Western Michigan University
ScholarWorks at WMU

Dissertations | Graduate College

1-2011

New Media ICC Profiles Construction and Concerns

Reem El Asaleh
Western Michigan University

Follow this and additional works at: https://scholarworks.wmich.edu/dissertations

Part of the Chemical Engineering Commons, Engineering Science and Materials Commons, and the Materials Science and Engineering Commons

Recommended Citation

Asaleh, Reem El, "New Media ICC Profiles Construction and Concerns" (2011). *Dissertations*. 342.
https://scholarworks.wmich.edu/dissertations/342

This Dissertation-Open Access is brought to you for free and open access by the Graduate College at ScholarWorks at WMU. It has been accepted for inclusion in Dissertations by an authorized administrator of ScholarWorks at WMU. For more information, please contact wmu-scholarworks@wmich.edu.

NEW MEDIA ICC PROFILES CONSTRUCTION AND CONCERNS

by

Reem El Asaleh

A Dissertation
Submitted to the
Faculty of The Graduate College
in partial fulfillment of the
requirements for the
Degree of Doctor of Philosophy
Department of Paper Engineering, Chemical Engineering, and Imaging
Advisor: Paul Dan Fleming III, Ph.D.

Western Michigan University
Kalamazoo, Michigan
December 2011

NEW MEDIA ICC PROFILE CONSTRUCTION AND CONCERNS

Reem El Asaleh, Ph.D.

Western Michigan University, 2011

With the advent of the modern digital technology, users can now capture an image and reproduce it between different media, such as display it on LCD monitor or tablet computer, print it on desktop printer or send it to a printing press. The challenge has been then to maintain the accuracy of image colors during this reproduction, which has led to the development of Color Management Systems. Using these systems, the color reproduction across-media will be accomplished using device ICC profiles that describe each device's color characterization data in a standardized format based on International Color Consortium (ICC) specifications.

ICC profiles use a multidimensional Lookup Table (LUT) to map the device independent space to the device colorant space. This LUT is constructed based on an estimated characterization device model (using data fitting functions and a set of measurement data) to speed the transformation performance. The attempts of this research are to study all the factors that affect the accuracy of different device characterization models and to reveal some important fundamentals that influence the accuracy of constructing an equivalent device profile. Different digital devices were employed: a scanner, two different LCD monitors and an RGB printer. A plausible model for each device was provided, which also was used to smooth the measurement noise. An equivalent LUT was constructed based on that model and stored inside an equivalent ICC

profile for each device using a customized C++ program and an open source library. Different evaluation tests were employed and some promising results were achieved.

UMI Number: 3496370

All rights reserved

INFORMATION TO ALL USERS
The quality of this reproduction is dependent on the quality of the copy submitted.

In the unlikely event that the author did not send a complete manuscript
and there are missing pages, these will be noted. Also, if material had to be removed,
a note will indicate the deletion.

UMI 3496370

Copyright 2012 by ProQuest LLC.

All rights reserved. This edition of the work is protected against
unauthorized copying under Title 17, United States Code.

ProQuest LLC.
789 East Eisenhower Parkway
P.O. Box 1346
Ann Arbor, MI 48106 - 1346

© 2011 Reem El Asaleh

ACKNOWLEDGMENTS

I would like to thank god for blessings I have received and the motivation to keep me focused on my goals.

It is my pleasure to thank Dr. Paul D. "Dan" Fleming for his support and friendship. His knowledge was a strong contribution to my research and he was a wealth of information during my graduation years.

I would like to extend my thanks to Dr. Alexandra Pekarovicova and Dr. Karlis Kaugars for serving on my thesis committee and providing me with invaluable comments and suggestions for improving this dissertation.

I would like to thank X-Rite for their donation of i1Profiler software and for their technical help and support. Also an individual thank to Mr. Marti Maria for allowing me to use the open source library (LittleCMS) program; this was the foundation of my research. Mr. Maria was very supportive with the technical guidance he gave me.

Most of all I would like to thank my partner in this journey, my lovely husband, and my family for their support. If it was not for their wisdom I would not be where I am today.

Of course I would like to give a special thanks to my 6 year daughter, Haneen, and my two year son, Jassim, for patience when mom was busy working on this dissertation instead of playing with them.

Reem El Asaleh

TABLE OF CONTENTS

ACKNOWLEDGMENTS ii

LIST OF TABLES viii

LIST OF FIGURES ix

CHAPTER

1. INTRODUCTION 1

1.1. Color Standards 2

1.2. Why Color Management? 2

1.3. Device Color Gamut 3

1.4. Dissertation Outline 3

1.5. Conclusion 4

2. LITERATURE REVIEW 5

2.1. Fundamentals of Color 5

2.1.1. Human Visual System 5

2.1.2. Color Spaces and Color Differences 7

2.2. ICC Color Management 9

2.2.1. Color Management System (CMS) 10

2.2.2. What are ICC Profiles 11

2.2.3. Profile Construction 12

Table of Contents- Continued

CHAPTER

2.2.4. Profile Models 14

2.3 Device Characterization Methods 16

2.3.1. Physical Models 17

2.3.2. Empirical Models 17

2.3.3. 3D Look-Up Tables 18

2.4 Gamut Mapping 19

2.4.1. Understanding Gamut Mapping 20

2.4.2. Rendering Intents 21

2.5 Conclusion 24

3. EXPERIMENTAL METHODS 26

3.1 Overview 26

3.2 Test Charts 27

3.2.1. Scanner Targets 27

3.2.2. Monitor Targets 28

3.2.3. Printer Targets 29

3.3 Measurements Conditions 29

3.4 Fitting Models Fundamentals 30

3.4.1. Least-Square Fitting Model 31

3.4.2. Polynomial Fitting Model 31

3.4.3. Transformation Requirements 32

Table of Contents- Continued

CHAPTER

3.5 C++ Programming Code 33

3.6 Notes Related to Constructing ICC Profiles 33

3.7. Data Analysis Procedure 34

3.8. Conclusion 35

4. EXPERIMENT 1: SCANNER 37

4.1 Introduction 37

4.2. Experimental Design 39

4.3. Scanner Model 40

4.4. Simulation Results 42

4.5. Conclusion 47

4.6. Future Works 48

5. EXPERIMENT 2: MONITOR 50

5.1. Introduction 50

5.2 Experimental Design 51

5.3 Phase #1: Monitors Physical Behaviors Evaluation 53

5.3.1. Experimental Design 53

5.3.2. Results and Discussion 54

5.4. Phase #2: Finding the Native Gamma 61

5.4.1. Experimental Design 61

Table of Contents- Continued

CHAPTER

5.4.2. Results and Discussion 61

5.5 Monitor Model 63

5.6 Simulation Results 71

5.7. Conclusion 77

5.8. Future Works 77

6. EXPERIMENT 3: PRINTER 79

6.1. Introduction 79

6.2 Experimental Design 81

6.3. Printer Model 83

6.4 Simulation Results 89

6.5. Conclusions 98

6.6. Future Works 98

7. CONCLUSION 99

7.1. Overview 99

7.2 Overall Findings 99

REFERENCES 101

APPENDICES

A. Scanner 108

B. Monitor 111

Table of Contents- Continued

APPENDICES

C. Printer..... 125

LIST OF TABLES

2-1. Matrix-based profiles required tags 15

2-2. LUT-based profiles required and additional tags..... 16

2-3. ICC profile tags and their corresponding rendering intents..... 22

3-1. Common required tags..... 33

4-1. Calculated determinant and RMSE..... 42

4-2. ΔE comparison between selected color patches of the training data and their equivalent values under different profiles 47

5-1. Configuration of computer system for monitor profiles..... 51

5-2. Calculated determinant and RMSE for different monitors..... 71

6-1. Calculated Jacobian determinant, Eigenvalues and RMSE for the constrained fit model..... 89

6-2. ΔE comparison between the training data of selected color patches and their equivalent values after applying different profiles on Adobe Photoshop..... 97

LIST OF FIGURES

2-1. Cross section of human eye structure 5

2-2. Rods and cones 6

2-3. ICC workflow 12

2-4. ICC profile structure 13

2-5. 3D projection of monitor and printer gamuts 20

2-6. Color transformation system's stages..... 21

2-7. Choosing appropriate rendering indents in Adobe Photoshop 22

3-1. IT8.7/2 targets from Kodak..... 28

3-2. LCD target provided by ProfileMaker..... 28

3-3. TC9.18 RGB test chart for Eye-one iO measuring device..... 29

4-1. Scanner characterization general schema 38

4-2. The xy-chromaticity plots of two lcms profiles: (A) the LS fit profile and (B) the polynomial fit profile 43

4-3. A 3D display of the gamut volume of two lcms profiles: (A) the LS fit profile and (B) the polynomial fit profile..... 43

4-4. The gamut volume of lcms profile (A) and ProfileMaker profile (B) 44

4-5. A 3D display of the gamut volume of lcms profile (A) and ProfileMaker profile (B) 45

4-6. The gray ramps of lcms profile (A) and ProfileMaker profile (B) 45

4-7. The primaries ramps of lcms profile (A) and ProfileMaker profile (B) 46

4-8. IT8.7/2 test chart after applying different profiles in Photoshop, polynomial lcms profile (A) and LS lcms profile (B)..... 46

5-1. Monitor characterization overall schema..... 51

LIST OF FIGURES-Continued

5-2. White and gray patches for monitor physical evaluation test 54

5-3. Brightness test results for Acer and LED monitors using an equivalent Lut-based profile that was build using ProfileMaker software. 55

5-4. Warm-up test using gray patch (up) and white patch (down) for Acer display 56

5-5. Warm-up test using gray patch (up) and white patch (down) for Apple cinema display 57

5-6. The CCT (in Kelvin) of the displayed white and gray patches on both Acer (up) and Apple display (down) monitors under different native profiles 59

5-7. The average CCT (in Kelvin) for a white background across different applications and platforms on both Acer and Apple display 60

5-8. Fit gamma graph of red vcgt channel in Acer display matrix-based profile 62

5-9. RGB and white patches 67

5-10. Average ΔE values for different fitting models compared with MeasureTool values for each display 68

5-11. Measurement data of the same LCD test chart in spectral mode (A) and in LAB mode(B) 69

5-12. The new average ΔE values for different fitting models compared with MeasureTool values for each display 70

5-13. The xy-chromaticity plots comparisons of different profile types for Apple (A) and Acer (B) monitors 72

5-14. The primary ramp comparisons of different profile types for Apple (A) and Acer (B) monitors 73

5-15. The gray ramp comparisons of different profile types for Apple (A) and Acer (B) monitors 73

LIST OF FIGURES-Continued

5-16. Average ΔE comparison between Photoshop data and different profiles and displays 74

5-17. Average ΔE comparison between DigitalColor Meter data and different profiles and displays 75

5-18. Average ΔE comparison between Photoshop and DigitalColor Meter of different profiles for Acer (up) and Apple cinema (down) displays 76

6-1. Printer characterization overall schema 80

6-2. Mitsubishi CP3020DA 81

6-3. xy-Chromaticity plot of Polynomial fit lcms profile and ProfileMaker profile for dye sublimation printer 84

6-4. Primary and secondary ramps of polynomial fit lcms profile (A) and ProfileMaker profile (B) for dye sublimation printer 84

6-5. xy-chromaticity plot of ProfileMaker profile (A) and our constrained fit lcms profile (B) for the dye sublimation printer 90

6-6. A 3D plot of ProfileMaker profile (A) and our constrained fit lcms profile (B) 90

6-7. A gray ramp plot of ProfileMaker profile (A) and our constrained fit lcms profile (B) 91

6-8. A gray ramp comparison between the training data (up) and the contents of the LUT of our constrained fit lcms profile (down) 92

6-9. Primary & secondary ramps plot of ProfileMaker profile (A) and our constrained fit lcms profile (B) 93

6-10. A cyan ramp comparison between the training data (up) and the contents of the LUT of our constrained fit lcms profile (down) 94

6-11. A magenta ramp comparison between the training data (up) and the contents of the LUT of our constrained fit lcms profile (down) 95

6-12. A yellow ramp comparison between the training data (up) and the contents of the LUT of our constrained fit lcms profile (down) 96

6-13. Color patches used to evaluate the printer profile 97

CHAPTER 1

INTRODUCTION

Other than viewing a colorful digital image on monitors or printing it on different substrates (such as T-shirts or papers), an important issue for publication or graphic industries in general, is to have a predictably accurate color appearance between different color devices, such as scanners, monitors or printers. To accomplish this goal, it's essential to study and understand color fundamentals, how colors are perceived by human eyes, the colors' mathematical identification, and the aim of color management, and factors that could affect the accuracy of color transformation across different media. All of these main topics, and more, were central to many investigations and research through the years and have led to developments of color systems and color consortia with one main goal: accurate color reproduction among media.

Moreover, due the wide existence of many digital devices, it becomes essential to achieve consistent results in a color reproduction system through a consistent imaging device characterization model. Many researchers have been conducted to produce better and accurate mathematical methods to describe the color behavior (or characterization) of different digital devices. Although better results have been reached, still these methods are not optimal and some irregularities occur.

This chapter will present an overall introduction about the fundamentals of color and Color Management System (CMS).

1.1. Color Standards

Light is visible for humans only if its wavelength falls between 400 to 700nm[1]. Special photoreceptor cells in the human eyes are responsible for interpreting their sensitivity to light and converting to signals that will be transferred to the brain through optical nerves. Despite the similarity of the vision process for all humans, the accuracy of interpreting colors is different depending on different factors, such as the human observers themselves [2], their gender, and age. Therefore, standards have been set and defined by the CIE (Commission Internationale de L'Éclairage), based on different color matching experiments that model the human visual system. Based on these standards, a set of color spaces were then developed and recommended by the CIE over the years to define the color in a mathematical way [3].

1.2. Why Color Management?

Color data cannot be transformed accurately across media, without the existence of the Color Management Systems (CMS) [4]. The basic goal for color management is to establish a communication between different devices and media in order to facilitate a consistence in transformation of color image between them [1]. The cross-platform ICC profile file asserts the modern ICC color management ambition by characterizing each device model, based on standards that were defined by the ICC (International Color Consortium). The connection between the device profiles will be made by a Color Management Model (CMM) to transfer color between them [5].

Device characterization methods come mainly in three approaches: physical, empirical and a mathematical using Look-up Table (LUT). Other alternative techniques combined one or two features from these approaches. However, there is no universal approach that can be applied for all types of color devices. [6]

1.3. Device Color Gamut

The new developments of digital devices allow each device to produce a different set of colors, which is referred to as its color gamut. Therefore, some of the captured image colors by digital cameras or scanners may not be accurately reproduced by printing devices or there will be a miss match situation. The allegation is that gamut mapping algorithms will be used to map these miss matching colors between different devices. The CMS contributes by providing different styles or rendering intents to handle the mismatching colors or the out-of-gamut colors. The accuracy of the selected Gamut Mapping Algorithm (GMA) is influenced by the selection of the appropriate rendering intents. [7] (See chapter 2 for more details).

1.4. Dissertation Outline

Chapter 2,"Literature review", will discuss in detail the basic fundamentals of colors in terms of how the human eye can see color and how colors are interpreted into numbers. It also defines a Color Management System and explains its basic components such as ICC profiles. Other interesting topics include device characterization methods and gamut mapping.

Chapter 3,"Experimantal Methods", provides an overview about the general experimental steps that were used in this study for different devices. It also introduces the general data analysis procedures that were conducted to evaluate our results. It is necessary to read this chapter because it contains many definitions that will be used in later chapters.

Chapter 4, 5 and 6 focuses on Scanner, Display and RGB printer experiment respectively. Each chapter introduces an overview of the device characterization process and specifies the experimental design. It gives details of data evaluation results as well. Finally, each chapter includes a summary of the experiment with suggested topics of future works.

1.5. Conclusion

Overview issues of color fundamentals and color management system were introduced along with a description of the contents of this study. More details about the discussed topics are provided in the following chapter.

This study concentrates in developing a plausible mathematical way to describe the color behavior of different digital devices that will lead to enhanced performance of their ICC profiles. In addition, it will highlight some basic fundamentals of constructing ICC profiles using programming code.

CHAPTER 2

LITERATURE REVIEW

2.1. Fundamentals of Color

2.1.1. Human Visual System

Figure (2-1) shows a side section of the human eye structure. As incident light enters the eye, it's projected onto the retina at the back of the eye after it has been focused by both the cornea and the eye lens. The main function of the retina is to interpret the light into signals that are transmitted by the optical nerves to the brain to be processed.[8, 9]

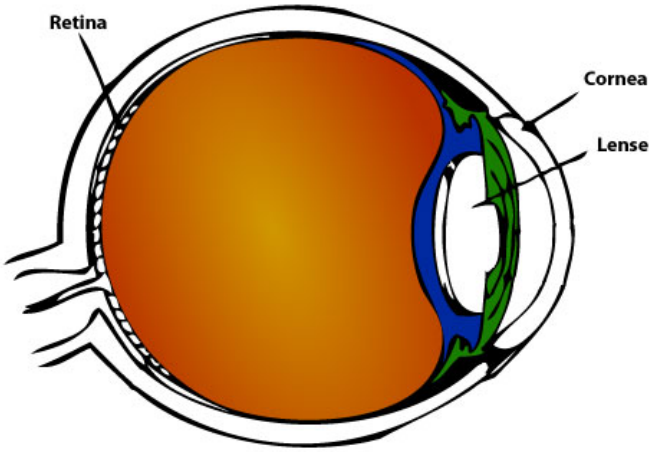

Figure 2-1: Cross section of human eye structure

A network of photosensitive cells is incorporated with the Retina's thin layer cell structure. These photosensitive cells are responsible for the visual system of the eye and are divided into two basic types: Rods and Cones (see **Figure 2-2**). [10] Rods only work at low luminance levels or gray shades, which means that they cannot see colors. In contrast, cones work at high luminance levels, but they can see colors and in fact they are divided into three basic types, based on their sensitivity of the visual spectrum. These types are *Long- wavelength (L), Middle- wavelength (M)* and Short-*wavelength (S)* cones. They also can be referred to *RGB* based on their sensitivities to red, green and blue colors, respectively. [11, 12]

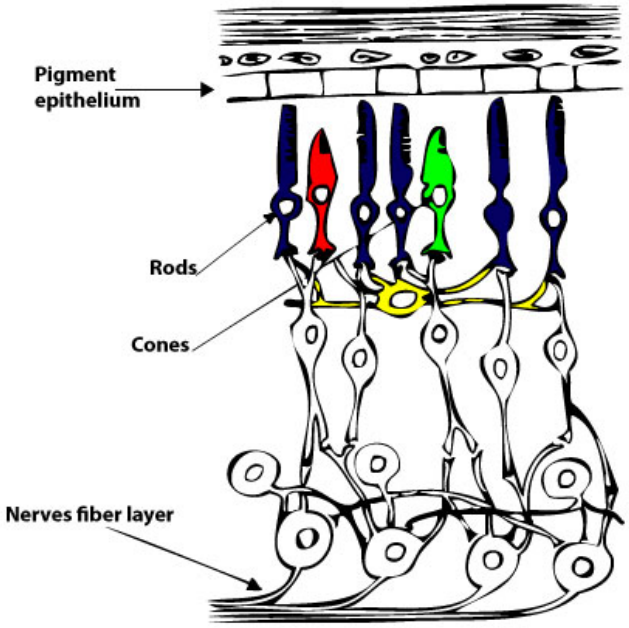

Figure 2-2: Rods and cones

Due to the different sensitivities of the rods and cones functions, the human visual system is able to work under a range of luminance levels. The color vision of the cones is referred to as *Photopic Vision* or *Bright-light Vision*, while the black and white vision of

the rods is referred to as *Scotopic Vision* or *Dim-light Vision*. It is interesting to know that there is variation in the distribution of the rods and cones across the retina surface. [2,13]

Despite the fact that all human eyes process color the same way, color interpretation can be different from one observer to another. One of the reasons is related to the eye lens function, where it also works as a filter by absorbing and scattering both UV and short-wavelength (blue region) radiation. As humans get old, the ratio of these phenomena increases and the lens become more yellow. Thus, the response of the color will be significantly different between different observers. [9,14] Other reasons that could affect the perception of color could be related to either physical or physiological factors. To average the variation of the color perceptions, CIE (Commission Internationale de L'Éclairage) has defined in 1931 a set of *standard observers* that are based on the human visual system. [3]

2.1.2. Color Spaces and Color Differences

Whether an image has been captured by a scanner, displayed on a monitor or printed by a printer, its color values are strongly dependent on the device characteristics [15]. For instance, CRT monitors have phosphor channels that define the RGB primaries, as well as RGB filters in scanners. However, each device will reproduce different amounts of RGB values, even if they are identical brands. Moreover, colors in printers are reproduced in terms of CMYK primaries and depend on pigment or colorant types, toners or printer devices. Therefore, the printed color will have different appearance. Consequently, each device produces a different amount of color or color gamut. [16]

Typical additive devices, such as monitors and scanners, use the RGB color space, which is based on the additive color theory, where colors are produced in terms of RGB primaries. Printers on the other hand, use the CMYK color space that is based on the subtractive color theory, where the printed colors absorb some colors of light and reflect others. These types or color spaces are also defined as device-dependent color spaces. [15]

The device-independent color spaces are defined based on CIE colorimetric measurements (i.e. do not depend on any devices) and they are basically used to convert between different color spaces. Examples of these color spaces are CIEXYZ and CIELAB [16]. CIEXYZ was developed by CIE in 1931, where the XYZ primaries (or tristimulus values) define colors based on the CIE standard observer [17]. To overcome the non-uniformity perceptual problem of the CIEXYZ colorspace, CIE recommended in 1976 the CIELAB (or CIE 1976 L*a*b*) space [18]. CIELAB is a three-dimensional color space, where the axis of **L*** represents the illumination of a color, while the **a*** axis represents the red-green opponent end color and the **b*** axis represents the blue-yellow opponent end [19]. The CIELAB space also was noted as a uniform color space. Another uniform color space recommended by CIE was the CIELUV (or CIE 1976 L*u*v*) color space [20].

Based on the uniformity of the CIELAB color space, the Euclidean distance between two colors in the three-dimension space will be a numerical way to measure the perceptual difference between them [21]. Color difference (or $\Delta\mathbf{E}$) is quantified based on the following formula:

$$\Delta E^*_{ab} = [(\Delta L^*)^2 + (\Delta a^*)^2 + (\Delta b^*)^2]^{1/2} \quad (2.1)$$

Color difference is an important way to evaluate the differences between original and reproduction color (i.e. color images displayed on monitors and printed by printers).

Similarly, if colors are represented in polar coordination (i.e. using the LCH color space to express the color in terms of chroma and hue angle) the color difference can be also calculated as follows [22]:

$$\Delta E^* = [(\Delta L^*)^2 + (\Delta C^*_{ab})^2 + (\Delta H^*_{ab})^2]^{1/2} \quad (2.2)$$

$$\Delta H^*_{ab} = [(\Delta E^*_{ab})^2 - (\Delta L^*)^2 - (\Delta C^*_{ab})^2]^{1/2} \quad (2.3)$$

Note that ΔE^* and ΔE^*_{ab} are identical by construction.

2.2. ICC Color Management

In the imaging system world, where different digital devices exist (e.g. scanners, digital cameras, monitors and printers), each with its unique color characterization and color space, it is required to have reliable color reproduction among these devices. *Color Management* comes into place to assure consistence color transformation and appearance across assorted color devices or media [4]. The importance of using color management then led to the formation of the ICC (International Color Consortium) to define standards that can be used for characterizing these devices, which then were represented in special computer files called *Profiles*. [23]

2.2.1. Color Management System (CMS)

Controlling and achieving reliable color reproduction across different devices is the main goal of color management systems (CMS). Four main procedures [24] need to be employed, as part of CMS manipulation, to achieve accuracy. Two procedures involve *calibrating* and *characterizing* each device that is involved in the transformation [4]. The device needs to be optimized prior to calibration, to achieve *consistency* (the third procedure) in its behavior. Without consistency, especially in forward and reverse transformations, the whole CMS is worth little. Device calibration involves adjustment of device response in order to match an established condition [25]. Characterizing the device involves using instruments, such as a colorimeter and spectrophotometer, to measure the device response for color signals (from color test charts) that are sent to it. As a result of this procedure, the gamut of the device is calculated and the characterization data are used to create a special computer file called an *"ICC Profile"*, which is an important part of the CMS [26]

The *converting* process is the fourth process in CMS, which involves converting an image between two different color spaces via the ICC profile. For instance a printer profile would be employed to convert a displayed RGB image into printer CMYK color space, in order to print it [24]. Therefore, an accurate ICC profile would results an accurate color conversion between different color spaces.

Transforming color information from one medium to another or, in other words, from one color space to another (such as from monitor to printer) can be accurately achieved if the calibrating and characterizing procedures of the media have been

accurately accomplished. [27] To facilitate this transformation, a combination of application software (such as Photoshop), operating system software (such as ColorSync for Mac OS or WCS and ICM for Windows) and Color Management Modules (CMM) are used. [23]

2.2.2. What are ICC Profiles

The first version of the ICC (International Color Consortium) profile was developed in 1993, as a result of establishing the ICC by eight industrial vendors [28]. The main reason to create such files is to ease mapping color across different imaging devices (scanners, monitors, printers, etc.) by capturing each device's color characterizations and storing them in special tags. This information is then used to remap the device color space to a standard color space, as defined by the ICC (PCS or Profile Connection Space), to establish a communication across different devices. At this stage, the PCS can use either CIELAB or CIEXYZ device independent color spaces as the standard colors pace, as defined by the ICC [29].

The CMM uses the information stored in the profile to combine different device profiles and perform a consistent color transformation across them [2] (see **Figure 2-3**).

Figure 2-3: ICC workflow

2.2.3. Profile Construction

An ICC profile is a cross-platform computer file that contains data (text and numbers); these data are divided into three main parts: a fixed size profile header, which includes homogeneous information that can be found in all profiles, a variable size tag table and the tagged element data [23] (see **Figure 2-4**).

The information set inside the profile header is used to describe the profile and it can be found in all profiles. The completed information will facilitate working with the profile by different applications without corruption [30].

The tag table comes after the profile header and it includes tag counters, which is the total number of tags inside the tag table, each tag's signature, a pointer to the actual tag data location and the size of the tag data element in bytes [29].

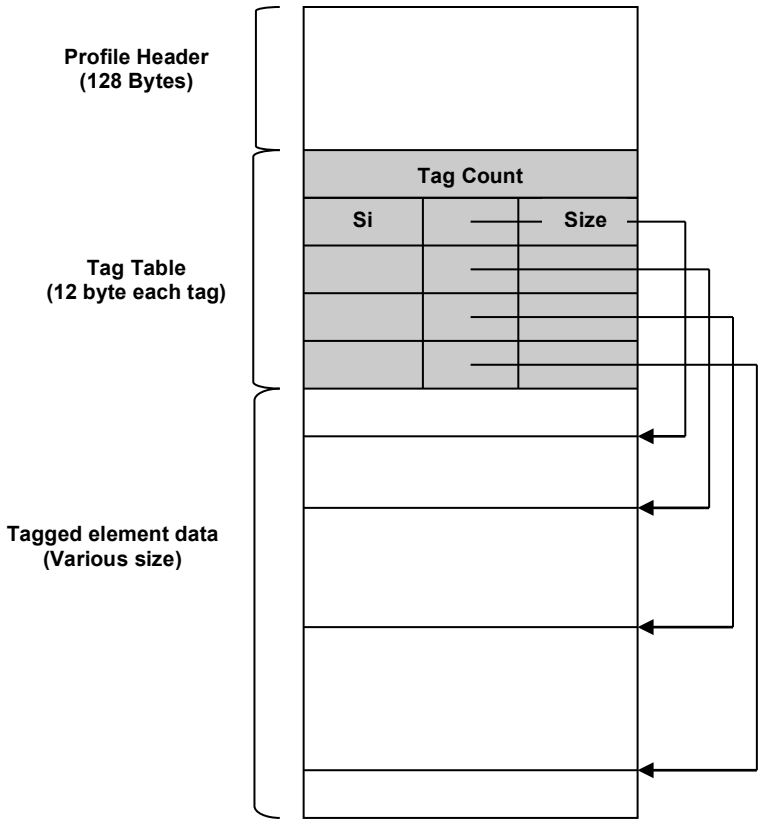

Figure 2-4: ICC profile structure [30]

Generally ICC profiles come in seven different types; Device profiles, which include input (for scanners and digital cameras), display (for monitors) and output (for printers and presses) profiles, DeviceLink profiles, ColorSpace Conversion profiles, Abstract profiles and Named Color profiles [28] . Each of these has a different set of tags (required, optional and private) and therefore the total size of the profile depends on its type [28].

The required tags, as described by ICC specifications [30], contain all sets of information that enhance the CMM functionality of the requested color mapping. [31] Although the absence of the optional tags will not cause problems in the profile performance, they can enhance it [31]. In addition, companies can add specific tags into a

profile, which can be used to enhance its performance within that company's application. These kinds to tags are called Private tags. [29]

2.2.4. Profile Models

For accurate color space conversion to and from the PCS, two algorithm models are used: the Matrix/TRC model and the LUT (Lookup table) model. Therefore ICC profiles are divided into two models (Matrix-base and LUT-base profiles), based on the calculation algorithm that is used to convert between color spaces [28]. The type of the profile model can be determined by the user of the profiling software.

For implementing these models, each model is required to have a special set of data, which are stored in a special tag type. [28] Therefore, the CMM will use these data in performing the conversion between different color spaces through the standard PCS color space.

2.2.4.1. The Matrix/TRC Model

This model structure involves:

The 3 one dimensional LUTs are represented by the Tone Reproduction curves (TRC) [31]. To transfer color between input and output tables, a linear interpolation calculation is performed [32]. In this model the PCS will only use the CIEXYZ standard

color space [30]. The Matrix/TRC model is generally valid for CRT displays, but it can be useful for any device for which the transformation to the PCS is nearly linear such as Scanners.

For displays, the TRC curves also determine the gamma value of the display. Therefore, matrix-based profiles are generally used in monitors, or RGB devices, and they are simple and produce small size profiles [31]. The following tags are required to be included in a Matrix-based profile [28]

Table 2-1: Matrix-based profiles required tags

	Tag name	Tag
Colorants tags	redMatrixColumnTag	rXYZ
	greenMatrixColumnTag	gXYZ
	blueMatrixColumnTag	bXYZ
TRC tags	redTRCTag	rTRC
	greenTRCTag	gTRC
	blueTRCTag	bTRC

2.2.4.2. LUT Model

In contrast with the matrix-base profiles, the LUT-base profiles are complex and large size profiles. The following is the LUT model structure [31]:

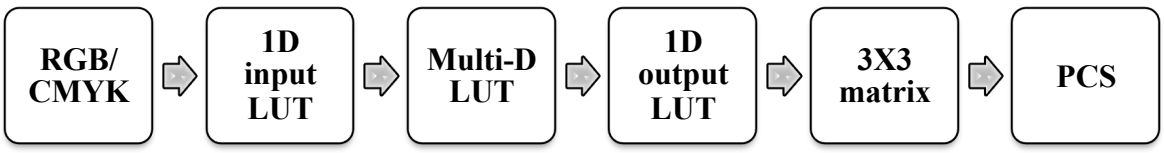

However, other possible combinations of the LUT-model's elements can be used since it is not a requirement to use all the transformation elements. The LUT-based profile can be used in all kinds of device profiles (input, display and especially output) [23]. **Table (2-2)** displays the required tags that need to be included in the LUT-based profile. In addition, **Table (2-2)** displays also additional tags that might be found in input and display LUT-based profiles and they're required in output LUT-base profiles.[30]

Table 2-2: LUT-based profiles required and additional tags

	Tag name	Tag
Required Tags	AToB0 Tag	AToB0
	BToA0 Tag	BToA0
Additional Tags	AToB1 Tag	AToB1
	BToA1 Tag	BToA1
	AToB2 Tag	AToB2
	BToA2 Tag	BToA2

2.3. Device Characterization Methods

A displayed image on a monitor that has an RGB colorant space must be converted to a printer CMYK colorant space in order to be printed. This conversion can be accomplished only through a CIE color space. The process of creating a model of the relationship between a device colorant space and CIE color space is known as device characterization [6].

There are three main approaches that are used for characterizing a device: physical models, empirical models and 3D Look-up tables (LUT) [33]. Combined elements from these approaches also can be used in the color transformation procedures.

2.3.1. Physical Models

Physical models require some measurements to construct a mathematical relationship between the device input and the output signals. Kubelka-Munk [34] and Neugebauer [35] equations printer models and the gain-offset-gamma (GOG) CRT display model are examples of this approach [6].

Physical models, or other model-based approaches, consume less time for predicting a characterization function and they generate smooth models. In case some parameters of the device have been changed, the re-deriving of the characterization model would be straightforward [26]. On the other hand, the model-base approach is complex to derive and not sufficiently accurate [36]. In addition, because this approach depends mainly on the device technology, the accuracy of the generated model is influenced by the extent of representing the device physical behavior in the generated model [37].

2.3.2. Empirical Models

In contrast with physical models, empirical models require a large set of measurements to construct a characterization function [26]. They are not obviously connected to the physical behavior of a device and often involve the using of regression or interpolation techniques to derive a direct relationship between the device color space

and the CIE colorimetric space [33]. The polynomial regression model is one example of this approach.

However, they have poor performance toward the edge of the device gamut. In addition, errors might be produced due to the large set of measurements. This approach is widely used for characterizing scanner and output devices [6].

2.3.3. 3D Look-up Tables (LUT)

The multidimensional LUT is a 3D table that accurately transforms colors between two color spaces that are not related to each other (i.e. device colorant space and device independent color space such as CIE LAB or XYZ). [33]

The entries of the LUT can be constructed from direct measurements or through either physical or empirical approaches. These entries cover the gamut of the characterized device but do not include all the lattice points. For instance, an RGB device, such as monitor where it has 3 color channels, each channel has up to 256 values (8-bit), the total possible sample measurements would be over 16 million. A 3D LUT can be constructed with 17x17x17 entries with a total of 4,913 lattice points. This could speed up the process of color transformation and minimize the computational cost. [38]

For the other lattice points that are not included in the LUT, an interpolation method is employed to approximate the function value. The larger the number of LUT entries, the less the interpolation error could occur. But this could affect negatively on the process speed and the memory required for the computation. [33]

The most common interpolation methods that can be used are trilinear, prism, pyramid and tetrahedral. They differ in the way the lattice points are selected, the accuracy of results and complexity. [39]

The LUT methods are used for forward and backward transformations as well and provide more accurate results than the other device model methods [36]. The ICC profile is an example of a system that implements a LUT for color transformation among color spaces.[28]

2.4. Gamut Mapping

The amount of colors that can be produced by coloring device, or medium, is defined as its color gamut [6]. As a result, the media gamut can be expressed as the color volume (a three dimension shape); therefore the color space boundary can be also referred as the gamut boundary [40]. Specifically, in CIELAB space, this volume represents the number of colors that can be generated within a ΔE tolerance of $\sqrt{3}$. [41]

Using the fact that each device has its own color gamut, it is obvious that some colors cannot be reproduced between two different media [7] For example, generally RGB devices, such as monitors or scanners, have a larger gamut than CMYK devices, such as printers, which means that some colors that can be displayed in monitor cannot be printed by a printer or, in other words, they will be out-of-gamut (see **Figure 2-5**). Thus, the procedure of mapping the mismatch or the out-of-gamut colors from reproduction media to and from original media is defined as gamut mapping.[42]

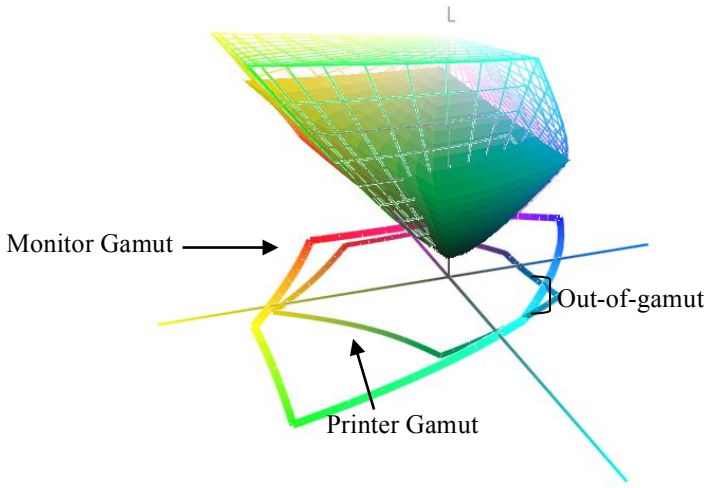

Figure 2-5: 3D projection of monitor and printer gamuts

2.4.1. Understanding Gamut Mapping

The main aim of gamut mapping is "to ensure the closest overall color appearance between the reproduction and the original image" [43], which can be realized using the gamut mapping algorithms (GMA) or techniques. [44]

Transforming color between different media can be accomplished within five stages, as shown in **Figure (2-6)**, which can be referred to as a color transformation system [42]. This system comprises three main components: device characterization, color appearance model and gamut mapping [43] Device characterization is the procedure of rendering device signals as referred to the human visual system [24], where the color appearance model was defined by CIE TC 1-34 as: "any model that includes predictors of at least the relative color appearance attributes of lightness, chroma, and hue" [45].

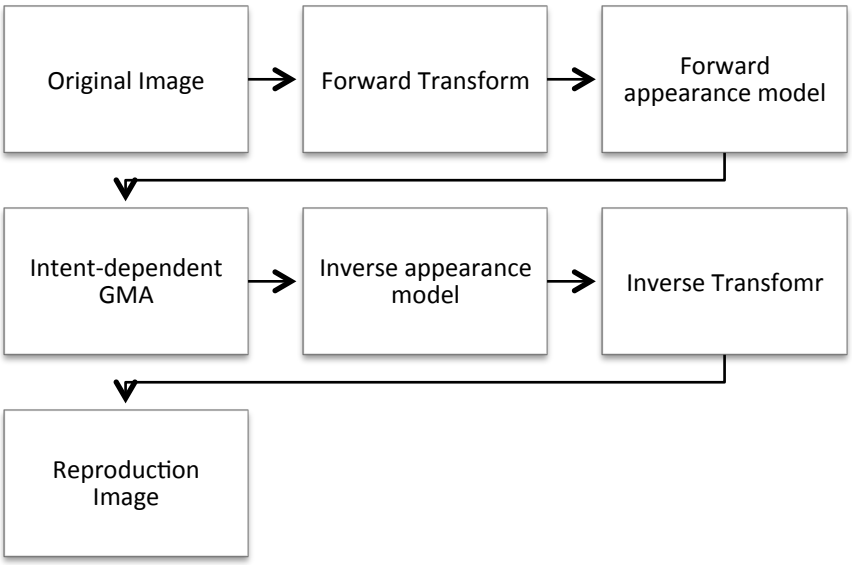

Figure 2-6: Color transformation system stage. (Adapted) [46]

2.4.2. Rendering Intents

The ICC has defined four different methods or styles that are used by the CMM to handle replacing the out-of-gamut colors or to form a gamut mapping. These methods are Perceptual, Relative colorimetric, Absolute colorimetric and Saturation [50]. Specifying rendering intent will help setting a corresponding GMA to achieve an accurate color reproduction across media [43]

Software, such as Adobe Photoshop, allows users to select between different rendering methods (see **Figure 1-7**). To chose between different rendering methods, it's important to know the gamut volume of devices that are concerned and understand the specific image type. [48]

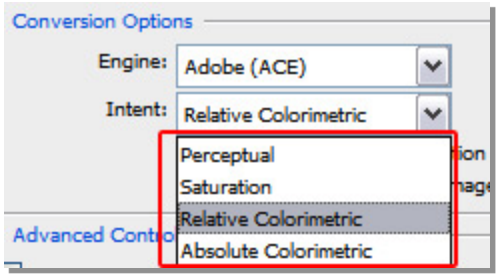

Figure 2-7: Choosing appropriate rendering indents in Adobe Photoshop

In the LUT-based profiles each of the AToBx Tags and BToAx Tags represent different rendering intent models, where the BToAx tags (PCS-to-Device lookup table) represent the reverse calculation methods of AToBx tags [5] as shown in **Table (2-3)**

Table 2-3: ICC profile tags and their corresponding rendering intents

Tag Name	General description	Rendering Intents
A2B0 Tag	Device-to-PCS lookup table	Perceptual
A2B1 Tag	Device-to-PCS lookup table	Media-Relative colorimetric
A2B2 Tag	Device-to-PCS lookup table	Saturation

2.4.2.1. Perceptual Intent

This intent works by mapping the original color gamut to the final gamut (or printer gamut) [5]. However, this rendering method might cause some color change from original image to final. But, on the other hand, it maintains the best color appearance [28]. Therefore, perceptual intent is suited for images that are not required to have exact color matches, such as with pictorial or photographic-type images. [15]

2.4.2.2. Media-Relative Colorimetric Intent

This rendering is accomplished by matching the white point of the medium to the final input or output device [2]. The accuracy of mapping the in-gamut color makes this intent suitable to use in images where exact color mapping is required, such as in company logo images [23]. For the out-of-gamut colors, this intent tries to map them to the closest available color within the gamut, which might be lost in some cases or might be mapped to the same position of other similar out-of-gamut colors [49].

2.4.2.3. Absolute Colorimetric Intent

Despite the similarity to the relative colorimetric intent, where it is used for the images that required exact color matching, the absolute colorimetric intent doesn't allow changing the white point of the original to final device [28]. However, if we have an output profile as the original, that has a yellowish white point, the absolute intent maps the color of the final image to match exactly that yellowish white point. The use of this intent is useful for simulating between different devices, such as proofing on monitors how the actual image will look when it's printed. [48]

According to ICC specifications, "this definition of ICC-absolute colorimetry is sometimes called "relative colorimetry" in CIE terminology, since the data have been normalized relative to the perfect diffuser viewed under the same illumination source as the sample". [30]

2.4.2.4. Saturation Intent

For business images, such as charts or pie charts, where more bright and vivid colors are required, saturation intent must be used [5]. The intent is accomplished by moving the in-gamut colors to the edge of the final device gamut.[49]

2.5. Conclusion

CIE has set observes standards which were the basis of the mathematical interpretations of how human see colors. The developed device-independent color spaces XYZ and LAB were also based on the CIE standards.

“What You See Is What You Get” is the overall goal of using color management system especially when utilizing different color devices. The 4C's of the CMS are: calibration, characterization, consistency and converting. its essential to ensure the accuracy of each process of the CMS to achieve consistent color appearance across digital media.

ICC profile is the most important element of the CMS as it holds all the required information to perform the color transformation across media. This chapter discussed the profile's structure and its models.

To build an ICC profile for a device its need to be characterize in a mathematical way to find the mapping model between the device-dependent color space and the independent color space. Three different models are existing each has its advantages and disadvantages.

The selection of an accurate device characterization model could ease the selection of the appropriate Gamut mapping algorithm to map between two different devices each with its unique gamut.

CHAPTER 3

EXPERIMENTAL METHODS

3.1. Overview

To achieve a consistent color appearance for an image across media, each digital device needs to be accurately calibrated and characterized. The characterization methods for input, display and output devices are different depending on device physical properties. Consideration of the fundamentals of each device characterization method is essential for achieving consistent results in a color reproduction system. The aim of this research is to control all the elements that could influence the possibility of having a conceivable model that characterizes scanners, printers and display devices. The intent is to smooth the device gamut by reducing the effects of inaccurate measurements.

This study utilizes three different devices: a flatbed scanner, two different LCD monitors and a dye sublimation printer. Different test charts are used for each device, which will provide both the device color space and the independent color space information. This information will be employed to design a characterization model for each device and a corresponding ICC device profile will be constructed using a customized C++ program as our profile editor. Different evaluation tests will be operated to test both the performance of the constructed ICC profile and the developed characterization model for each device. This chapter will discuss the target test charts for each digital device, some basic fundamentals related to the characterization models and a

number of useful notes regard the measurement conditions and several ISO standards that need to be known of before constructing an ICC profile.

3.2. Test Charts

Generally, a device characterization process requires the use of a suitable reference target or test chart that contains a specific set of color patches that cover a device color gamut. The selection of the test chart depends on many factors and these factors differ based on the selected device to be characterized (i.e. scanner, printer, LCD or CRT, etc...).

3.2.1. Scanner Targets

For a scanner device the reference target is usually accompanied with a reference file that contains the associated CIE XYZ/LAB values of each color patch. And thus, the equivalent RGB values will be collected from the scanned image of that chart. Usually the selection of the scanner test chart depends on the selected scanned material (i.e. transmission or transparency and reflection materials). The most common test charts are IT8 charts and Hutch Color (HTC) targets. The different between them is that IT8 targets meets ISO 12641:1997 [50] standards and HTC do not but it is still accepted in some profiling software. [51]

There are two kinds of IT8 targets: IT8.7/1 for transmission materials and IT8.7/2 for reflection materials. Both kinds can be provided by different companies such as Kodak, FUJI and Agfa [51]. For our scanner device, the selected target for this study was Kodak Q60 IT8.7/2-1993. (See **Figure 3-1**)

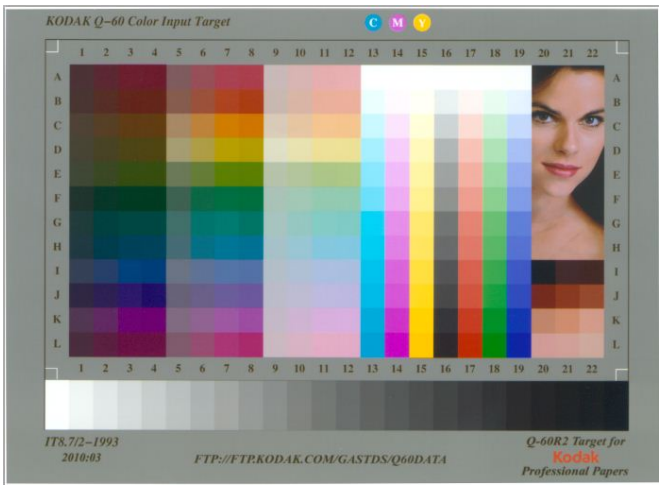

Figure 3-1: IT8.7/2 targets from Kodak

3.2.2. Monitor Targets

Generally, there are no specific designed test charts for monitors. However, some profiling software, such as ProfileMaker, provides two different targets that are designed for CRT and LCD respectively (See **Figure 3-2**). These targets contain a set of RGB color patches which will be flashed on the screen one at a time while a measurement device collects the corresponding XYZ/LAB values. For our two LCD monitors the selected target was LCD test chart as shown in **Figure (3-2)**.

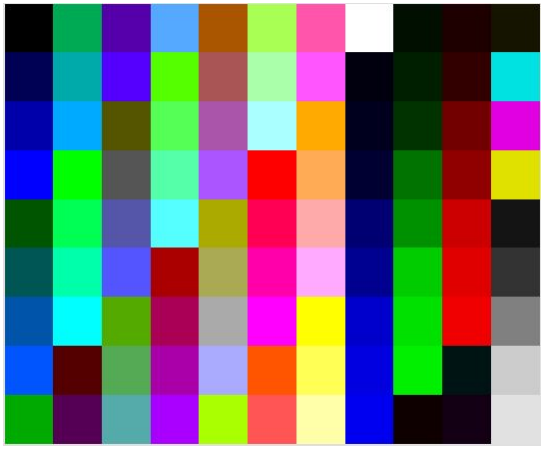

Figure 3-2: LCD target provided by ProfileMaker

3.2.3. Printer Targets

The selection of the reference target for a printer deepened on many factors such as the selection of the printing process, printed material, type of ink used and the measurement device as well. The IT8.7/3 target has been used for a long time and it follows ISO 12640 standers [52]. However, ECI2002 is considered as the enhanced version of the IT8.7/3 and was widely used for many CMYK printing application [53]. In addition, TC9.18 target was designed for RGB printers, such as our dye sublimation printer, which contains 936 different RGB color patches and was the selected target for this study as well. (See **Figure 3-3**)

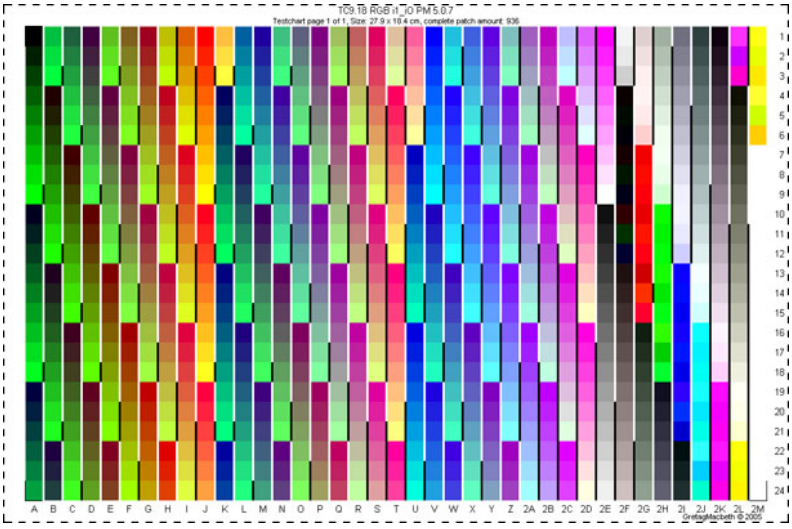

Figure 3-3: TC9.18 RGB test chart for Eye-one iO measuring device

3.3. Measurements Conditions

Colors in general will appear differently if they are observed under different illuminants. Therefore CMS have paid a lot of attention to what is called "*Chromatic adaptation*" .To simplify the definition of the chromatic adaptation; let's refer back to the

human eye. For instant, if a user wants to compare a displayed image on a screen with a printed copy of the same image under a different illuminant. If the user turns his head quickly between the two images he can clearly observe the difference in the color appearance. but If the user maintains looking at any of the images for a little while his eye will naturally adapted the color to the applied illuminant and he will be convinced that the two images looks similar. Bradford and CMCCAT97 are the commonly used models for the chromatic adaptation process. [30]

Based on ISO 13655 standards [54], the measurement of any reference target should be collected under CIE illuminant D50 to avoid any error in the measurements due to instrument's fluorescence. When the actual reference illuminant or chromaticity is different than D50 a chromatically adaptation or correction is utilized at the ICC profile building time. [53]

3.4. Fitting Model Fundamentals

All tested devices will be characterized based on a LUT table model, where its entries will be populated through an empirical approach, which was previously discussed at section 2.3.2. This approach utilizes a regression model to estimate it coefficients. For this study, two different regression models will be used: the Least-square linear fitting model (for scanner and monitor) and the nonlinear polynomial model (for all tested devices).

3.4.1. Least-Square Fitting Model

Let ***P*** contain **n** measurement elements which correspond to X, Y or Z and ***Q*** be an **mxn** matrix that holds the number of terms where ***C*** will hold the best-fit corresponding of **m** coefficients. The linear function can be expressed as:

$$\boldsymbol{P = QC + E} \qquad \textbf{(3.1)}$$

Where ***E*** is the residual error that has **n** elements. If we find $\hat{\boldsymbol{C}}$ that minimize ***E*** such that

$$\hat{\boldsymbol{C}} = (\boldsymbol{Q}^T \boldsymbol{Q})^{-1} (\boldsymbol{Q}^T \boldsymbol{P}) \qquad \textbf{(3.2)}$$

Where $\boldsymbol{Q}^T$ is the matrix transpose. Then $\hat{\boldsymbol{C}}$ will be denoted as the *Least-square solution*.[33,55]

3.4.2. Polynomial Fitting Model

For some digital devices, such as a CRT, the use of linear Least-squares model to characterize the device would be sufficient. Other devices require a higher order model such as a polynomial. The order of this model can increased up to **n-1** order, where **n** is the number of variables. In addition, the same form of this model can be used for both forward and inverse color transformation. [26]

A 2nd-order polynomial model was selected for this study, with a total of 9 terms. A forward transformation model from RGB to XYZ can be expressed as follow: [55]

$$\begin{bmatrix} X \\ Y \\ Z \end{bmatrix} = \begin{bmatrix} c_{1,1} & c_{1,2} & c_{1,3} & c_{1,4} & c_{1,5} & c_{1,6} & c_{1,7} & c_{1,8} & c_{1,9} \\ c_{2,1} & c_{2,2} & c_{2,3} & c_{2,4} & c_{2,5} & c_{2,6} & c_{2,7} & c_{2,8} & c_{2,9} \\ c_{3,1} & c_{3,2} & c_{3,3} & c_{3,4} & c_{3,5} & c_{3,6} & c_{3,7} & c_{3,8} & c_{3,9} \end{bmatrix} \begin{bmatrix} R \\ G \\ B \\ RG \\ RB \\ GB \\ R^2 \\ G^2 \\ B^2 \end{bmatrix} \quad \textbf{(3.3)}$$

3.4.3. Transformation Requirements

Let ***M*** be the **3x3** matrix that holds either the coefficients of the Least-square model or the linear coefficients of the polynomial model. For a well-behaved forward transformation, ***M*** should satisfy both the non-singularity and a constant sign Jacobian determinant conditions. A non-singular matrix is an invertible matrix that is also diagonally dominant [56]. This condition is very important for both monitor and printer devices to insure the forward and inverse transformation between different color spaces.

For the Jacobian determinant's sign, a positive sign indicates a linear transformation from RGB to XYZ. While for CMY devices the nonlinear transformation from RGB to CMY enforces a negative Jacobian sign. Overall, a constant sign must be maintained through all transformation points which reflect stable transformation performance. In addition, a non-zero Jacobian determinant value indicates that the transformation function is continuously differentiable and thus it is invertible [57]. Section 3.7 in this chapter will demonstrate the general form of calculating the determinant.

3.5. C++ Programming Code

Microsoft visual studio 2008 and VC++ was used to design and customize our profile editor code. This new code was designed with assistance of LittleCMS 2.2 (LCMS) library, which is a compilation of an open source program (designed by Marti Maria) that can be used to construct and edit ICC profiles and it fully supports the newest ICC specifications. [58]

The advantage of having our code is that the underlying cause of any irregular behavior that might be resulted from insufficient device characterization model can be examined in more detail. This will make possible the removal of the irregular behavior from the constructed profile and provide a valid characterization of the device within the limits of human color vision.

3.6. Notes Related to Constructing ICC Profiles

As discussed briefly at section 2.2.3, ICC profiles consists of optional and required tags. Among all profile types four tags are common and required as well which are listed at **Table (3-1)**.

Table 3-1: Common required tags

Tag name	Tag
Profile Description tag	desc
Media Whitepoint tag	wtpt
Copyright tag	cprt
Chromatic Adaptation tag	chad

The Media Whitepoint tag consists of the tristimulus value of the media whitepoint values as measured from the reference target. The chromatic adaptation tag contain the chromatically adaption matrix that is used when the reference illuminant is not a D50. [53]

In this study, both the scanner and printer test chart's measurements were taken under D50 illuminant. Based on ICC specifications [30], the CLUT in AToBx tag need to be built as a relative colorimetric LUT. This step is actually achieved by scaling all the fit values that result from the fitting model to the ratio of the D50 whitepoint value to actual measured whitepoint under D50 illuminant and then save the result in the CLUT of the A2B tag. The actual measure whitepoint value should be saved in the Media whitepoint tag in the ICC profile and this value will be then used to perform an absolute/relative colorimetric conversion.

For monitor device the test chart measurement were recorded under the native illuminant which is different than D50. Therefore all the measurements required to be chromatically adapted to D50 before converting them to relative colorimetric. In addition, a D50 value should be saved in the Media whitepoint tag of the monitor ICC profile despite whatever the actual measure whitepoint. [53]

3.7. Data Analysis Procedure

To evaluate the performance of the tested profiles, several tests were employed depend on the tested device. Overall, the Jacobian determinant and the Root Mean Square Error (RMSE) were calculated to test the accuracy of the selected fitting model for each device.

For a forward transformation $\boldsymbol{P}$ from RGB to XYZ, the Jacobian matrix $\boldsymbol{J_P}$ can be expressed as follow [59]:

$$\boldsymbol{J_P} = [\boldsymbol{\nabla X}, \boldsymbol{\nabla Y}, \boldsymbol{\nabla Z}]^{\boldsymbol{T}} \quad \textbf{(3.4)}$$

where $\boldsymbol{\nabla}$ symbolize the *gradient* (for instance the $\boldsymbol{\nabla X} = \left[\frac{\partial X}{\partial R} \quad \frac{\partial X}{\partial G} \quad \frac{\partial X}{\partial B}\right]$). And the determinant ***det(P)*** of a **3x3** matrix $\boldsymbol{J_P}$ can be calculated as follow [13]:

$$\boldsymbol{det(J_P)} = \begin{vmatrix} \boldsymbol{a} & \boldsymbol{b} & \boldsymbol{c} \\ \boldsymbol{d} & \boldsymbol{e} & \boldsymbol{f} \\ \boldsymbol{h} & \boldsymbol{i} & \boldsymbol{a} \end{vmatrix} = \boldsymbol{aei + bfg + cdh - ceg - bdi - afh} \quad \textbf{(3.5)}$$

RMSE reflects the statistical error of the estimation that is the calculated standard deviation of the difference between the reference and the estimated values and can be expressed as follows [60]:

$$\boldsymbol{RMSE} = \sqrt{\frac{\sum_{i=1}^{n}(x_{1,i} - x_{2,i})^2}{N}} \quad \textbf{(3.6)}$$

Moreover, the performance of the tested profiles for different devices was evaluated in terms of color difference ΔE between the reference data and the predicted once.

3.8. Conclusion

This chapter highlights different topics that are related to the proceeding experiments in this study. It distinguished between different target charts for each digital

device. Moreover, for all digital devices some ISO standards need to be employed at the measurement time of the target test to limits any variations that could cause due using different measurement devices.

This chapter demonstrates also the general form of two different fitting models that will be used in this study for different devices. In addition, the mathematical requirements that need to be achieved for a well-behave model are discussed.

Following the ICC specifications is essential for a precise profile. One of these specifications is to save the device LUT inside a profile as relative colorimetric where the whitepoint information can be used to covert to absolute colorimetric.

For evaluating the accuracy of the selected fitting model and the constructed ICC profile, different evaluation processes were employed and some procedures were discussed in this chapter as well.

CHAPTER 4

EXPERIMENT 1: SCANNER

4.1. Introduction

In addition to their lower prices and their great benefit of converting an image into a digital form, color scanners have become an important part in many digital imaging environments and especially for pre-press systems. These systems include, beside the scanner, monitors, digital printers as proofer and plate making, where digital image data are exchanged across them. Therefore, for an accurate and consistent color appearance of this image across different media, the use of a *Color Management System* (CMS) becomes a must.

In the case of a scanner device, the characterization process involves generating a mapping or transformation function between its RGB colorant space and CIE LAB or CIE XYZ, the device-independent space. The overall characterization process is performed by scanning a target test chart that contains a set of color patches and mapped its RGB values with its equivalent LAB or XYZ values that were generated by measuring the same test chart using a color measurement device [1] (See **Figure 4-1**). This map or transformation is nonlinear due to non-colorimetric characterization of scanners. [2]

Generally, scanner characterization methods can be implemented either by an empirical approach such as polynomial regression method or by mathematical approach

by using a 3D Look Up Table (LUT), where again it's entries can be constructed from through either physical or empirical approaches [3]. The color characterization data will then be saved inside an ICC (International Color Consortium) input profile.

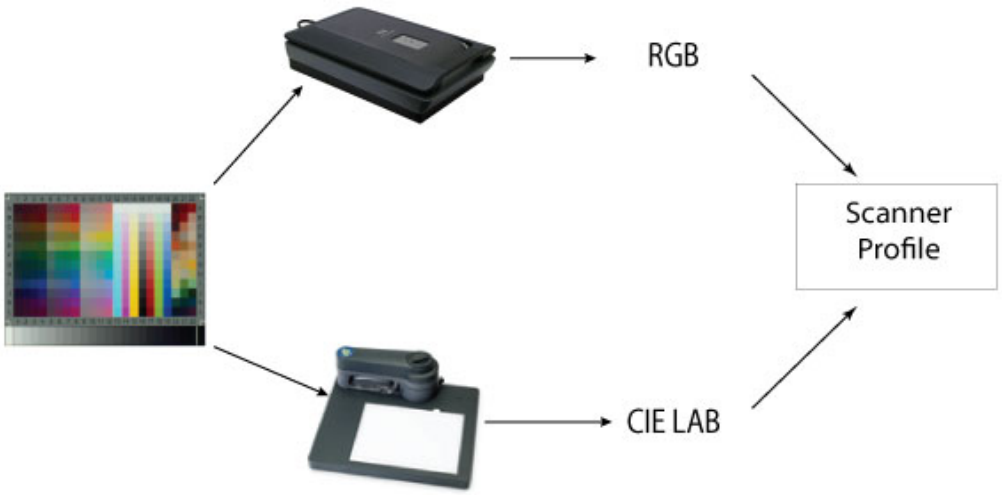

Figure 4-1: Scanner characterization general schema

Since scanners are non colorimetric, the existence of linear transformation matrix that can linearly transform RGB to XYZ or LAB would require a complex characterization method and might not be accurate. More discussions about the linearity of a scanner can be found in the Farrell and Wandell paper [4]. Therefore, scanners are accurately profiled using LUT-base profiles.

This experiment provides better understanding of the fundamentals behind the process of constructing scanner ICC profiles. In addition, we propose a plausible scanner characterization model, which minimizes the noise from measuring processes and produces a smooth transformation.

4.2. Experimental Design

For a scanner characterization process, a Kodak Q60 IT8.7/2-1933 test chart target is scanned by an HP ScanJet G4050 at 300 dpi and the image file was saved as a Tiff (or *Tagged Image File Format*) file. All automatic color correction features were disabled. The RGB values of the IT8 color patches where collected from the saved tiff image in Adobe Photoshop CS5. The same IT8 target was also measured using X-Rite i1iO scanning spectrophotometer and MeasureTool software to generate the XYZ values as our selected PCS. Using both the RGB values and the measured XYZ values, which are our training data, a mapping function between them was derived using Minitab 15. The Jacobian determinant was used to evaluate the rate of change in the developed transformation function.

Using our customized C++ profile, a 3D LUT with a 33 x 33 x 33 grid points was constructed using the coefficients of the mapping functions and saving it inside the AToBx tag as part of generating a scanner profile. The selected combination of A2Bx tag's elements is:

Another ICC profile was built using X-rite ProfileMaker 5.0 software using the scanned test target image and the measured XYZ values as a reference file. Chromix ColorThink 3.0 Pro software was used to visualize the gamut volume of the resulting ICC profiles.

4.3. Scanner Model

Different scanner characterization models were discussed in many papers [5-9]. The most common model was the polynomial regression method, which has proved its consistency.

For this experiment two different characterization models were used: the Least-squares fit model (LS), which represent the linear transformation and a polynomial fit model that represents the non-linear transformation.

The following is the generated linear LS mapping function between the RGB values and XYZ values of IT8 target using Minitab:

$$\mathbf{X} = \mathbf{0.54} + \mathbf{0.120R} + \mathbf{0.114G} + \mathbf{0.00147B} \qquad (\mathbf{3.1})$$

$$\mathbf{Y} = \mathbf{0.53} + \mathbf{0.0501R} + \mathbf{0.210G} - \mathbf{0.0207B} \qquad (\mathbf{3.2})$$

$$\mathbf{Z} = \mathbf{0.59} - \mathbf{0.0225R} + \mathbf{0.0177G} + \mathbf{0.198B} \qquad (\mathbf{3.3})$$

While the following is the generated second degree polynomial mapping function also using Minitab:

$$\mathbf{X = 0.54 + 0.0282R + 0.0049G - 0.0054B + 0.00013RG - 0.00005RB - 0.00018GB + 0.00041R^2 + 0.00048G^2 + 0.00028B^2} \qquad \mathbf{(3.4)}$$

$$\mathbf{Y = 0.53 + 0.0064R + 0.0302G - 0.0115B + 0.0001RG - 0.00006RB - 0.00012GB + 0.00023R^2 + 0.00076G^2\ 0.00018B^2} \qquad \mathbf{(3.5)}$$

$$\mathbf{Z = 0.59 - 0.0109R - 0.0106G + 0.0362B + 0.00008RG - 0.00007RB + 0.000043GB + 0.000033R^2 + 0.000098G^2 + 0.000749B^2} \quad \textbf{(3.6)}$$

The intercept values in the two models are actually the measured black point from the gray scale section in the IT8 test chart. This black point value was deducted from all XYZ values of the training data and a regression model was then conducted through Minitab to generate the coefficients of both the Linear LS and the polynomial models as presented in **equations** (**3.1-3.6)**. The reason of using that black point as an intercept value is to correct the black point mapping, which was due to either measurement noise or the device physical behavior.

Let *M* be the 3x3 matrix that holds the linear terms coefficients of the generated polynomial fit functions **(equations 3.4-3.6)** as follow:

$$\mathbf{M} = \begin{bmatrix} 0.0282 & 0.00494 & -0.00542 \\ 0.00641 & 0.0302 & -0.0115 \\ -0.0109 & -0.0106 & 0.0362 \end{bmatrix} \quad \textbf{(3.7)}$$

Although our matrix satisfies the diagonal dominant condition, for a scanner device the invertability condition is omitted, because it is not necessary and there are no B2Ax tags in an input profile that could hold the inverse transformation from PCS to RGB colorant space.

However, a well-behaved scanner transformation matrix should have a positive Jacobian determinant which reflects a sensible scanner response. In other words it should be invertible, even though it doesn't need to be for the profile. **Table (4-1)** displays the

calculated determinant and the RMSE (root mean square error) values for both fitting models (linear LS and polynomial). The calculated determinant value for the polynomial fit model represents the average determinant value of all LUT entries that are stored in the A2B tag of the constructed lcms profile. While the RMSE value represents the average RMSE error computed for each X, Y and Z transformation functions.

For both fitting models (linear LS and polynomial) the calculated determinant values were positive which indicates a well-behaved one-to-one RGB to XYZ transformation. Moreover, we can observe the higher RMSE value of the linear LS fit over the non-linear polynomial fit model which signifies the poor performance of the LS model.

Table 4-1: Calculated determinant and RMSE

	LS	**2nd degree Polynomial**
Jacobian determinant	0.0040	0.0054
RMSE	7.7227	0.9172

4.4. Simulation Results

Figure (4-2) demonstrates the xy-chromaticity plots for the two different input profile gamuts. Both profiles were constructed the same way using our profile editor the only difference is the characterization fitting model that is used to build the A2B LUTs. ICC profile (a) demonstrates the LS linear transformation model where ICC profile (b) demonstrates the polynomial model. In the LS fit profile a small part of its gamut volume is located outside the chromaticity diagram, which indicates the existents of non-visible

colors, where the polynomial regressing profile not only its boundaries are inside the chromaticity diagram but also has a smoother gamut volume shape. A clear demonstration of the out-of-gamut points in the LS model are shown in **Figure (4-3)**.

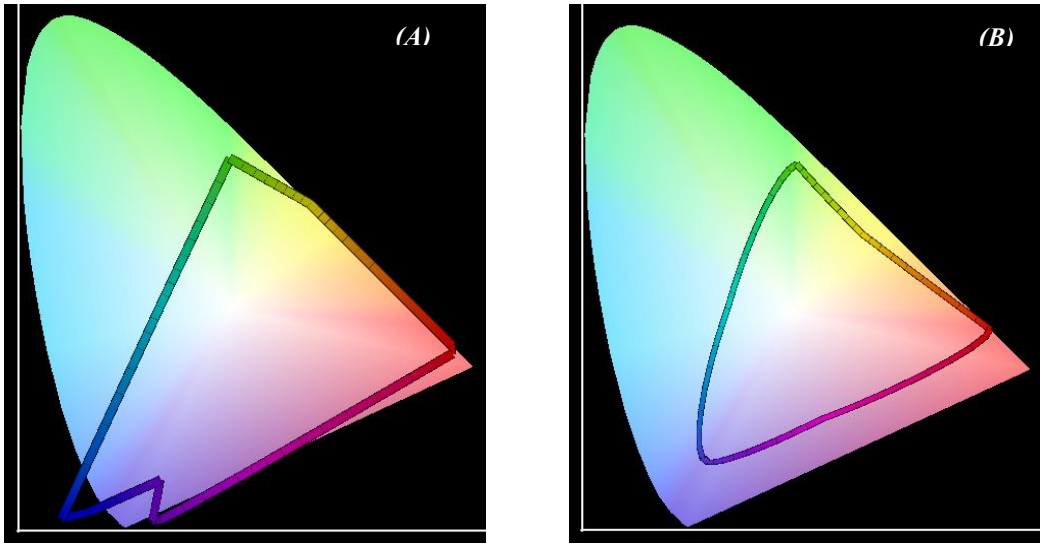

Figure 4-2: The xy-chromaticity plots of two lcms profiles: (A) the LS fit profile and (B) the polynomial fit profile

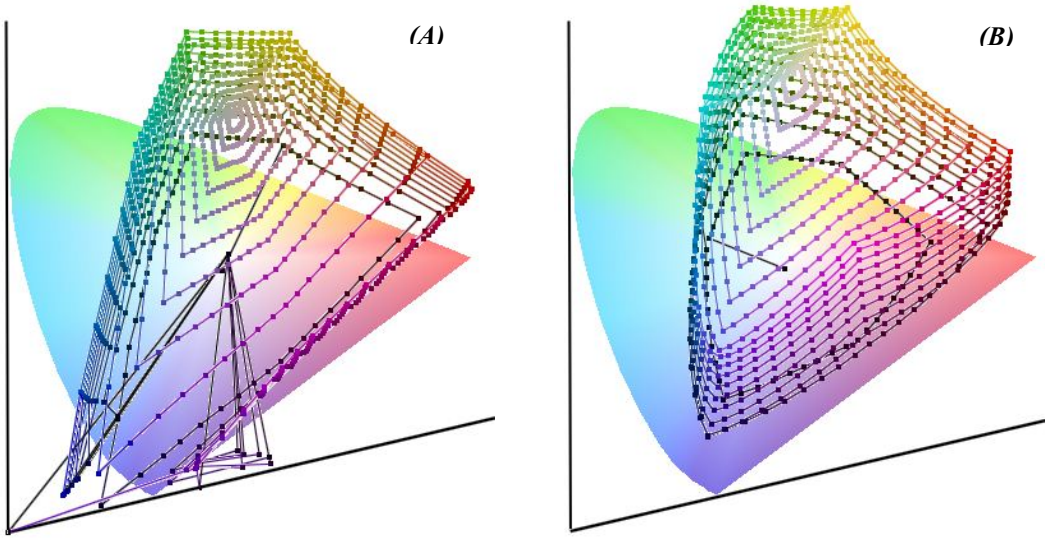

Figure 4-3: A 3D display of the gamut volume of two lcms profiles: (A) the LS fit profile and (B) the polynomial fit profile

Figure (4-4) demonstrates a comparison between our input profile (a) that was constructed by our profile editor and using a polynomial regression model (which will be denoted as *"Lcms Profile"* referring to the open source library that was used to build our profile editor) and an input profile that was constructed by X-rite ProfileMaker (b). Again our lcms profile has the smoothest gamut volume boundaries and has a smaller gamut volume amount as well.

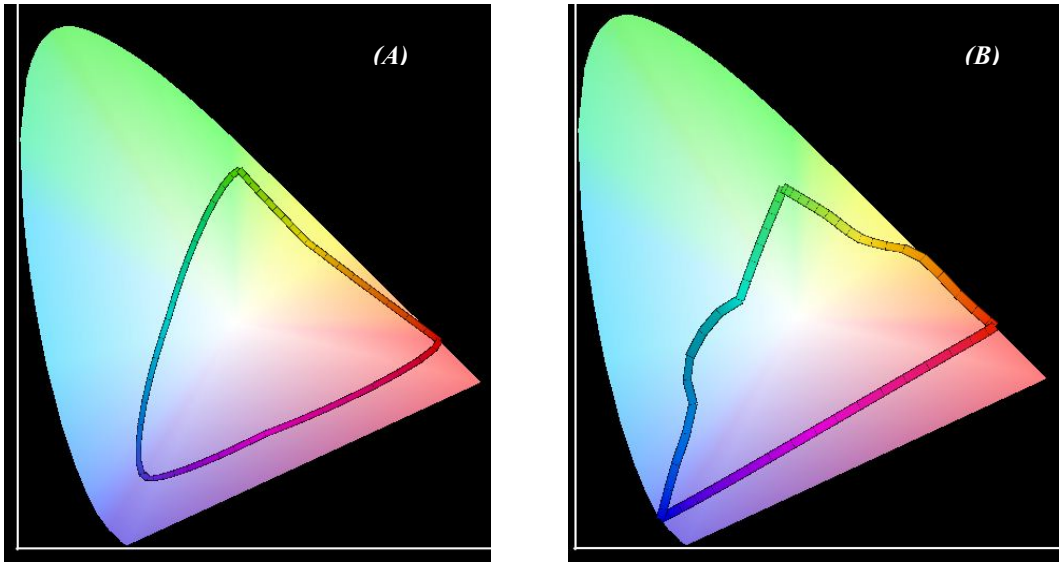

Figure 4-4: The gamut volume of lcms profile (A) and ProfileMaker profile (B)

Another way to compare between these two profiles is demonstrated in **Figure (4-5)**. This figure represents 3D plots of the profile's gamut volume showing every point inside the CLUT. There is an obvious conflict between the two profiles in terms of the noise points that are occurred in the ProfileMaker profile (b). Also, is seen the smooth gamut volume surface of the lcms profile (a) especially toward the edges.

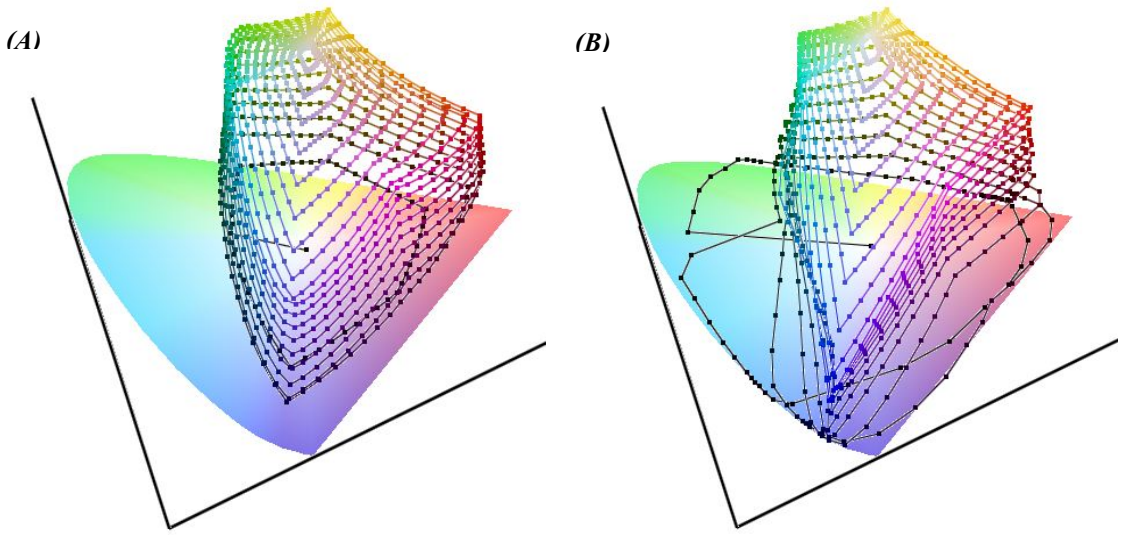

Figure 4-5: A 3D display of the gamut volume of lcms profile (A) and ProfileMaker profile (B)

Figure (4-6) and **(4-7)** shows the gray ramp and the RGB primaries ramp, respectively, of both our lcms profile and the ProfileMaker profile (More analyzing figures can be seen in the appendix). While ProfileMaker profiles shows some raggedness in both gray and primaries ramps our lcms profiles shows smoother curves.

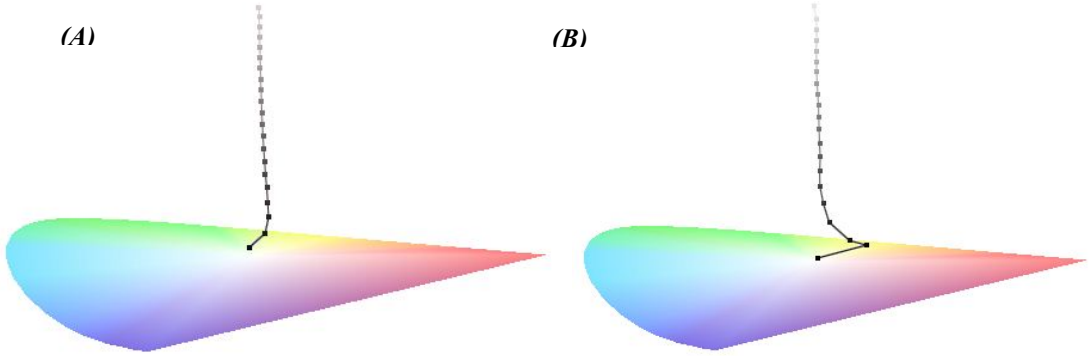

Figure 4-6: The gray ramps of lcms profile (A) and ProfileMaker profile (B)

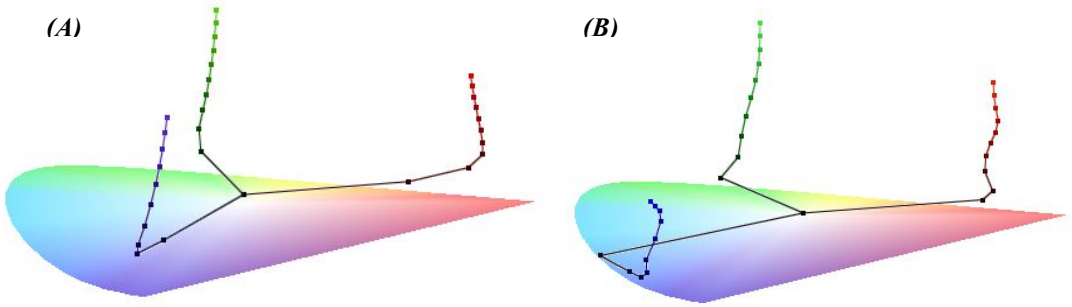

Figure 4-7: The primaries ramps of lcms profile (A) and ProfileMaker profile (B)

The next evaluation test was conducted using Adobe Photoshop CS5. **Figure (4-8)** represents the two lcms profiles with different empirical models (polynomial and linear LS fit) after applying them on IT8.7/2 test chart on Photoshop. Without taking any measurements the different between the two profiles is noticeable. The LS fit profile (b) has washed out colors over the polynomial fit (a). In contrast, when applying the ProfileMaker profile, the different between the polynomial fit lcms profile and the ProfileMaker was not significantly noticeable and therefore it was required to do some actual measurements to evaluate the difference.

Figure 4-8: IT8.7/2 test chart after applying different profiles in Photoshop, polynomial lcms profile (A) and LS lcms profile (B)

Table (4-2) represents the ΔE comparison between the measured LAB values for selected patches of the IT8.7/2 test chart after assigning both lcms profile and the ProfileMaker profile in Photoshop and their equivalent LAB values from the training data

Table 4-2: ΔE comparison between selected color patches of the training data and their equivalent values under different profiles

	ΔE (Profile Maker)	**ΔE (lcms Profile)**
Mean	4.10	3.42
Max	6.48	12.91
STD	1.64	3.52

As seen on the table, the average ΔE for both profiles is less than 5 showing a plausible behavior. Despite to the higher average ΔE value of the ProfileMaker, the lower value of the standard deviations gives another side of the story. Some color patches, especially in the shadow areas, under the lcms profile had recorded a higher ΔE where the maximum value is higher than 12 which explain the higher standard deviation value. However, other color patches had the opposed reaction and had recorded a really low ΔE values than 1 of compared to the same patches under ProfileMaker profile. Detailed data can be seen in (**Appendix A**)

4.5. Conclusion

We were able to show the enhanced performance of the Polynomial regression model over the linear regression model and whatever model that is used by ProfileMaker.

However, it's not the optimum one as numbers still show high ΔE in shadows and highly saturated colors.

4.6. Future Works

- Even if we don't actually use the inverse transformation in case of a scanner, but this doesn't mean that this information should not exist. Therefore, our future works here is to study and conduct an inverse transformation model based on an acceptable forward model.

- ΔE comparisons between our lcms profile and the training data shows some outlier values (Cyan and Yellow) which lead to more investigation to understand the cause of it. Keeping in mind that our polynomial fitting model is actually built to transform RGB to XYZ values and the measured LAB values are calculated from these XYZ. Thus, a study could be conduct here to evaluate the uniformity of ΔXYZ between the training data and the calculated and the uniformity of the equivalent LAB.

- What we didn't do in this experiment is overcome the non-uniformity of the scanning spots in the scanner, especially when we want to measure the native behavior of the device. To achieve that the test chart needs to be scanned at least 3 times and each time the position of the test chart should be changed and then by averaging the measured values we would at least guarantee that we cover that variance.

- Even though we know that we have switched off any color adjustments or corrections, there is still the issue of the scanner gamma that still appears in the scanner controlling options. This issue requires more investigations to see its effects on the accuracy of the built ICC profile.

CHAPTER 5

EXPERIMENT 2: MONITOR

5.1. Introduction

CRT (Cathode Ray Tube) and LCD (Liquid Crystal Display) are two widespread types of display technologies. E-papers (Electronic Papers), LED (Light-Emitting Diode display) and OLED (Organic Light-Emitting Diode display) are some new developments of display technologies. LCDs have more advantages than CRT in terms of stability, brightness and sharpness, besides their high resolution, which make them more acceptable as display devices [26].

Generally, display devices are used not only for displaying purposes, but also they are playing an important role at different digital applications from graphic design to prepress Soft Proofing[61-62], where a client can preview the final product on the screen before the actual printing. Therefore, monitors are required to have good color reproduction, which reflects an accurate device characterization.

Figure (5-1) demonstrates the overall process of characterizing an LCD monitor. Generally, there are two test charts that are available for the characterization process: CRT and LCD test charts. Each chart consists of a set number of color patches that covers the monitor gamut. A measuring device is usually employed to measure each color patch while it's flashed on the monitor. The measurement data consist of the RGB / LAB

or XYZ pairs for each color patch. Profiling software will then use these data to form both a forward (RGB to XYZ/LAB) and inverse (XYZ/LAB to RGB) color transformation model and store it in a suitable monitor profile. [63]

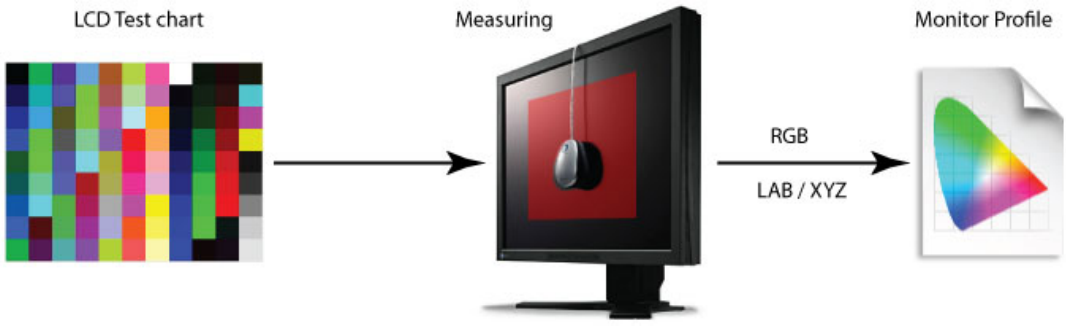

Figure 5-1: Monitor characterization overall schema

The purpose of this experiment is to provide a plausible universal characterization model that can be use to describe different LCD monitors and minimize any measurement noise. This experiment also gives a better understanding of the fundamentals behind constructing a monitor ICC profile.

5.2. Experimental Design

A dual quad tower Mac Pro with two LCD monitors was used to assist this experiment with the following specifications:

Table 5-1 Configuration of computer system for monitor profiles.

Monitors	24" Apple Cinema Display, 1920x1200, LED backlight 20" Acer, 1680x1050, Fluorescent backlight
Video Card	ATI Radeon HD 4870
Operating systems	MacOS 10.6 and Windows 7

It was important to study the physical properties of our monitors before constructing any specified display profile and thus different native profiles were used for this purpose. This study was divided into two phases: (1) evaluating the physical behavior of the monitors, (2) determining the system gamma value. X-Rite ProfileMaker Pro 5.0.9 and Monaco PROFILER 4.8.3 software were used to construct all native profiles, with the assistance of an Eye-One Pro spectrophotometer as a measuring instrument. These applications offer an LCD test chart that contains around 98 different color patches that cover the color gamut of a monitor.

Based on the generated gamma value from phase 2, diverse display profile types (Matrix and LUT-based) were constructed using our profile editor (these will be denoted as lcms profiles). Two different device models were used to characterize our monitors the linear Least-square model and the nonlinear 2^{nd} degree polynomial model which was generated using Minitab for the RGB to XYZ transformation. Based on these models, a 3D LUT with 33 gird points was assembled and stored inside the AToB Tags as a part of generating a LUT-based display profile. A similar combination of the AToB tag elements that was used with scanner device in Chapter 4 is also used with the monitor profile.

In addition, other LUT-based profiles were built for each monitor (ACER and Apple) using new profiling software called “X-rite i1 Profiler” and we used that for comparison purpose.

5.3. Phase #1: Monitors Physical Behaviors Evaluation

5.3.1. Experimental Design

A set of native white point ICC profiles were constructed for each display using the two profiling software. The constructed profiles represent the two ICC profile models i.e. matrix and LUT-based profiles. All the profiles had the same gamma setting (a 1.8 gamma value). The profiles were then selected as the system monitor profile for each display. The main goal of using native profiles was to evaluate the real behavior of the display without any color corrections.

Each evaluated display has a different backlight (LED and Fluorescent backlights) and therefore, warm-up and brightness tests were applied to evaluate both displays. For the warm-up test, a uniform square white (255,255,255) and a gray (100,100,100) patch were constructed in Adobe Photoshop CS5 software and displayed alternatively every two minutes (see **Figure 5-2**). The patche tristimulus values were measured by an Eye-One Pro Spectrophotometer in the intermediate of each period starting from a cold powered up to a total of 2 hours. For the brightness test, the same white patch was displayed on each monitor. Both displays were set to different brightness levels and the tristimulus value of the white patch was measured at each brightness level. The steps of these tests resemble steps to a previous experience in Fairchild and Wyble [64] with an Apple flat LCD display.

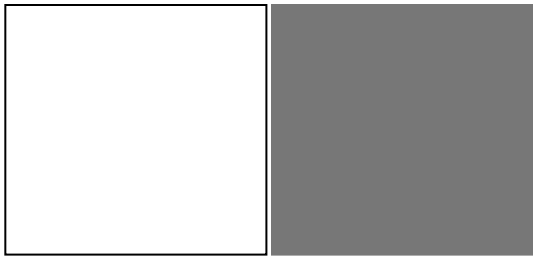

Figure 5-2: White and gray patches for monitor physical evaluation test

5.3.2. Results and Discussion

Usually, an ICC profile does not have a significant effect on the physical properties of a monitor. However, the information that is stored inside the ICC profile would change the contrast of the video card while the brightness levels or the color temperature should not be affected by a selected profile.

Figures (5-3) illustrates the tristimulus values of the displayed white patch under different brightness levels for both tested displays (Acer and Apple cinema) when an equivalent native LUT-base profile were applied for each monitor. As expected, the XYZ values of the white patch that was displayed on the Apple cinema display decreased with the decreasing of the display's brightness levels. The fluorescent backlight has a different behavior where the XYZ values of the white patch remain stable and then start decreasing when the brightness level reaches 60%. In addition, despite that the brightness level was "0%", the measured XYZ values of the white patch at that level were higher than those for the Apple cinema display and weren't even close to 0!. This observation may result from the Apple Monitor adjustment being done in software, via the video controller of course, while the Acer has an on board monitor adjustment. More figures and results using other native profiles can be seen in **Appendix B**.

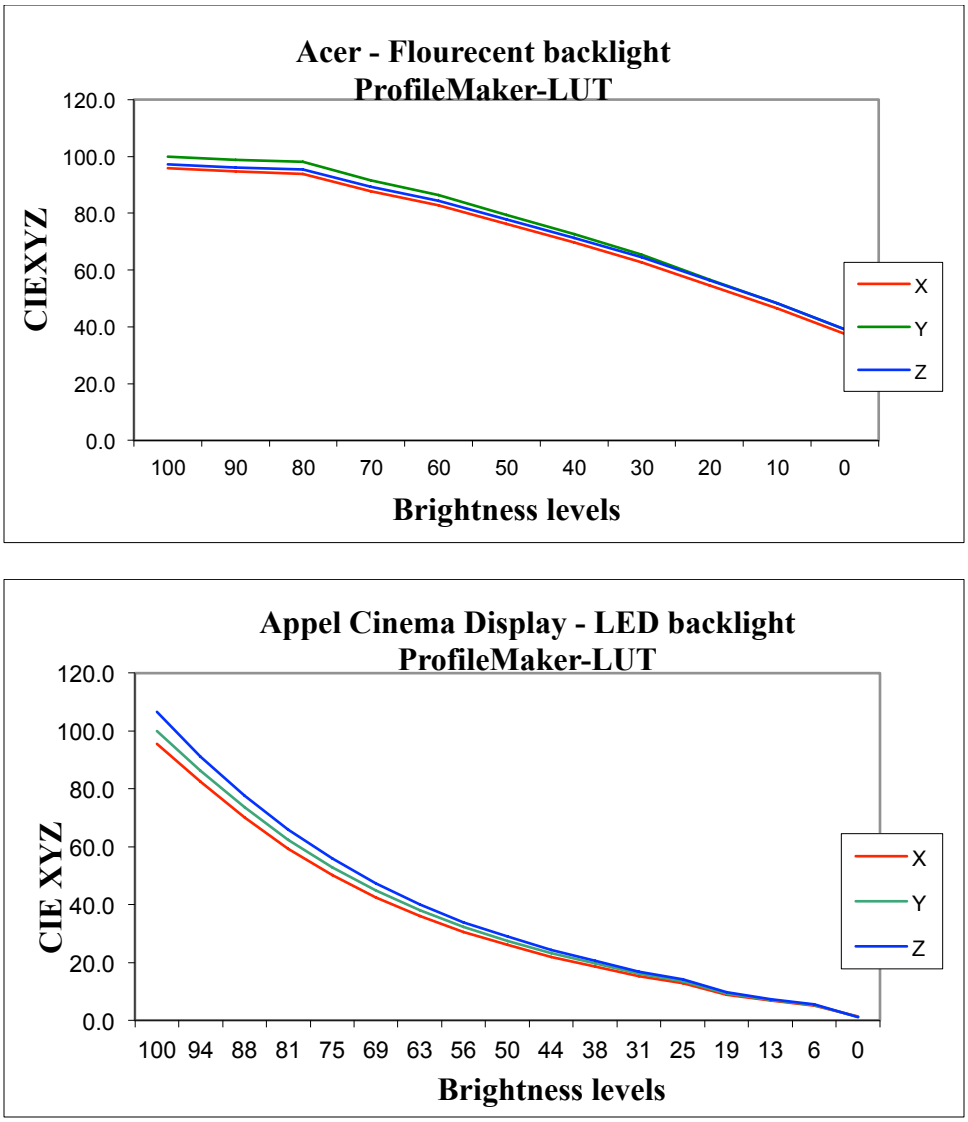

Figure 5-3: Brightness test results for Acer and LED monitors using an equivalent Lut-based profile that was build using ProfileMaker software

Figures (5-4 and 5-5) show the tristimulus values of both displayed white and gray patches over the 2-hour warm-up test for Acer and Apple Cinema display, where the applied profiles were the matrix-based profiles that were constructed by MonacoProfiler software.

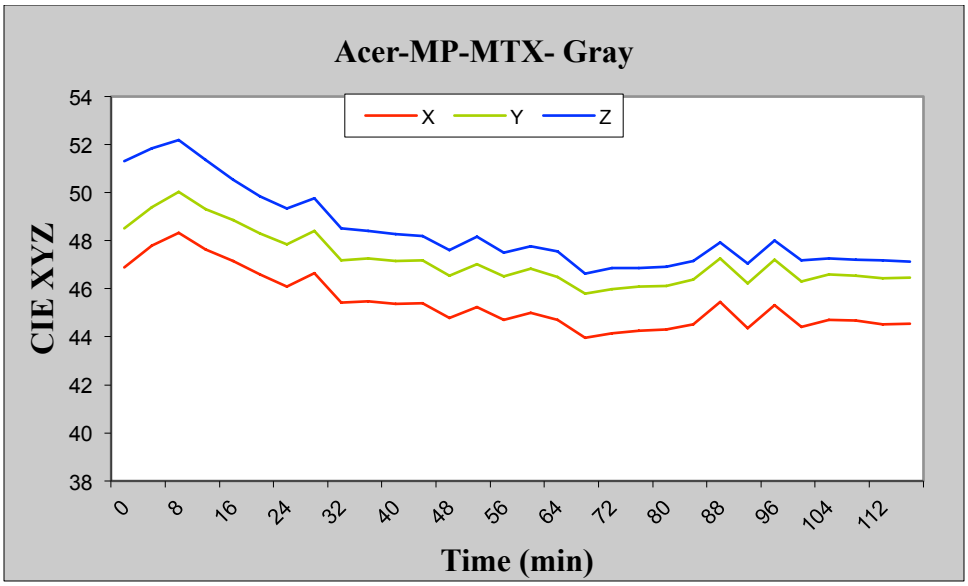

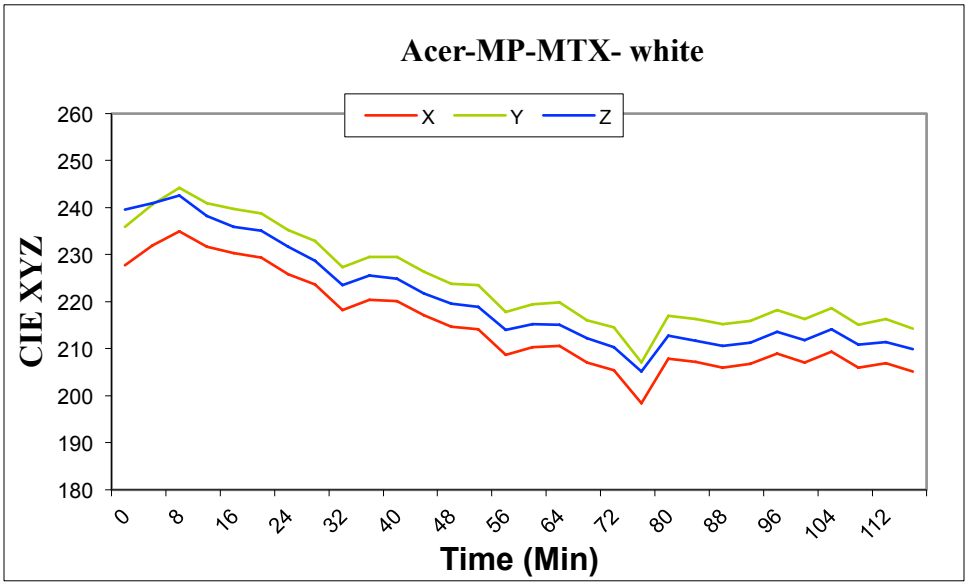

Figure 5-4: Warm-up test using gray patch (up) and white patch (down) for Acer display

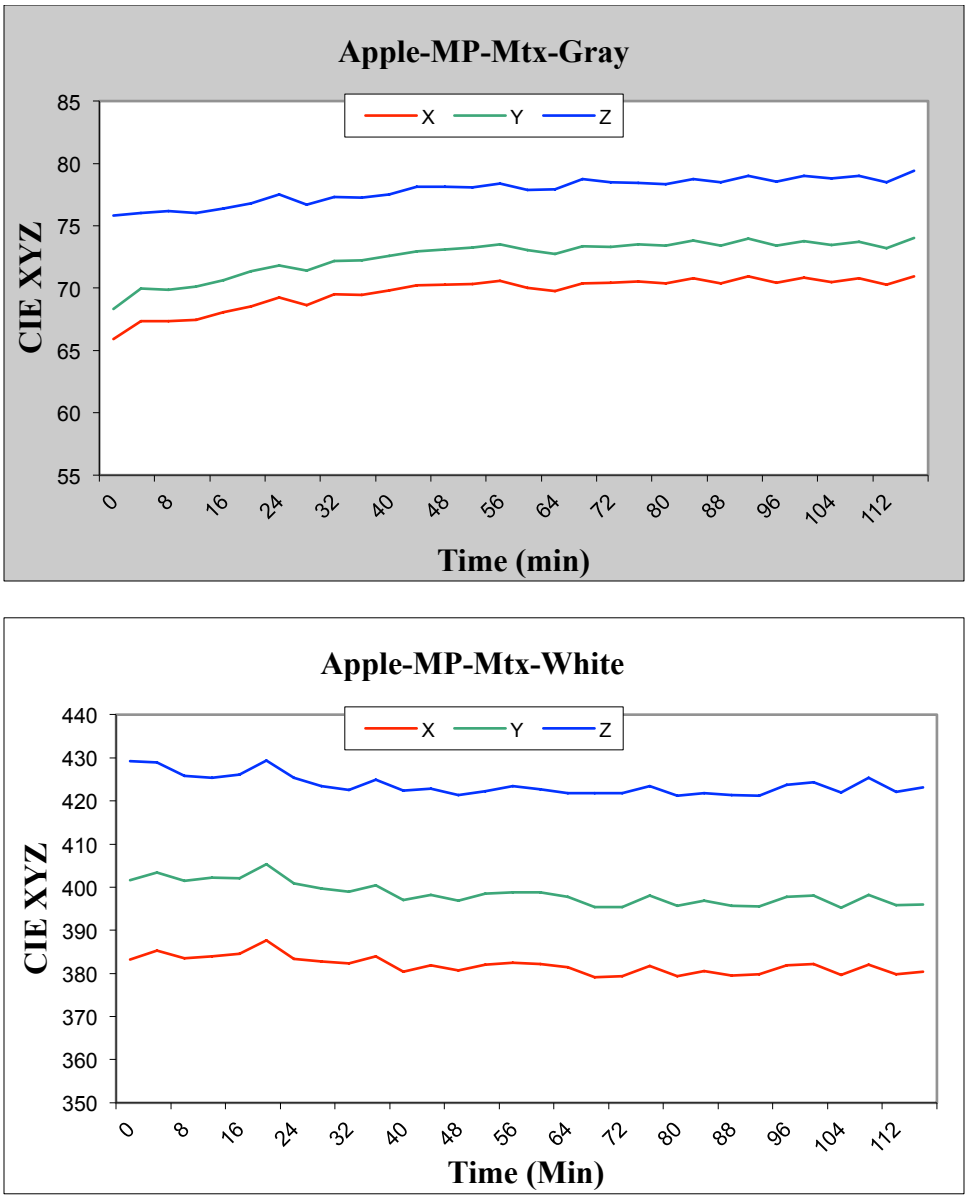

Figure 5-5: Warm-up test using gray patch (up) and white patch (down) for Apple cinema display

Overall, the measured XYZ for both gray and white patches on the Apple cinema display record higher values than those measured on the Acer display. For the LED backlight monitor, the output levels of the white patch were mostly stable for the whole 2-hour test period and the same results were obtained for the gray patch under all tested profiles (matrix-based and LUT-based). On the other hand, in the case of the fluorescent backlight monitor, the output levels for the white patch decreased with the passage of the

2-hour time test, where the output levels for the gray patch under profiles that were constructed by ProfileMaker software had a different behavior than those that were constructed by MonacoProfiler. There, the measured XYZ values for gray level under profiles constructed by MonacoProfiler were more correlated to each other than those constructed by ProfileMaker, where the Z values were significant higher.

Next, the average value of the Correlated Color Temperature (CCT) was calculated for the white and gray patches of the whole warm-up test interval for each display, using the measured XYZ values of both patches. **Figure (5-6)** shows the CCT of the displayed white and gray patches on both Acer monitor and Apple LED monitor under different native profiles.

For an accurate gray level display, the CCT of the white and the gray patches need to be near to each other. This is not the case for either display. These results might be due the lack of equal gamma in the RGB channels, where equal RGB values should produce a natural gray level.

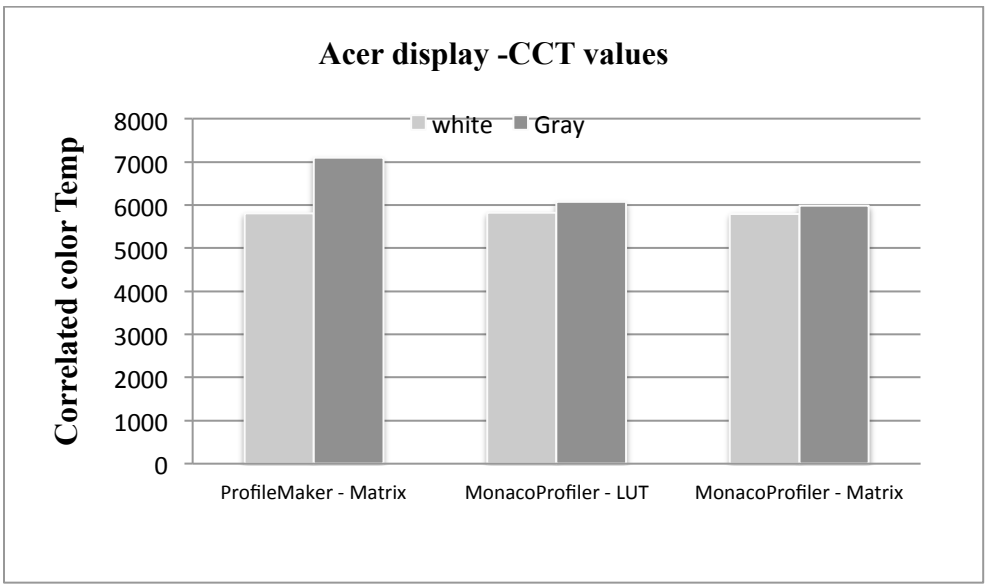

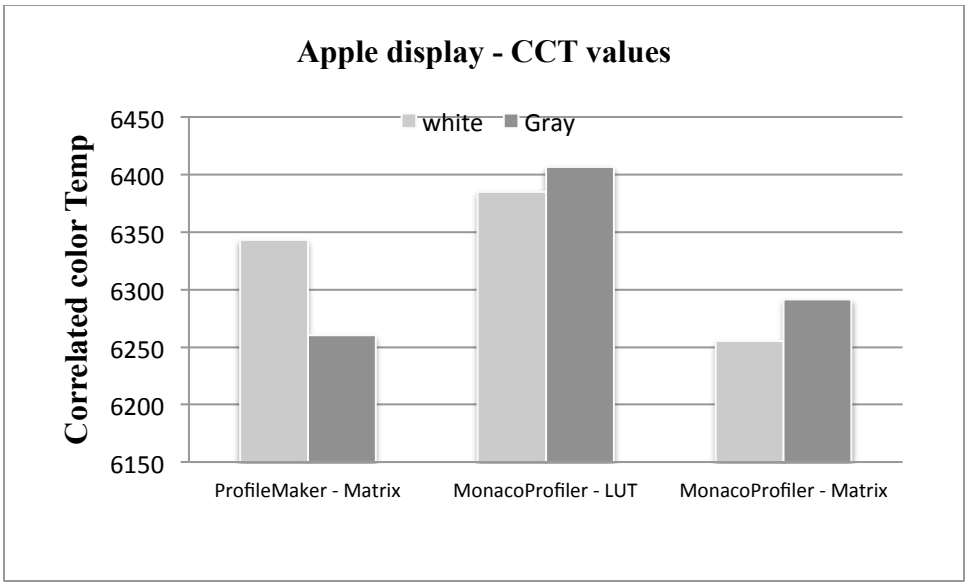

Figure 5-6: The CCT (in Kelvin) of the displayed white and gray patches on both Acer (up) and Apple display (down) monitors under different native profiles

Since both monitors use the same video card it would be expected that the CCT of a displayed white patch would not be affected by the selecting operating system or by the displayed application. Therefore, the XYZ values of a white patch were measured three different ways: the patch was displayed in Adobe Photoshop and measured through MeasureTool, using the "Spot" option with the assistance of an Eye-one Pro. In addition, a text reference file was constructed that had only the RGB value of the white point (255, 255, 255) and stored inside the MeasureTool and the white patch was again measured through the MeasureTool but using the "Chart" option. This option will assure that the display will use its native behavior and will display the white patch in front of a black background. Also under the Windows platform, an empty folder was open which has a white background and the equivalent XYZ values were measured again through the MeasureTool and the "Spot" option. While in Mac platform a white patch was displayed

in the Preview software. The chromaticity values were calculated for each application and across platforms using the following equation:

$$x = \frac{X}{X+Y+Z} \qquad y = \frac{X}{X+Y+Z} \tag{5.1}$$

Based on the average values of the calculated chromaticity, the CCT values were computed across platforms for each monitor and are presented in **Figure (5-7).**

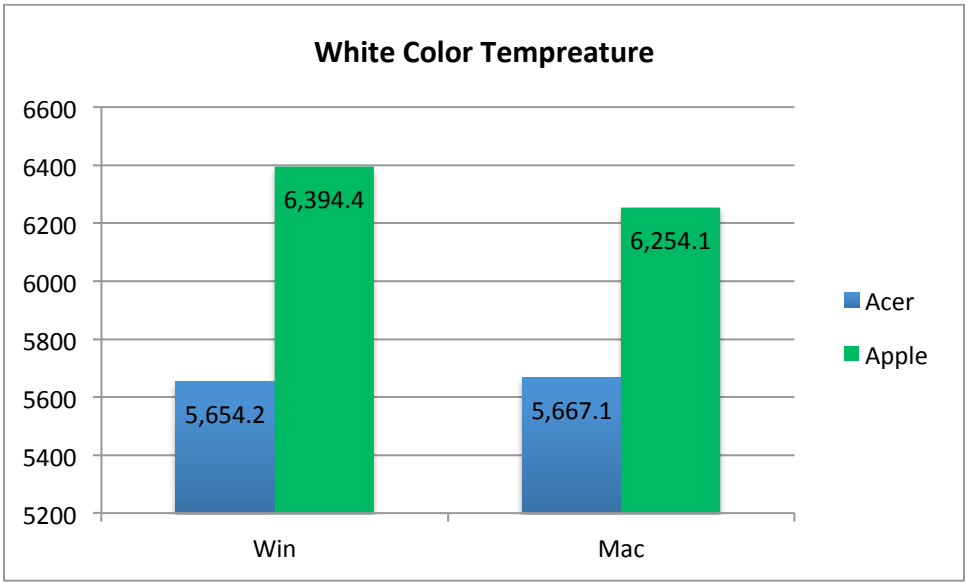

Figure 5-7: The average CCT (in Kelvin) for a white background across different applications and platforms on both Acer and Apple display

It was surprising to discover that the incidence of a very small variation in the calculated chromaticity within different platforms result in clear differences in the calculated CCT for the Apple monitor across platform as opposed to the Acer monitor. The difference between the chromaticity values within applications and across platforms for the Apple monitor occurred at the third digit after the decimal point, i.e. in Windows the x chromaticity from Photoshop was 0.31212 and for the folder background was

0.31552, while for Acer the difference occurred at the fourth digit after the decimal point. This slight change in Apple display chromaticity values had its effect on the calculated CCT. (See **Appendix B** for detailed measurements)

5.4. Phase #2: Finding the Native Gamma

5.4.1. Experimental Design

Phase two starts with controlling the video card gamma of the two displays through the Video Card Gamma Tag (vcgt), which is part of the monitor ICC profile structure. The actual task that is performed by this tag is to adjust the contrast (or the gamma) of the display by adjusting the contents of the video card look-up table [65].

New native white point profiles were constructed, but with a gamma value of 1. The vcgt tag data were read from the constructed profiles using our profile editor. The contents of the vcgt tag were constructed as RGB channels. Linear regression, in Minitab 15, was then used to find the slope between each range and the respective vcgt channel value. The inverse value of the graph slope represents the actual displayed gamma for each RGB channel. The average gamma value of the RGB channels will be considered as the native gamma of that certain display.

5.4.2. Results and Discussion

Recalling the fact that the matrix-based profiles are a special case of LUT-based profiles, as their structures are less complex, it is easier to control the tags in the matrix-based profiles to avoid any noise or error that could be caused from measuring

procedures [66] Thus, phase 2 was conducted using Matrix-based monitor profiles. Moreover, ProfileMaker was the only profiling software that was used to construct the new set of the monitor profiles using a gamma value of 1 due to lack of ability to set the same gamma value in Monaco Profiler software. **Figure (5-8)** illustrates one example of fit gamma graph to red channel obtained in Minitab software using a matrix-based profile for the Acer display. The axes of the graph represent the log red channel values from the vcgt tag against the log range values.

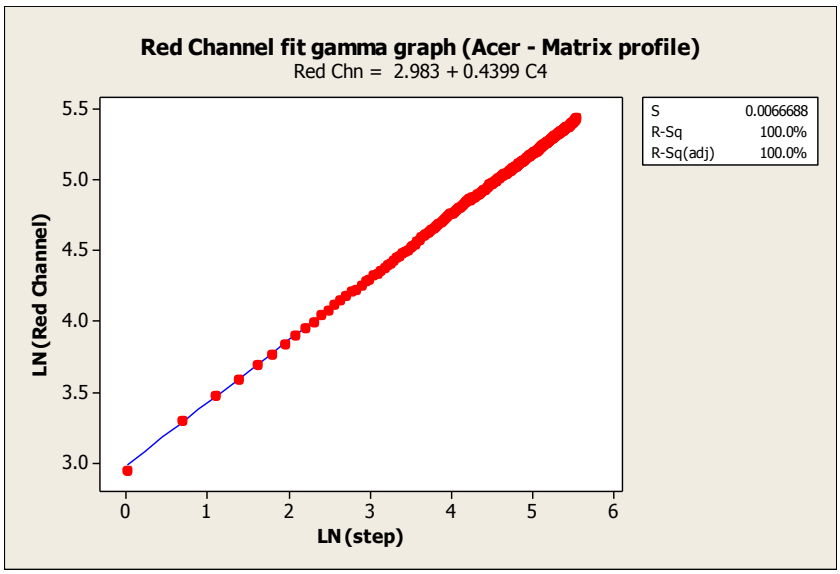

Figure 5-8: Fit gamma graph of red vcgt channel in Acer display matrix-based profile

The inverse value of the graph slope represents the actual displayed gamma and in our experiment it would be considered as the native gamma of the display. The calculated gamma value for Acer was close to 2.2, while for the Apple display was closer to 2.1. For accurate behavior of a monitor profile with proper gamma setting, the effective vcgt gamma value should be 1. Thus, the vcgt contents of the matrix-based profiles set for both display that had the new native gamma were read again using the C++ program code

and were plotted in Minitab. The resulting values of the affective vcgt gamma value for both displays were 1, which indicates an accurate behavior of the new set of matrix-based profiles.

5.5. Monitor Model

Using the gamma values from phase 2 for each Acer and Apple displays LUT-based native whitepoint profiles were constructed again on different platforms (Mac and Windows) using ProfileMaker 5.0.9 software and their measurement data were saved. Then by using X-rite MeasureTool software, a general reference file for the Acer monitor was constructed by averaging the equivalent measurement data between Mac and Windows platforms. For the Apple display, due to the previous results of the CCT variation across applications and platform as stated in section 5.3, both measurement data for Mac and Windows were normalized to Y=100 and then averaged in Microsoft Excel to generate a general reference file for the Apple display. These general reference files will be our training data for each monitor.

For this experiment, the same fitting models that were used with the scanner in chapter 4 were again used with the monitor. The two fitting models are the Least-square (LS) linear model and the 2nd degree polynomial model for nonlinear transformation.

For monitor devices, the general form of a forward linear transformation from RGB to XYZ is:

$$\begin{bmatrix} X' \\ Y' \\ Z' \end{bmatrix} = \begin{bmatrix} X_{R,max} & X_{G,max} & X_{B,max} \\ Y_{R,max} & Y_{G,max} & Y_{B,max} \\ Z_{R,max} & Z_{G,max} & Z_{B,max} \end{bmatrix} \begin{bmatrix} (R/255)^{\gamma} \\ (G/255)^{\gamma} \\ (B/255)^{\gamma} \end{bmatrix} \quad \textbf{(5.2)}$$

where γ is the display "gamma" value. The entries of the local transformation matrix would be obtained from the measured RGB primaries from the training data.

Based on the general form of **(5.2)**, the input values (RGB color values) should be normalized by dividing them by the maximum color intensity, which is 255. This indicates that the output values from this matrix are normalized too. To obtain that, XYZ values of training data should be divided by the Y value of the whitepoint to give $X', Y'$and Z'. As stated previously, the Apple display's training data were already normalized before the averaging between Mac and Windows measurements, while for Acer display the average training data were not normalized, and therefore the normalization process is required before testing any model.

In addition, and based on the resulted values in phase 2, the gamma values for Acer and Apple monitors are 2.2 and 2.1 respectively, which indicates that the color transformation wouldn't be linear, unless the input values were raised to the gamma power. Below are the generated LS fitting models for the Acer monitor:

$$\mathbf{X' = 0.19 + 48.40\,R' + 30.80\,G' + 13.20\,B'} \qquad \textbf{(5.3)}$$

$$\mathbf{Y' = 0.19 + 27.40\,R' + 64.00\,G' + 8.54\,B'} \qquad \textbf{(5.4)}$$

$$\mathbf{Z' = 0.19 + 0.45\,R' + 8.93\,G' + 69.90\,B'} \qquad \textbf{(5.5)}$$

where R', G' and B' are the linearized RGB input values. The LS fitting model for Apple cinema (or LED monitor) will be:

$$\mathbf{X' = 0.10 + 41.68\,R' + 36.01\,G' + 17.85\,B'} \quad \textbf{(5.6)}$$

$$\mathbf{Y' = 0.11 + 21.01\,R' + 72.21\,G' + 7.01\,B'} \quad \textbf{(5.7)}$$

$$\mathbf{Z' = 0.18 + 0.66\,R' + 9.49\,G' + 97.30\,B'} \quad \textbf{(5.8)}$$

The intercept values again represent the measured black point, which is also denoting as the black-level flare. The intention is to use the intercept value from the Minitab software but these values were negative and therefore the measured black point was use. The occurrence of this value was due to the physical properties of the monitor backlight [67]. The effect of this flare was discussed in many researches [64,67,68], where the common intention was to remove it from the measurement data before generating any models, which was the same intention in this experiment. However and as previously discussed in chapter 3, we re-plug the black-level flare back to our model to maintain the captured native behavior of our characterized device.

Equations (5.6-5.8) were used to construct the Matrix-based profiles and a linear LS LUT-based profile for each monitor using our profile editors. In addition, the linear RGB and XYZ values from the training data were used with Minitab to build the forward regression nonlinear polynomial model for each monitor. The following functions demonstrate the Acer forward model:

$$X' = 0.19 + 47.0\,R' + 30.5\,G' + 11.9\,B' + 0.8\,R'G' + 0.8\,R'B' + 0.4\,G'B' + 1.1\,R'^2 + 0.17\,G'^2 + 1.27\,B'^2 \quad (5.9)$$

$$Y' = 0.19 + 26.9\,R' + 64.1\,G' + 6.08\,B' + 0.734\,R'G' + 0.582\,R'B' + 0.461\,G'B' + 0.30\,R'^2 - 0.282\,G'^2 + 2.42\,B'^2 \quad (5.10)$$

$$Z' = 0.19 + 1.2\,R' + 10.9\,G' + 62.4\,B' + 0.3\,R'G' + 0.52\,R'B' + 1.03\,G'B' - 0.7\,R'^2 - 2.13\,G'^2 + 7.58\,B'^2 \quad (5.11)$$

and the followings are for Apple cinema display:

$$X' = 0.10 + 42.1\,R' + 35.7\,G' + 17.7\,B' - 0.135\,R'G' - 0.081\,R'B' - 0.049\,G'B' - 0.426\,R'^2 + 0.328\,G'^2 + 0.255\,B'^2 \quad (5.12)$$

$$Y' = 0.11 + 21.3\,R' + 72.4\,G' + 6.8\,B' - 0.2\,R'G' + 0.002\,R'B' - 0.08\,G'B' - 0.2\,R'^2 - 0.367\,G'^2 + 0.365\,B'^2 \quad (5.13)$$

$$Z' = 0.18 + 1.09\,R' + 10.1\,G' + 95.3\,B' + 0.0\,R'G' - 0.157\,R'B' - 0.140\,G'B' - 0.148\,R'^2 - 0.469\,G'^2 - 1.55\,B'^2 \quad (5.14)$$

All these models were used to construct the non-Linear LUT-based profiles using our profile editor for each monitor.

Since there were two different algorithms that were used to construct our training data for each monitor (i.e. using manual averaging and MeasureTool averaging) it is important to evaluate the performance of the constructed models based on these data for each display comparing with what actually displays. This was achieved by employing color difference tests between predicted and measured sets of RGB primaries along with

white color patches (see **Figure 5-9**) in CIELAB space. The predicted data correspond to the LUT entries inside the A2B tag of each constructed profile that represents each fitting model. In addition, keeping the fact that Measure tool, and because it uses a measuring device, actually measures what it is really displaying under the native device illuminant, therefore, the measurement data were compared with the native LUT data (i.e. before they are chromatically adapted to D50).

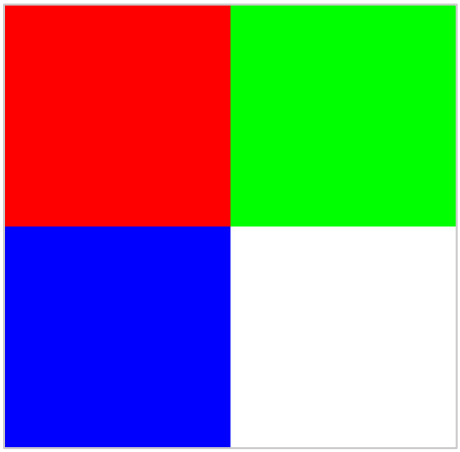

Figure 5-9: RGB and white patches

Figure (5-10) demonstrate the average ΔE of each fitting model and for each display. The higher ΔE that was recorded for Acer display among the fitting models confirms that the training data that were used to construct both models were not accurate compared with the Apple display values. (See **Appendix B** for detailed data)

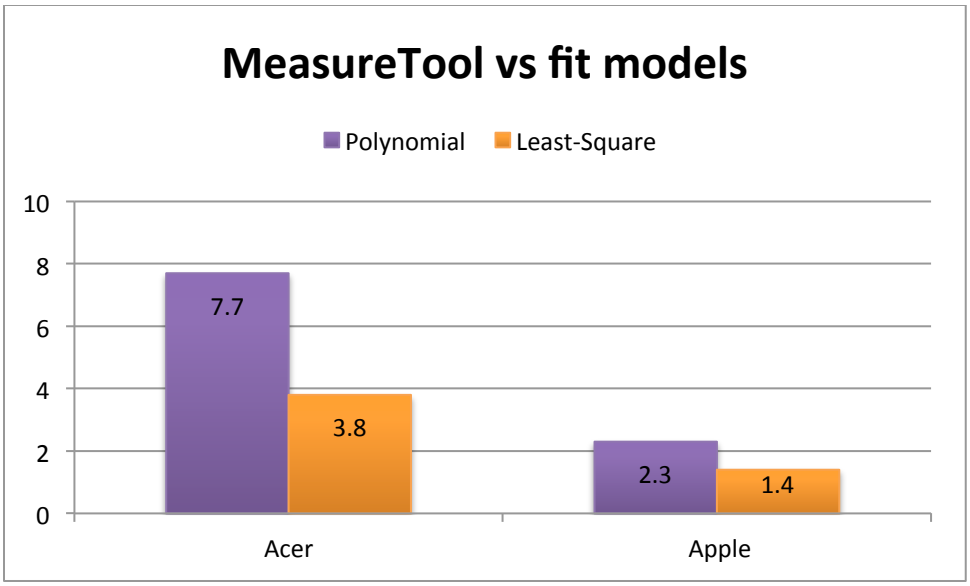

Figure 5-10: Average ΔE values for different fitting models compared with MeasureTool values for each display

Although both ProfileMaker and MeasureTool measure the same LCD test chart, ProfileMaker records the measured data in terms of spectral values (see **Figure 5-11-A**) which leads us to use MeasureTool to average the training data and export them to LAB values so we can read the equivalent XYZ and LAB values for each color patch. On the other hand, in MeasureTool software a user has the option of using the spectral data or not and thus we have selected it to not. Therefore, the measured data were automatically recorded as LAB values (see **Figure 5-11-B**).

(A)

File Edit Format View Help

```
LGOROWLENGTH    9
CREATED "8/13/2011"  # Time: 11:09
INSTRUMENTATION "Unknown"
MEASUREMENT_SOURCE      "Illumination=Unknown   ObserverAngle=Unknown   WhiteBase=Abs   Filter=Unknown"
ILLUMINATION_NAME       "Emission"
OBSERVER_ANGLE  "2"
KEYWORD "SampleID"
KEYWORD "SAMPLE_NAME"
NUMBER_OF_FIELDS        41
BEGIN_DATA_FORMAT
SampleID        SAMPLE_NAME     RGB_R   RGB_G   RGB_B   nm380   nm390   nm400   nm410   nm420   nm430
nm440   nm450   nm460   nm470   nm480   nm490   nm500   nm510   nm520   nm530   nm540   nm550   nm560
nm570   nm580   nm590   nm600   nm610   nm620   nm630   nm640   nm650   nm660   nm670   nm680   nm690
nm700   nm710   nm720   nm730
END_DATA_FORMAT
NUMBER_OF_SETS  99
BEGIN_DATA
1       A1      0.00    0.00    0.00    0.0019  0.0011  0.0016  0.0018  0.0021  0.0058  0.0097  0.0077
0.0057  0.0067  0.0092  0.0139  0.0074  0.0037  0.0027  0.0019  0.0090  0.0122  0.0030  0.0020  0.0061
0.0097  0.0062  0.0097  0.0107  0.0033  0.0046  0.0023  0.0019  0.0028  0.0019  0.0037  0.0051  0.0089
0.0107  0.0067
2       A2      0.00    0.00    85.00   0.0020  0.0016  0.0021  0.0097  0.0382  0.1424  0.2475  0.2202
0.2018  0.1604  0.1422  0.1650  0.0777  0.0209  0.0085  0.0054  0.0226  0.0242  0.0042  0.0035  0.0077
```

(B)

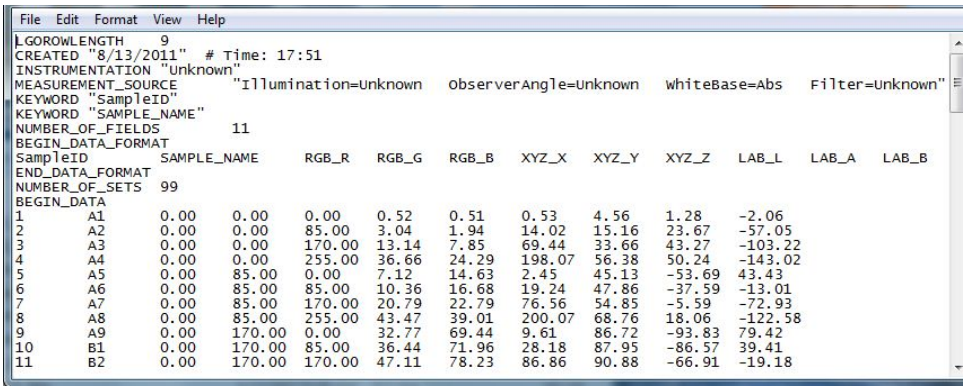

File Edit Format View Help

```
LGOROWLENGTH    9
CREATED "8/13/2011"  # Time: 17:51
INSTRUMENTATION "Unknown"
MEASUREMENT_SOURCE      "Illumination=Unknown   ObserverAngle=Unknown   WhiteBase=Abs   Filter=Unknown"
KEYWORD "SampleID"
KEYWORD "SAMPLE_NAME"
NUMBER_OF_FIELDS        11
BEGIN_DATA_FORMAT
SampleID        SAMPLE_NAME     RGB_R   RGB_G   RGB_B   XYZ_X   XYZ_Y   XYZ_Z   LAB_L   LAB_A   LAB_B
END_DATA_FORMAT
NUMBER_OF_SETS  99
BEGIN_DATA
1       A1      0.00    0.00    0.00    0.52    0.51    0.53    4.56    1.28    -2.06
2       A2      0.00    0.00    85.00   3.04    1.94    14.02   15.16   23.67   -57.05
3       A3      0.00    0.00    170.00  13.14   7.85    69.44   33.66   43.27   -103.22
4       A4      0.00    0.00    255.00  36.66   24.29   198.07  56.38   50.24   -143.02
5       A5      0.00    85.00   0.00    7.12    14.63   2.45    45.13   -53.69  43.43
6       A6      0.00    85.00   85.00   10.36   16.68   19.24   47.86   -37.59  -13.01
7       A7      0.00    85.00   170.00  20.79   22.79   76.56   54.85   -5.59   -72.93
8       A8      0.00    85.00   255.00  43.47   39.01   200.07  68.76   18.06   -122.58
9       A9      0.00    170.00  0.00    32.77   69.44   9.61    86.72   -93.83  79.42
10      B1      0.00    170.00  85.00   36.44   71.96   28.18   87.95   -86.57  39.41
11      B2      0.00    170.00  170.00  47.11   78.23   86.86   90.88   -66.91  -19.18
```

Figure 5-11: Measurement data of the same LCD test chart in spectral mode (A) and in LAB model (B)

Moreover, averaging the normalized data or un-normalized data has its influence on the calculated ΔE. Therefore, the algorithm that was used with setting the training data for Apple display was also used for Acer display and thus the following represent both the Least-squares and the polynomial fit models based on the new training data:

$$X' = 0.11 + 49.00\,R' + 29.85\,G' + 15.71\,B' \qquad (5.16)$$

$$Y' = 0.11 + 27.15\,R' + 63.34\,G' + 9.22\,B' \qquad (5.17)$$

$$Z' = 0.16 + 0.43\,R' + 8.14\,G' + 86.44\,B' \qquad (5.18)$$

$$X' = 0.11 + 49.8\,R' + 33.1\,G' + 19.6\,B' + 0.8\,R'G' + 0.8\,R'B' + 0.4\,G'B' + 1.1\,R'2 - 2.94\,G'2 - 3.91\,B'2 \qquad (5.19)$$

$$Y' = 0.11 + 28.3\,R' + 70.3\,G' + 9.40\,B' + 0.700\,R'G' + 0.713\,R'B' + 0.445\,G'B' - 0.819\,R'^2 - 7.10\,G'^2 - 0.357\,B'^2 \qquad (5.20)$$

$$Z' = 0.16 + 1.2\,R' + 12.6\,G' + 105\,B' + 0.6\,R'G' + 0.63\,R'B' + 0.88\,G'B' - 0.7\,R'^2 - 3.11\,G'^2 - 20.5\,B'^2 \qquad (5.21)$$

Figure (5-12) show the new evaluation results for the new fitting models for the Acer display compared with the Apple display. The difference between the old models in **Figure (5-10)** and the new models is noticeable with the lower ΔE value for the Acer display, from which we conclude that the training data are accurate. (See **Appendix B** for detailed data)

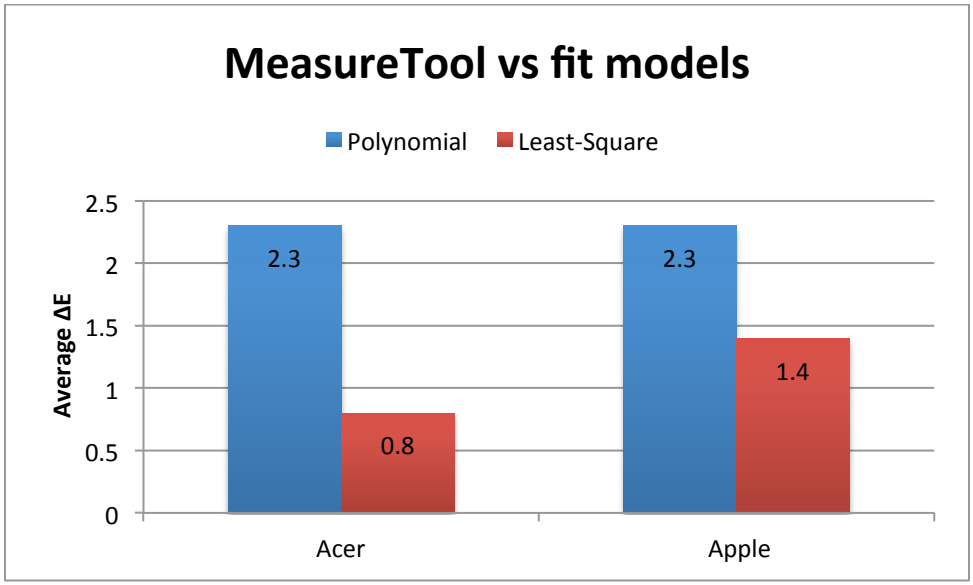

Figure 5-12: The new average ΔE values for different fitting models compared with MeasureTool values for each display

Proceeding with another evaluation for both LS fitting and the Polynomial fitting behavior, Jacobian determinant and RMSE tests was employed and the results are displayed in **Table (5-2)**. The determinant value for the polynomial fit model was calculated from the average determinant values of all LUT entries inside the constructed lcms profile. While the RMSE error is the average computed error value for each X, Y and Z transformation functions.

The overall positive results for the determinant indicate well-behaved models for both monitors. In addition, despite the overall lower RMSE values, the Apple monitor models yielded the lowest RMSE errors that are less than 1 for both models. Moreover, The polynomial fit was slightly more accurate than the LS for both displays.

Table 5-2: Calculated determinant and RMSE for different monitors

	Acer		**Apple cinema**	
	LS	**Polynomial**	**LS**	**Polynomial**
Jacobian Determinant	1.977×10^5	2.198×10^5	2.193×10^5	2.166×10^5
RMSE	1.5817	1.1535	0.4583	0.2861

5.6. Simulation Results

Figure (5-13) represents an xy-chromaticity plot for LS LUT-based lcms profile, Polynomial LUT-based lcms profiles and i1 profiler's profile for both Acer and Apple monitors. Overall, all plotted profiles wither for Acer or Apple monitors are so close that it is difficult to distinguish between them.

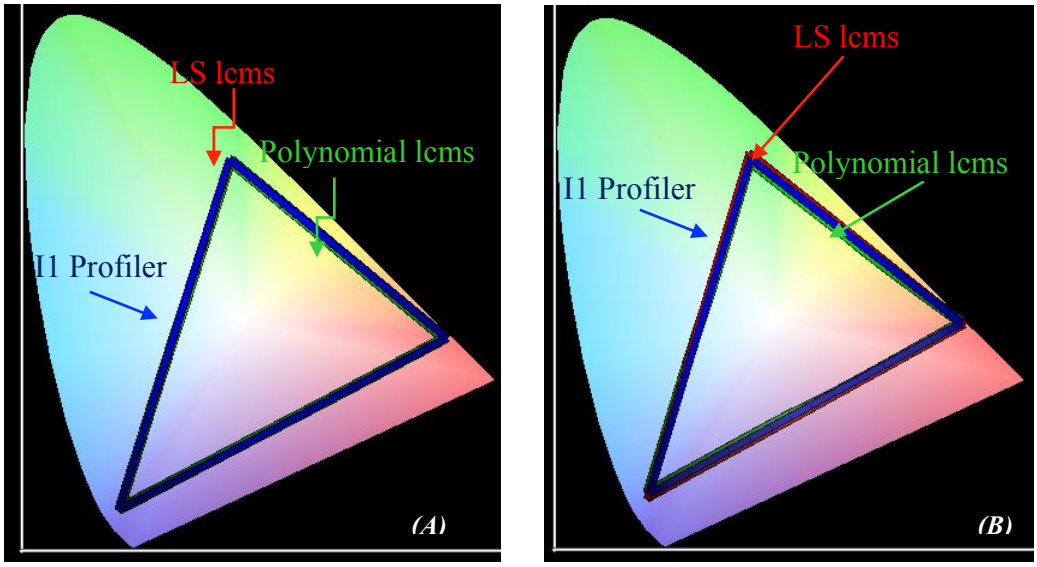

Figure 5-13: The xy-chromaticity plots comparisons of different profile types for Apple (A) and Acer (B) monitors

For the next comparison, only the polynomial fit profile was used since all lcms profiles are close. **Figure (5-14)** and **(5-15)** provides more detailed looks on the constructed profiles. **Figure (5-14)** show the primary ramps in both polynomial fit lcms profile and i1 Profiler's profile for both Acer and Apple monitors. They clearly show the convergence of the primary ramps between the two profiles. However, for both Acer and Apple monitors the black point of the constructed polynomial's profile records the actual measured values, while for the i1 profiler the black records a zero value. This explains the difference in the black point plotting between the two profiles.

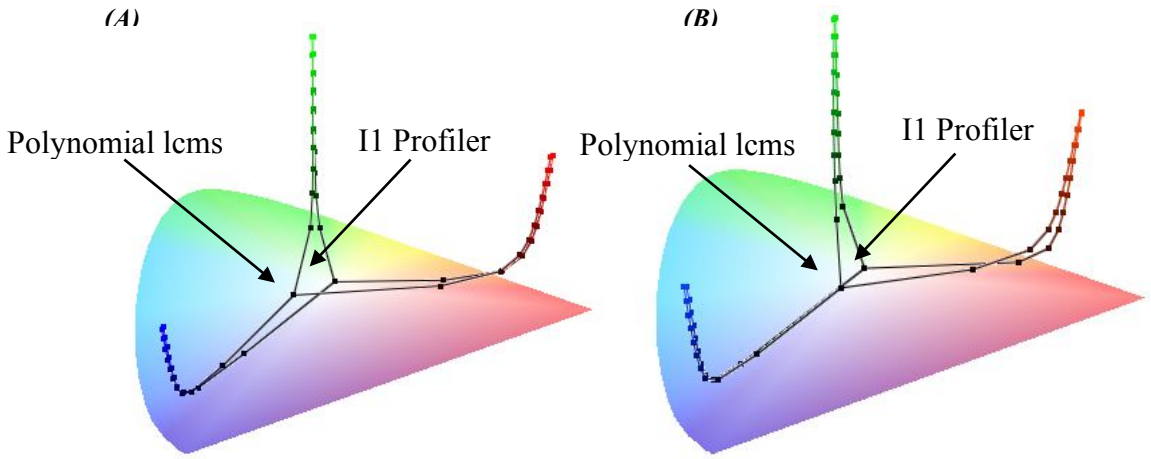

Figure 5-14: The primary ramp comparisons of different profile types for Apple (A) and Acer (B) monitors

The gray ramp comparison between the polynomial profile and the i1 profile for different monitors is shown in **Figure (5-15).** Despite the convergence between the two profiles toward the whitepoint value, it's obvious the significant difference between them toward the black point value.

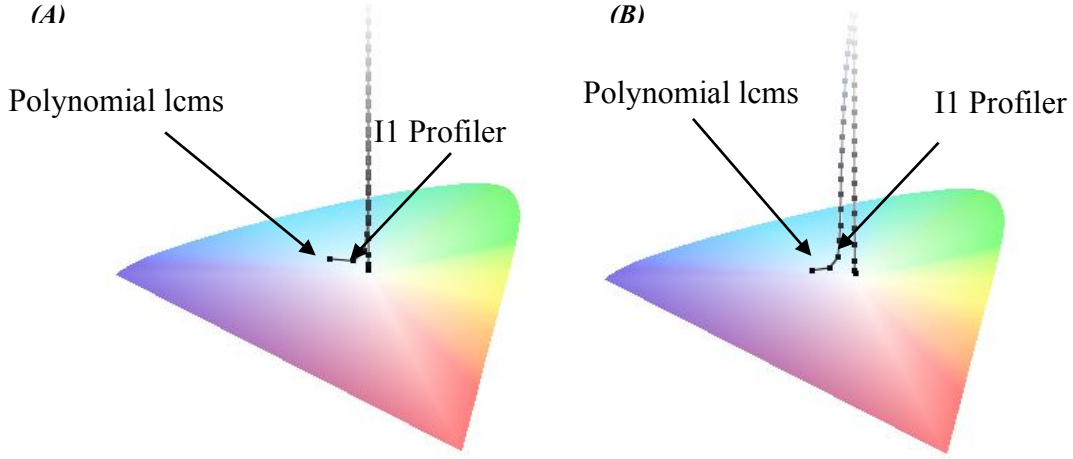

Figure 5-15: The gray ramp comparisons of different profile types for Apple (A) and Acer (B) monitors

Using the same RGB set in **Figure (5-9)**, ΔE values were collected between the predicted and the measured data to evaluate the performance of the selected fitting

models. The measured LAB values were collected from the info pallet in Adobe Photoshop CS5 and from DigitalColor Meter while the predicted values represent again the LUT entries inside the A2B tag for each profile. Since the Matrix-base lcms profile and the LS LUT-based profile use the same LS model, this comparison is generated using the LS lcms and Polynomial fit lcms LUT-based profiles.

Refer to section 2.4 about the chromaticity adaption of the LUT entries to D50 illuminant before they are stored inside the A2B tag in the monitor ICC profile, both Photoshop and DigitalColor meter reads the contents of that LUT. Thus, the aim of this evaluation is to test how well each software will interpret these contents. The resulting data are represented in **Figure (5-16)** and **(5-17).** (See **Appendix B** for detailed data)

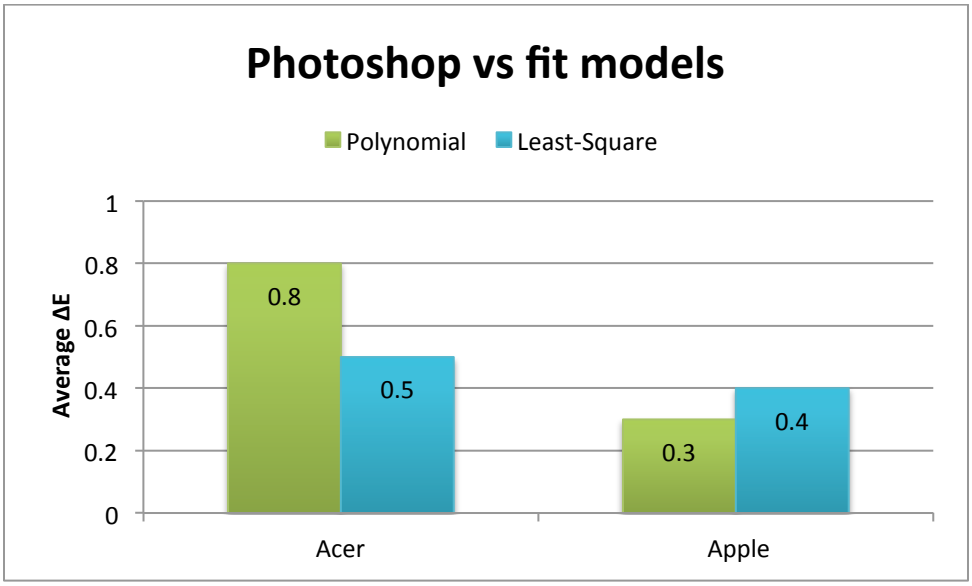

Figure 5-16: Average ΔE comparison between Photoshop data and different profiles and displays

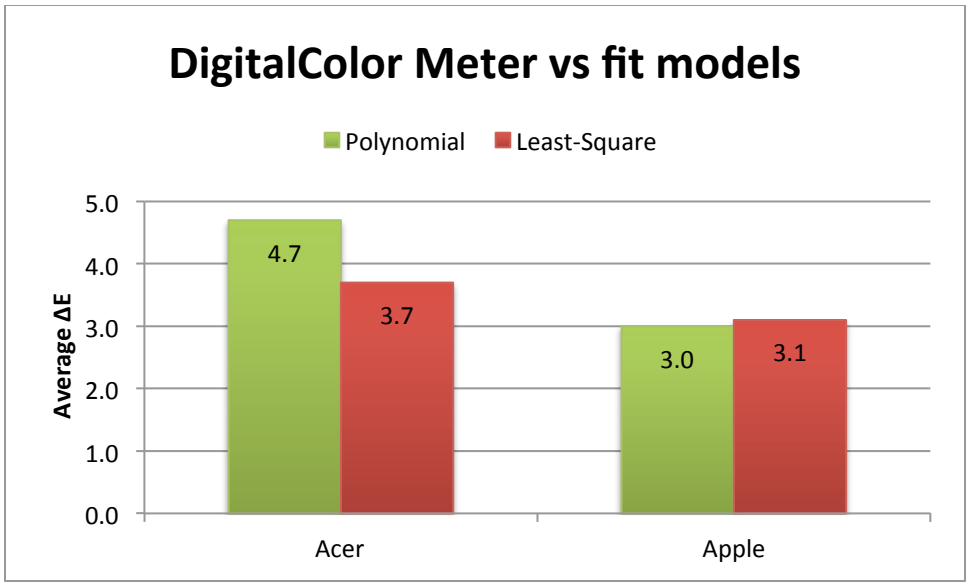

Figure 5-17: Average ΔE comparison between DigitalColor Meter data and different profiles and displays

The overall average ΔE values were less than 5 which is acceptable however, its very noticeable that Photoshop has significantly lower values across fitting models and for both displays over the DigitalColor Meter values. Another way to look at this variation is to compare the same values between Photoshop and DigitalColor Meter for each display as **Figure (5-18)** shows. For this comparison, i1profiler was also employed.

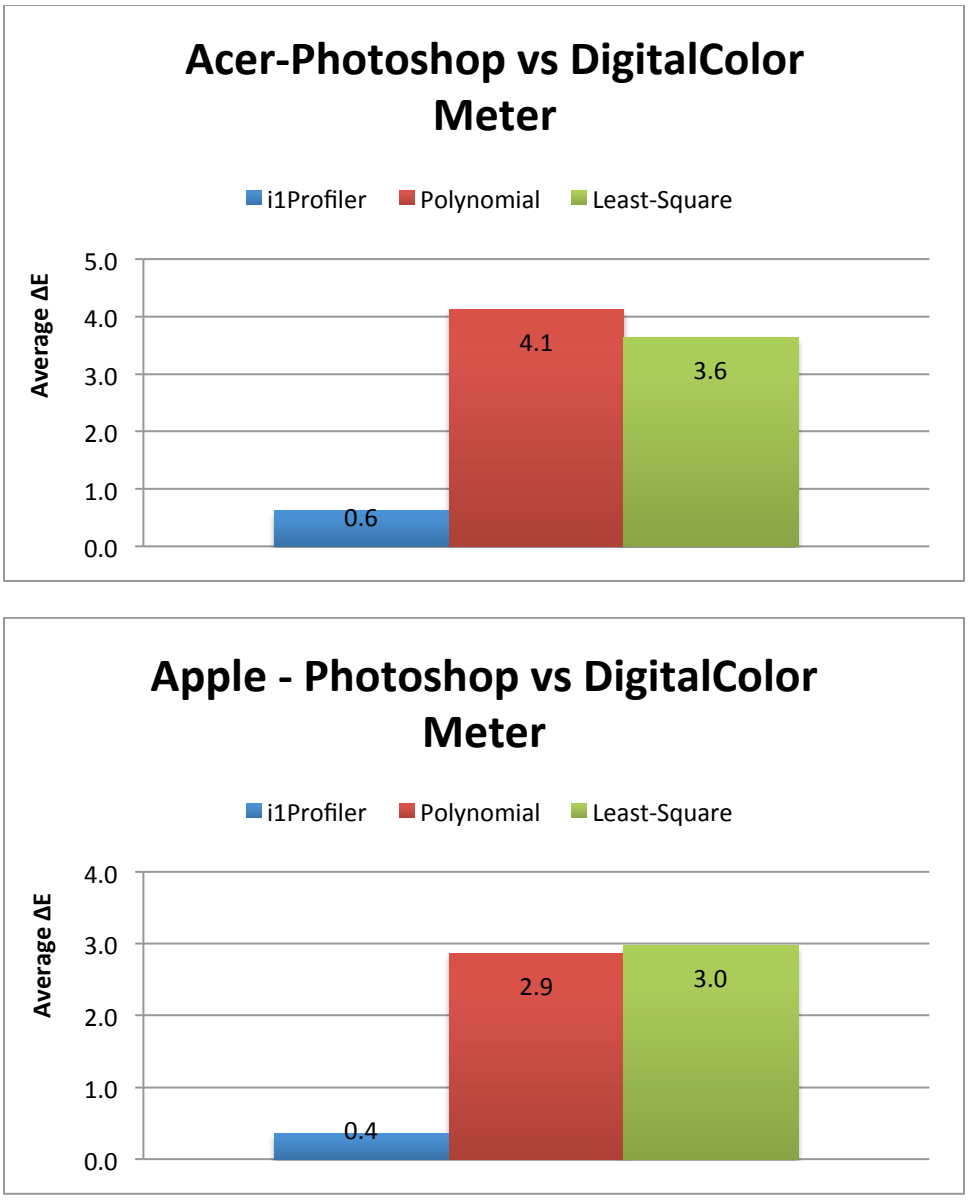

Figure 5-18: Average ΔE comparison between Photoshop and DigitalColor Meter of different profiles for Acer (up) and Apple cinema (down) displays

Overall i1Profiler has recorded the lowest ΔE values for both profiles, while values for Acer display were the highest. This variation could be due to the application itself and does not have anything with either the profile or the fitting model. (See **Appendix B** for detailed data)

In addition, comparing the fitting models themselves, it can be seen that the polynomial model has a better performance with Apple display over the Least-square model as oppose with Acer display and both Photoshop and DigitalColor Meter had recorded the same behavior.

5.7. Conclusion

Different results prove the unstable behavior of the Acer monitor with Fluorescent backlight over the Apple cinema display with LED backlight.

More concerns must be taken when selecting the appropriate algorithm to construct the training data that will be used to build the equivalent fitting models.

Both LS and polynomial fits record similar performance for characterizing different monitors with different backlights. Results have show that the polynomial fit was more consistent with the Apple display, while LS was more consistent with Acer display.

5.8. Future Works

- This research was focused on the forward transformation from RGB to PCS. However, the inverse transformation from PCS to RGB is also important for monitors and B2Ax tags are also required as part of LUT-based profiles. While this part was easy to conduct with the LS lcms profile by inverting the forward transformation matrix, for the nonlinear part it was quite complex. The goal is to find a better way to invert the proved accurate forward transformation model to

retrieve the actual recorded device-dependent values (the RGB values). This will require more investigations and studies to evaluate the existent models and probably be able to develop an enhanced inverse model.

- There are many types of displays that exist today. The challenge is to find a universal characterization model that accurately records the color behavior of these devices. Since the polynomial fitting model had proved its accuracy with LED displays, are we able to achieve the same results with others?

CHAPTER 6

EXPERIMENT 3: PRINTER

6.1. Introduction

Printers, in general, play different roles in graphic communication industries. Beside their default role of printing the final product using a desktop printer or a press, they are also used as proofers in a Prepress system. This step is a very important, which allows a client to preview the designed product's simulation before it's actually hit the press. Proofing can be also achieved using monitors in a process called "Soft proofing" [61-62]. Therefore, having a control on these devices in terms of colors is very essential.

Generally, Neugebauer model represents the physical characterization model for a printer where a common regression method represents the empirical model. A Color Look-up table (CLUT) is usually constructed based on the entries of any selected model. However, empirical models are widely used due to the reduction in the number of training sets and measurements error. [69]

The overall process of characterizing a printer and constructing an output profile is demonstrated in **Figure (6-1)**. Generally, an appropriate test chart would be selected, based on the selected measuring instrument, and printed without any color adjustment to maintain the native printer color. Next, the printed test chart would be measured using a measurement instrument such as i1iO, X-rite DTP70, X-rite DTP41, etc... The

measurement data usually consist of either the CMYK or RGB values of each color patches and their equivalent LAB and XYZ values. By employing any commercial profiling software, a mathematical transformation function will be generated for both forward (RGB/CMYK to PCS) and inverse (PCS to RBG/CMYK) transformation and will be used to construct an output profile for that particular printer and that particular paper.[70]

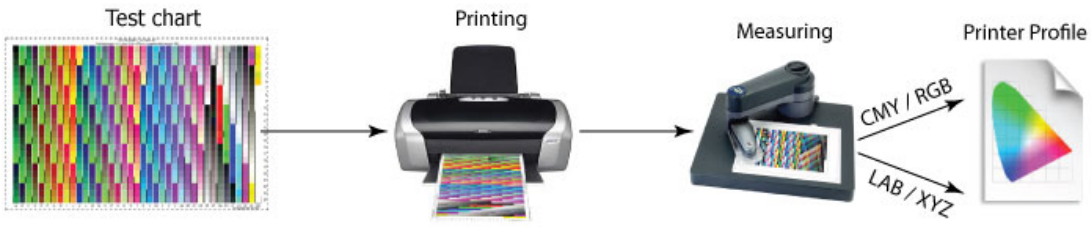

Figure 6-1: Printer characterization overall schema

Generally, most users define printers as CMYK devices. However, some printers can be operated as an RGB printer such as Epson inkjet or dye sublimation printers even if they are using CMYK inks. For such printers the printer driver internally conducts a color conversion from RGB to CMYK and therefore an RGB test chart need to be selected to build a corresponding RGB output profile. On the other hand, raster image processor (RIP) software are usually used to replace the printer driver and allow the user to interact with an RGB printer as a CMYK device. In this case, a CMYK test chart should be used to build a CMYK output profile. [71]

For an accurate color transformation from a printer device-dependent color space (CMYK or RGB) to PCS and due to the printing device complex color properties, only a

non-linear transformation model is employed and thus the constructed ICC profile should be a LUT-based profile.

The intention of this experiment is to construct a plausible RGB output profile based on a plausible characterization model for a dye sublimation printer, where no RIP software is available.[72]

6.2. Experimental Design

Using a previous output RGB ICC profile that was constructed using ProfileMaker 5.0.9 software for a dye sublimation printer (Mitsubishi CP3020DA – see **Figure 6-2**), the measurement data that were stored inside the private GretagMacbeth measurements tag (CIED tag) was read using SampleICC open source library code [73]. The ambition is to use the same measurement data to construct a new characterization model and a new profile using our customized profile editor.

Figure 6-2: Mitsubishi CP3020DA [74]

The measurement file reflects the measured RGB and the equivalent XYZ values of the 936 color patches of TC9.18 test chart that was measured using an X-Rite Eye One iO Spectrophotometer and used to construct the ProfileMaker ICC profile for the dye sublimation printer.

A 2nd degree polynomial fitting model was selected to be the printer characterization model as it has proved its accuracy with both scanner and monitor devices in chapter 4 and 5 respectively. This model was assembled using Minitab 15 and both RGB and XYZ values from the measurement file and it represents the forward transformation from RGB to CIE XYZ color space. In addition, a set of constraints were also employed to control the behavior of the transformation. These constraints were performed on the characterization model.

A Forward 3D LUT with 33 gird points that cover the printer RGB color space was constructed based on the characterization model and its equivalent constraints and was stored inside AToB Tag as a part of generating a printer profile. Again the selected combination of the AToB tag's elements was similar to those were used with both scanner and monitor device in Chapter 4 and 5 respectively.

In Addition, the same polynomial model was used to generate the inverse transformation model using Minitab software to transform from CIE XYZ to RGB color space and the generated LUT was stored inside the BToA Tag. The selected BToA elements will be similar to AToB tag however with a revised order as follow:

6.3. Printer Model

It important to note that we are trying to find a suitable characterization model for an RGB printer that is using a CMY ribbon, which means that the native color space of that device is actually a CMY colorspace.

The following functions demonstrate the forward regression polynomial model for our RGB printer to transfer from RGB to XYZ color spaces as resulted from Minitab software:

$$X = 1.72 + 0.0310R + 0.00257G - 0.0133B + 0.000790RG + 0.000051RB + 0.000113GB + 0.000245R2 - 0.000013G2 + 0.000109B2 \quad (6.1)$$

$$Y = 2.29 + 0.0236R - 0.00689G - 0.0085B + 0.000990RG + 0.000026RB + 0.000110GB - 0.000021R2 + 0.000237G2 + 0.000040B2 \quad (6.2)$$

$$Z = 3.91 - 0.0026R + 0.02010G - 0.0337B + 0.000185RG + 0.000217RB + 0.000740GB - 0.000123R2 - 0.000154G2 + 0.000340B2 \quad (6.3)$$

Looking at the liner terms of the X, Y and Z functions (**equations 6.1-6.3**), it's clearly shown the existence of some negative coefficients and the generated matrix that holds these coefficients will not be diagonal dominant. The calculated determinant of the transformation matrix was positive; however the eigenvalues were a set of negative and positive real numbers which reflects an unstable system behavior near the origin.

Moreover, the first derivatives at 255 along the primaries are negative which indicate a changing in the slop of the fitting curve or in another words generating unphysical fitting.

The following figures demonstrate different xy-chromaticity plotting of the resulted lcms profile compared with the original ProfileMaker profile that was built using the same training data.

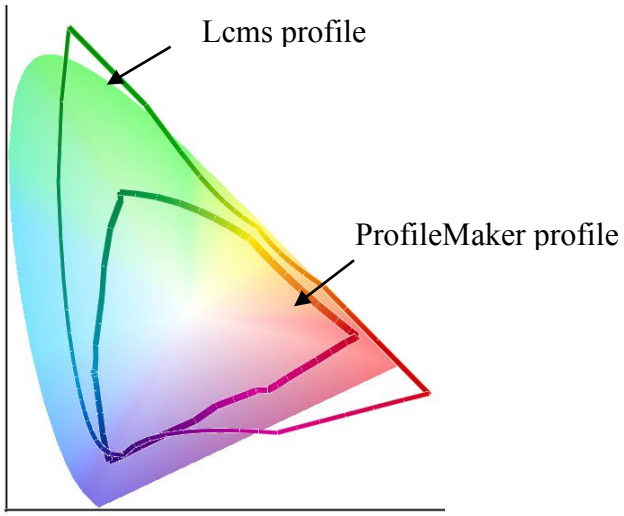

Figure 6-3: xy-Chromaticity plot of Polynomial fit lcms profile and ProfileMaker profile for dye sublimation printer

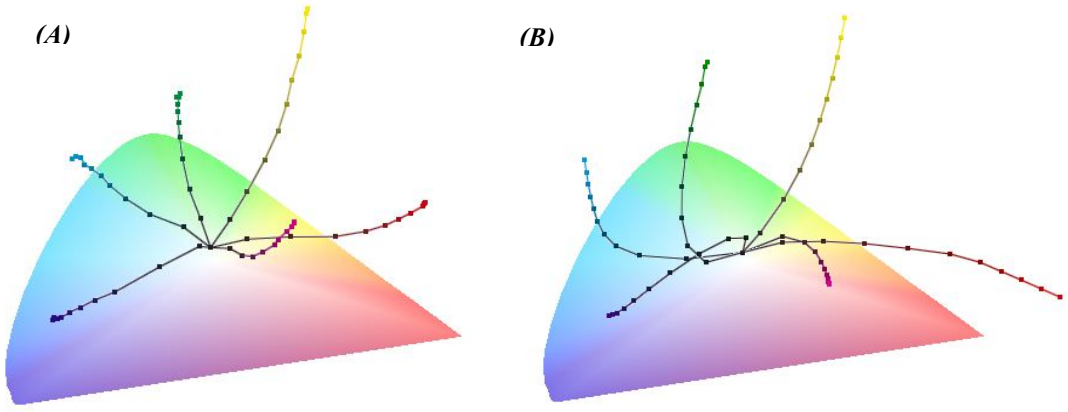

Figure 6-4: Primary and Secondary ramps of polynomial fit lcms profile (A) and ProfileMaker profile (B) for dye sublimation printer

It can be undoubtedly seen that the larger volume of the generated lcms profile using the polynomial fit. In Addition, both RGB and CMY ramps have strange hooks in the dark tone areas. Therefore, a polynomial regression model is not the right model to use with our printer, taking the fact that the native colorspace of our printer is CMY not RGB.

To overcome all of these problems, we have set constraints on the fitting function to force having a positive definite matrix and positive derivatives along the primaries and at the whitepoint as well.

For **G=B=0** the general form of **X** function with no intercept will be

$$\mathbf{X = aR + bR^2} \qquad \textbf{(6.4)}$$

Finding the derivative of **equation (6.4)**

$$\frac{\mathbf{dX}}{\mathbf{dR}} = \mathbf{a + 2bR} \qquad \textbf{(6.5)}$$

Based on the assumption that the derivative should be positive throughout the physical range of **R** (0-255) and that **X** should saturate at R=255, we can use **equation (6.5)** to find the value of b at R=255 corresponding to a maximum, we obtain the general constrained form of the X function (or X_f)

$$\mathbf{X_f = a\left(R - \frac{R^2}{510}\right)} \qquad \textbf{(6.6)}$$

A regression process on the training data for all **X** values at **G=B=0** was conducted to find the coefficient of $\mathbf{a_R}$. Similarly, we obtain the same steps to find the

new **G** and **B** equations with the new $\mathbf{a_G}$ and $\mathbf{a_B}$. Finally, the new training data for **X** values (will be noted as $\boldsymbol{X}^{*)}$ were conducted using the following equation:

$$\mathbf{X}^{*} = \mathbf{X} - \left(\mathbf{K} + \mathbf{a_R}\left(\mathbf{R} - \frac{\mathbf{R^2}}{\mathbf{510}}\right) + \mathbf{a_G}\left(\mathbf{G} - \frac{\mathbf{G^2}}{\mathbf{510}}\right) + \mathbf{a_B}\left(\mathbf{B} - \frac{\mathbf{B^2}}{\mathbf{510}}\right)\right) \qquad \textbf{(6.7)}$$

The ***K*** value represents the **X** value of the black point from the measurement data. The aim of including the black point in the subtraction function is to correct for the black point mapping, which was due to imperfect absorption in the black and measurement noise.

The ambition behind using this constraint is to conduct a new regression process with the new training data of $\mathbf{X}^{*}$ values to find the coefficient of the remaining cross terms (**RG**, **RB** and **GB**). Then we combine the new fitting function with the new functions of the **R**, **G** and **B** and the general form of the new fitting function for **X** will be:

$$\mathbf{X} = \mathbf{K} + \mathbf{a_R}\left(\mathbf{R} - \frac{\mathbf{R^2}}{\mathbf{510}}\right) + \mathbf{a_G}\left(\mathbf{G} - \frac{\mathbf{G^2}}{\mathbf{510}}\right) + \mathbf{a_B}\left(\mathbf{B} - \frac{\mathbf{B^2}}{\mathbf{510}}\right) + \mathbf{a_{RG}}\,\mathbf{RG} + \mathbf{a_{RB}}\,\mathbf{RB} + \mathbf{a_{GB}}\,\mathbf{GB} \qquad \textbf{(6.8)}$$

Finally, we perform the same steps to find the new fitting functions for both **Y** and **Z** values to have the same form of **equation (6.8)**.

These constraints will ensure a positive linear term of the fitting function, which will assure having positive derivatives along the primaries or zero at the end point of the primaries and having positive real parts of eigenvalues as well.

Next was to look at the gray ramp because a well-balanced gray ramp will insure a well-balanced overall color appearance. Therefore, we have set a new regression model on the new training data that resulted after applying **equation (6.7)** and for all $\mathbf{X}^*$ values where **R=G=B** to select the gray values. This regression model should give the sum of the cross terms coefficients (or b_{sum}) which will then give the **X** value of the whitepoint after adding it to the sum of the linear terms coefficients from **equation (6.8)**. Below is the selected regression model:

$$\mathbf{X_f = b_{sum}\, GB} \qquad \textbf{(6.10)}$$

Since **R** is equivalent to the **X** tristimulus value, we have select the **GB** term in our model because it was the only cross term in **X** transforming function that does not include the **R** value. However, the selecting of another cross term will not be effected since for this regression **R=G=B**.

By plugging the resulted term from **equation (6.10)** to **equation (6.7)**, we will have a new formula (see **equation 6.11**) that will be used to form a new training set. This set will be used to find the coefficients of the remaining cross terms (i.e. **RG** and **RB**) while noting that we still maintain the primaries coefficients.

$$\mathbf{X^* = X - \left(K + a_R \left(R - \frac{R^2}{510}\right) + a_G \left(G - \frac{G^2}{510}\right) + a_B \left(B - \frac{B^2}{510}\right) + b_{sum}\, GB\right)} \qquad \textbf{(6.11)}$$

A regression model will then be conducted using the new training data to find the new coefficients of the cross terms (b_{RG} and b_{RB}) as follow:

$$\mathbf{X_f = b_{RG}\,(RG - GB) + b_{RB}\,(RB - GB)} \qquad \textbf{(6.12)}$$

By now we have the coefficients of **RG** and **RB** and we have the sum of the cross terms coefficients, so it will be easy to find the exact coefficient of **GB** (or b_{GB}). The same algorithm will be applied for **Y** and **Z** where for **Y** the selected coefficient that will hold the sum of the cross terms value will be **RB** and for **Z** it will be **RG**.

At the moment we have to deal with both primaries and gray ramp next are the secondary ramps and these are represented by the cross terms in our model. So we had use the same regression model in **equation (6.12)** for **X**, **Y** and **Z** with the new resulted training data from **equation (6.11)** and for all $\mathbf{X}^*$, $\mathbf{Y}^*$ and $\mathbf{Z}^*$ where **R=G** and **B=0** for the yellow ramp, **R=B** and **G=0** for the magenta ramp and **G=B** and **R=0** for the cyan ramp. The aim of this step is to find improved coefficients of the cross terms that will fix the strange hooks of all secondary ramps at once (See **Figure 6-4**). The final printer model for this device is demonstrated as bellow:

$$\mathbf{X} = 1.16 + 0.163\left(\mathbf{R} - \frac{\mathbf{R}^2}{510}\right) + 0.0379\left(\mathbf{G} - \frac{\mathbf{G}^2}{510}\right) + 0.0237\left(\mathbf{B} - \frac{\mathbf{B}^2}{510}\right) + 0.000728\,\mathbf{RG} + 0.000059\,\mathbf{RB} + 0.000086\,\mathbf{GB} \quad (6.13)$$

$$\mathbf{Y} = 1.11 + 0.0770\left(\mathbf{R} - \frac{\mathbf{R}^2}{510}\right) + 0.112\left(\mathbf{G} - \frac{\mathbf{G}^2}{510}\right) + 0.00774\left(\mathbf{B} - \frac{\mathbf{B}^2}{510}\right) + 0.000873\,\mathbf{RG} + 0.000028\,\mathbf{RB} + 0.000077\,\mathbf{GB} \quad (6.14)$$

$$\mathbf{Z} = 1.1 + 0.000381\left(\mathbf{R} - \frac{\mathbf{R}^2}{510}\right) + 0.0360\left(\mathbf{G} - \frac{\mathbf{G}^2}{510}\right) + 0.110\left(\mathbf{B} - \frac{\mathbf{B}^2}{510}\right) + 0.000152\,\mathbf{RG} + 0.000148\,\mathbf{RB} + 0.000582\,\mathbf{GB} \quad (6.15)$$

Table (6-1) displays the calculated Jacobian determinant and RMSE for the constrained fit model. The Eigenvalues were computed from the linear part of **equations**

(6.13-6.15). The displayed determinant value is the average value of the calculated determinant over all LUT entries that were stored in the constructed lcms profile.

Table 6-1: Calculated Jacobian determinant, Eigenvalues and RMSE for the constrained fit model

	Printer lcms profile
Jacobian Determinant	0.00141
Eigenvalues	0.2038 0.0906 + 0.0129i 0.0906 - 0.0129i
RMSE	5.4611

After all the adjustments that we had on our characterization model we were able to get a positive sign for both the determinant and the real parts of the eigenvalues. However the RMSE record a high error value which gives a sign that our model still requires more adjustments.

6.4. Simulation Results

The aim of all the previous adjustments that we had on the printer characterization model is to try fixing the poor performance of the polynomial model in a way to have a plausible mode that can represent our device.

Despite all the adjustments that we had on our characterizing model the xy-chromaticity plot shows that we still have some missing parts. However, compared to the unconstrained polynomial fit profile in **Figure (6-3)**, our constrained fit lcms profile had an improved and smoother shape. In addition, looking at **Figure (6-5)** we can observe

some smoother parts in our profile than the ProfileMaker profile especially near the magenta areas.

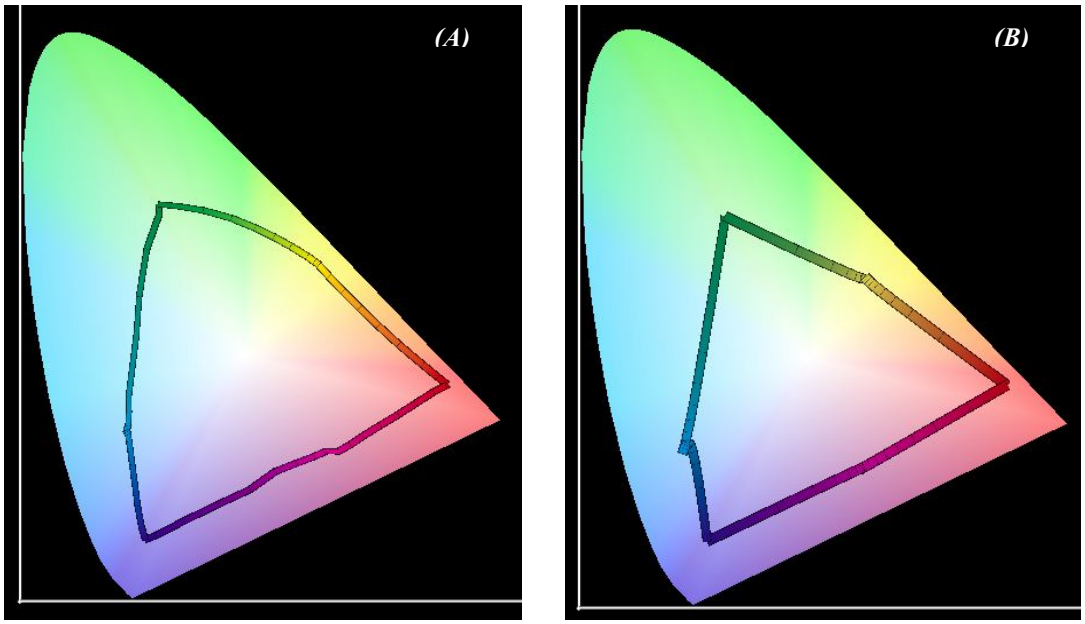

Figure 6-5: xy-chromaticity plot of ProfileMaker profile (A) and our constrained fit lcms profile (B) for the dye sublimation printer

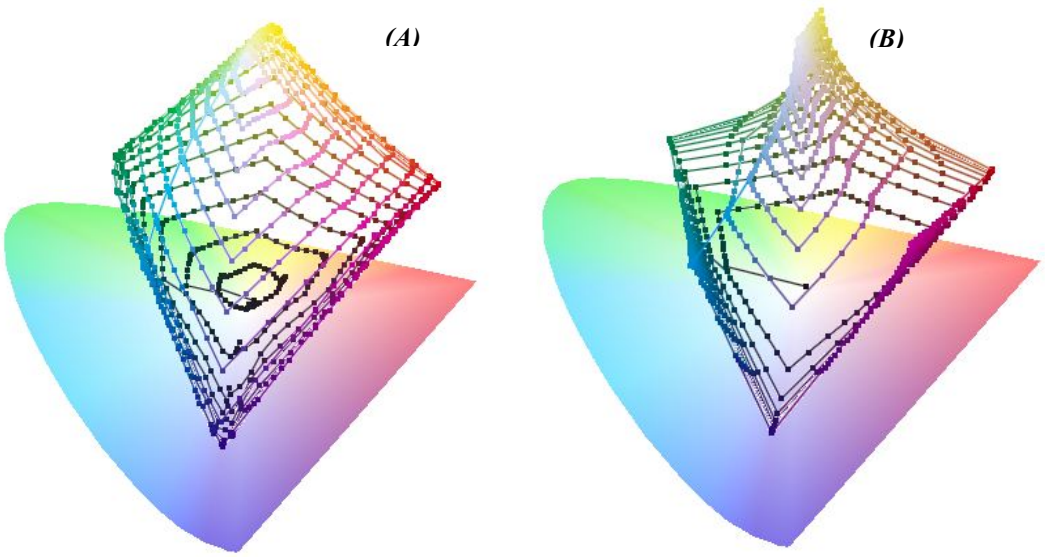

Figure 6-6: A 3D plot of ProfileMaker profile (A) and our constrained fit lcms profile (B)

3D gamut volume displays for both profiles are represented in **Figure (6-6)**. It's clearly see the shrinking volume of our constrained fit profile over the ProfileMaker profile which explains the lower gamut volume values that was calculated from our profile.

The gray ramp constrained that was discussed previously in section 6.3 and **equation (6.10)** has resulted a smoother gray ramp of our constrained fit profile over the ProfileMaker as demonstrated in **Figure (6-7)**.

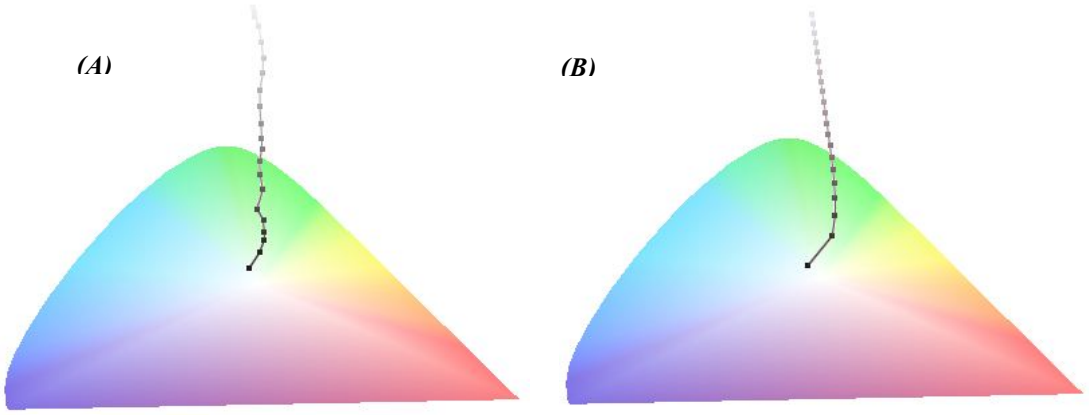

Figure 6-7:A gray ramp plot of ProfileMaker profile (A) and our constrained fit lcms profile (B)

In addition, **Figure (6-8)** represents a comparison of the gray ramp between the training data and the contents of the CLUT from our lcms profile. The smoothness results were clearly observed in the plotted XYZ curves from the LUT. (See **Appendix C** for detailed data)

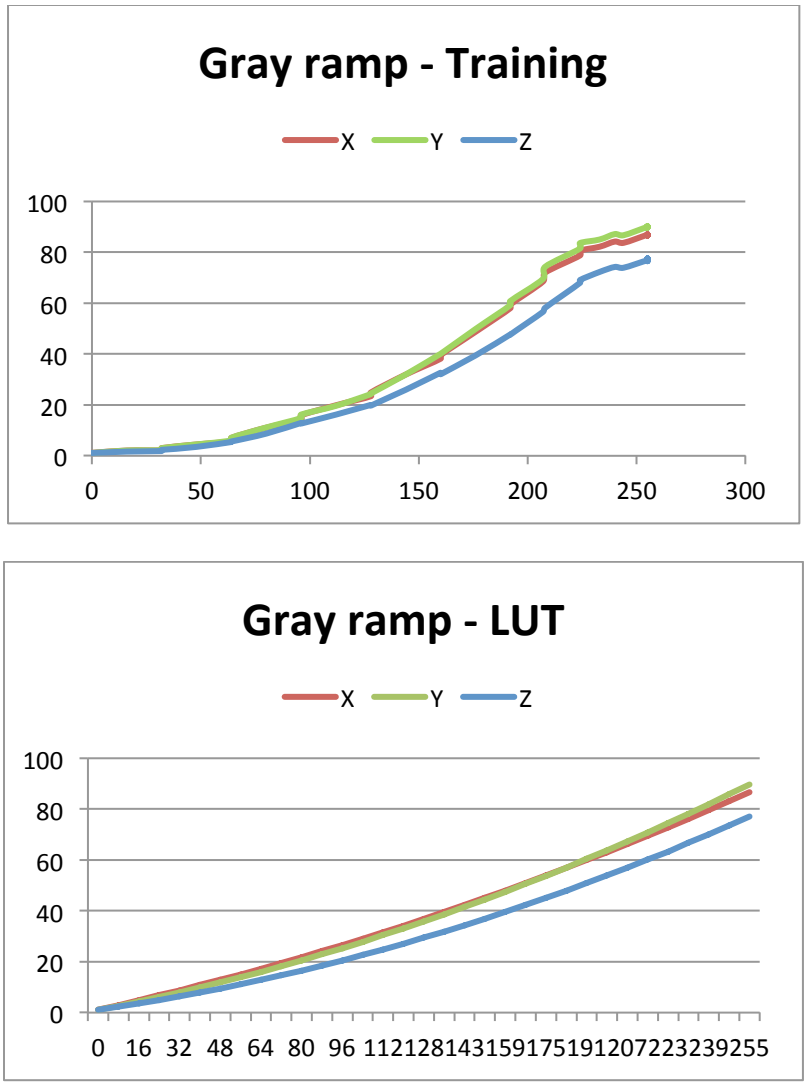

Figure 6-8: A gray ramp comparison between the training data (up) and the contents of the LUT of our constrained fit lcms profile (down)

Moreover, the same smoothing results were obtained for the primaries ramp as displayed in **Figure (6-9)**. For the secondary ramps the secondary constrain what was discussed in section 6.3 has fixed the ragged shapes that appeared in the ProfileMaker ramps. However, this constraint wasn't sufficient to fix the curvature of these ramps, which is obvious in the magenta and yellow ramps of the constrained fit profile. We were unable to try any new constraining method to fix this problem because we were out of terms to use. (See **Figure 6-9**)

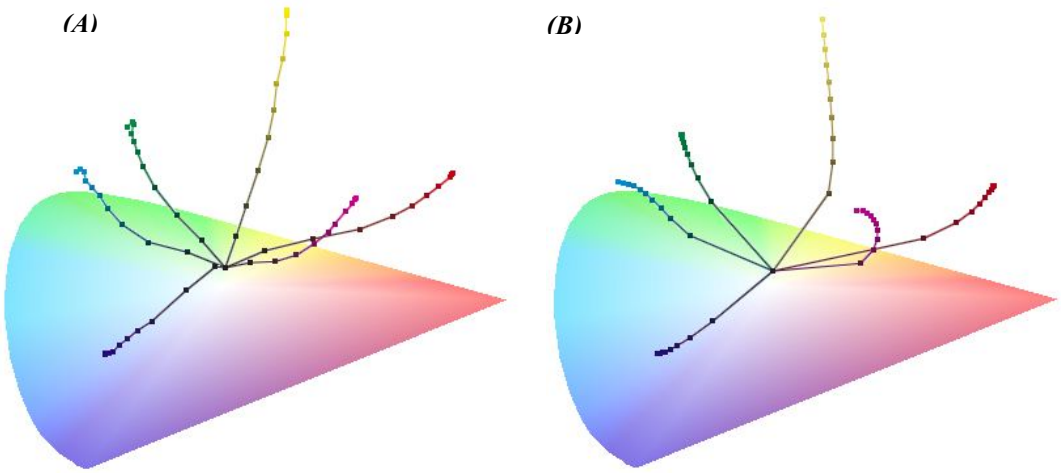

Figure 6-9: Primary and Secondary ramps plot of ProfileMaker profile (A) and our constrained fit lcms profile (B)

Another comparison between the training data and the contents of the CLUT in A2B0 tag of our constrained fit profile in terms of the secondary (CMY) ramps were represented in **Figures (6-10)** to **(6-12)** respectively. Overall, the plotting of the training set ramps are more likely represented by a higher order equation, which is possibly a cubic function, while the LUT plotting are represented by a quadratic term equation. (see **Appendix C** for detailed data)

For the cyan ramp (see **Figure 6-10**), despite the closing values of both X and Y curves, the Z values of the LUT record a significant higher values than the actual training data which explain the curvature of the cyan ramp in the xy-chromaticity plotting in **Figure (6-9)**.

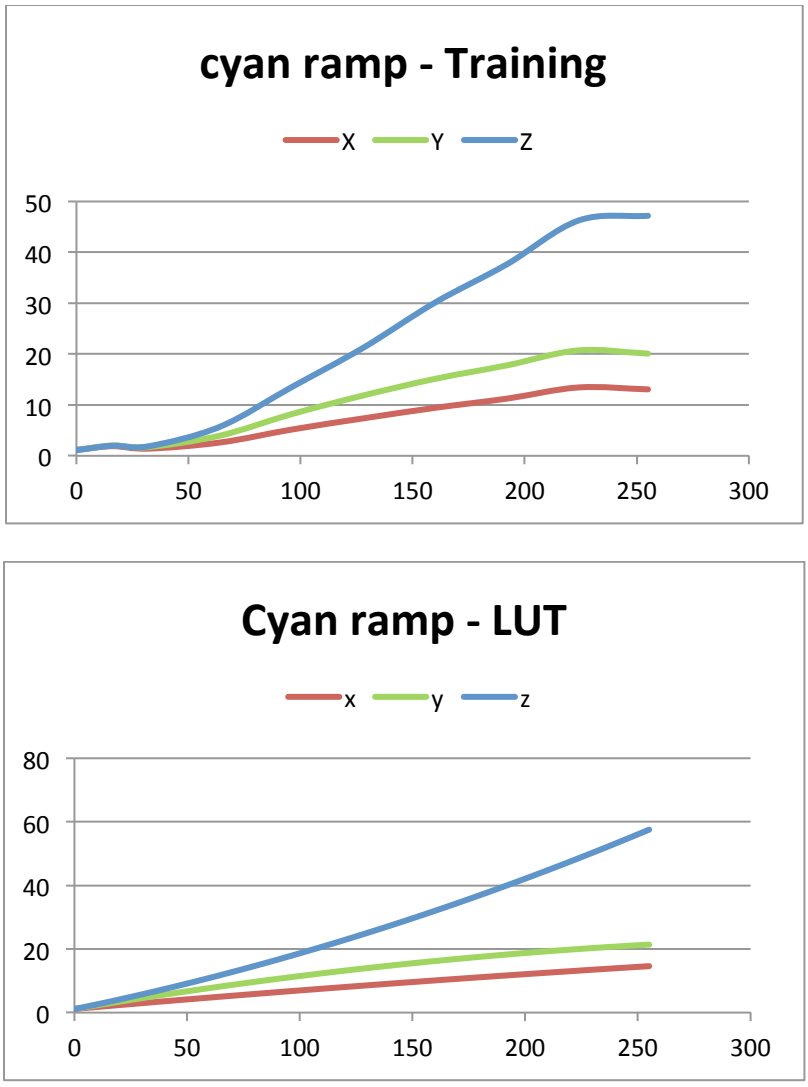

Figure 6-10: A cyan ramp comparison between the training data (up) and the contents of the LUT of our constrained fit lcms profile (down)

The same performance is noticed in the case of the Magenta ramp (see **Figure 6-11**). The Z values in the LUT are higher than what it should be as in the training data. This could also explain the diversity of the magenta ramp tower the blue region in **Figure (6-9)**.

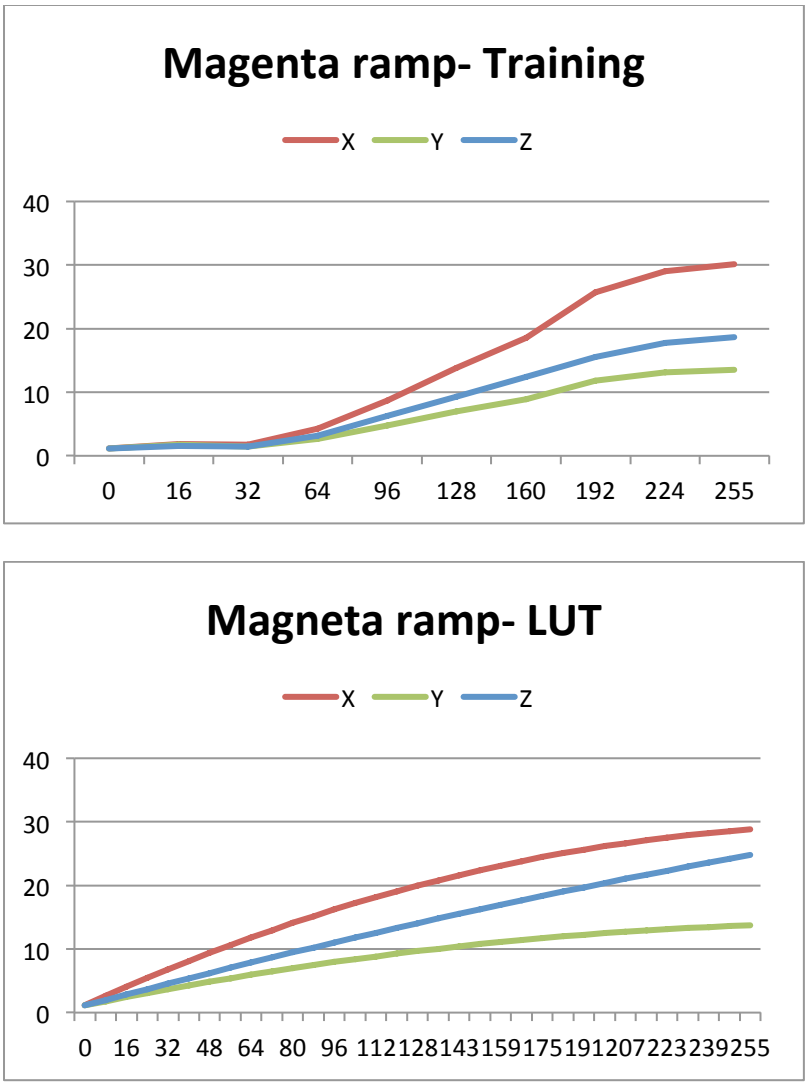

Figure 6-11: A magenta ramp comparison between the training data (up) and the contents of the LUT of our constrained fit lcms profile (down)

The Yellow ramp has the closest comparison between the data in the LUT and in the training data, despite a slightly higher value again in the Z curves. (see **Figure 6-12**)

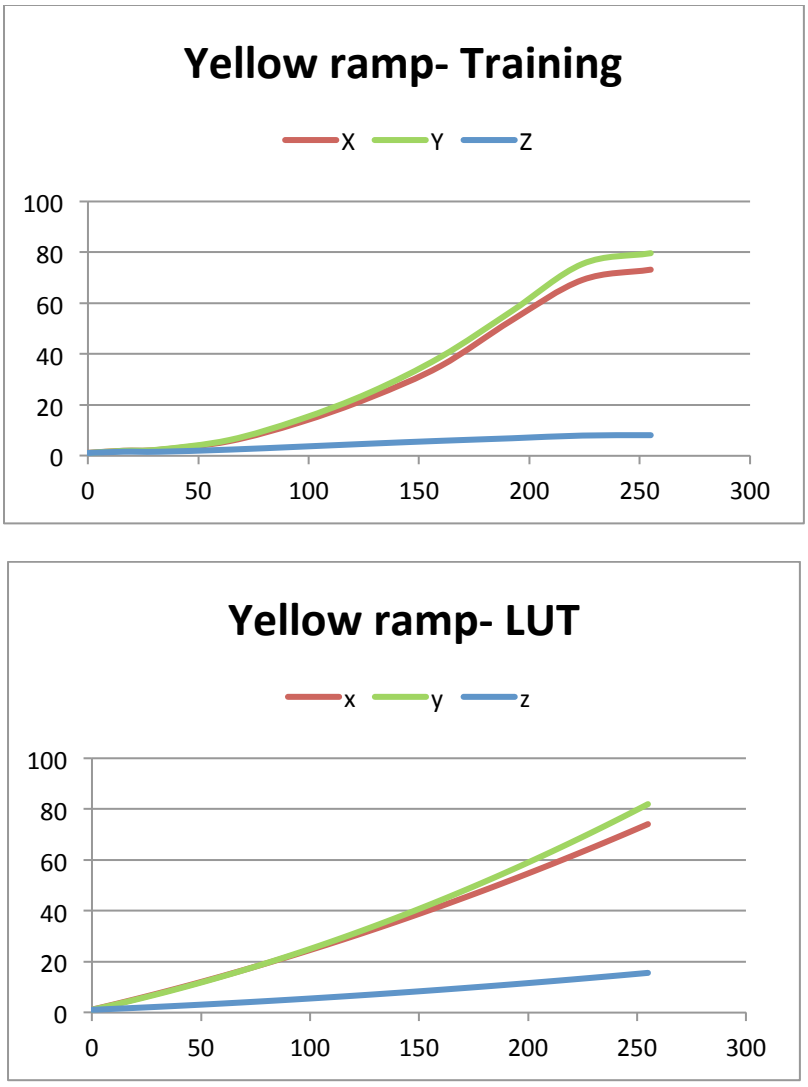

Figure 6-12: A yellow ramp comparison between the training data (up) and the contents of the LUT of our constrained fit lcms profile (down)

To evaluate the profiles performance, a set of primaries and secondary color patches along with black and white patches were assembled (see **Figure 6-13**) and displayed in Adobe Photoshop. Both our constrained lcms profile and the ProfileMaker profile were applied and their equivalent LAB values were collected from the info pallet in Photoshop. A ΔE was then calculated between each measured LAB value and the actual training values. The resulting comparisons are shown in **Table (6-2)**.

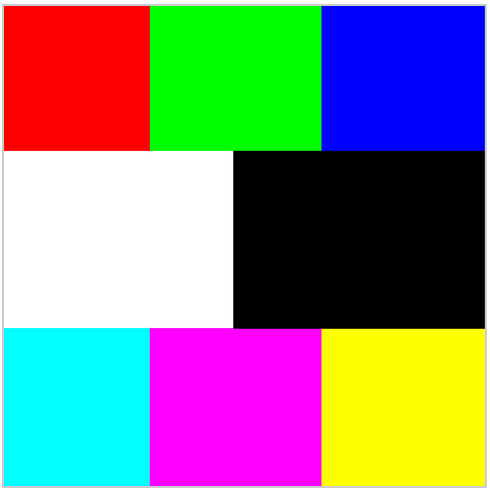

Figure 6-13: Color patches used to evaluate the printer profile

As expected the average ΔE between the training data and the ProfileMaker profile is lower than with our constrained fit lcms profile. In addition, ΔE of the secondary patches with our lcms profile has recorded higher values where the maximum value of 21.32 was related to the yellow patch which is expected since the previous results in this sections showed the poor performance of our characterization model toward the secondary ramps. Detailed data can be observed in **Appendix C**.

Table 6-2: ΔE comparison between the training data of selected color patches and their equivalent values after applying different profiles on Adobe Photoshop

	ΔE (ProfileMaker)	**ΔE (constrained lcms)**
Mean	0.39	8.02
Max	0.62	21.32
STD	0.19	7.03

6.5. Conclusion

The complex physical properties of a printer in general require a complex model to accurately characterize it. Results have showed that a 2nd order polynomial fitting model that has proved its accuracy with both scanner and monitor devices has poor performance with an RGB printer.

6.6. Future Works

- A high order regression model might be the right choice to characterize a printer device [75]. A suggested trend is to study different higher order models and use the evaluation result to develop a more enhanced model that can accurately describe the printer.
- This experiment again was focused on the forward transformation from RGB to XYZ. The inverse transformation is very important for a printer device and therefore our profile is not completed. More investigations need to be conducted to study this topic

CHAPTER 7

CONCLUSION

7.1. Overview

Among all the 4C's of the Color Management system (Calibration, Characterizations, Consistency and Converting) this research was focused on the Characterization process for different devices, due to its impotence to achieve a consistent color transformation across digital media.

An overview introduction about various color management topics was discussed in Chapters 1 and 2. Chapter 3 discussed the characterization models that were used for different devices, and highlighted the fundamentals of constructing ICC profile for different devices. Different characterization experiments were employed for different devices and a plausible results were achieved (Chapter 4-6). This chapter will demonstrate the common and the specific findings of this research.

7.2. Overall Findings

Generally, each digital device has its own physical properties and thus it will be difficult to find a universal model to characterize all of them and have a consistent transformation results. Results have shown that the linear Least-square model had a plausible performance with monitor devices as opposed to, due to the non colorimetric behavior of a scanner, scanning devices. In addition, a Polynomial fit model works very

well with both scanner and monitor devices unlike with a printer device, which is due to the complex structure of the printer device.

Chromatic adaptation needs to be employed if the measurement of the target charts were collected under a different illuminant than D50. This adaptation needs to take a place during the ICC profile constructing process and before populating the LUT entries.

The native white point color temperature of a monitor does not need to be D65 and it could differ across platform and across application.

For monitor devices, the calibration process can be conducted using different software. Both X-Rite ProfileMaker and MeasureTool can do the calibration process with the assistance of an Eye-One Pro measuring device, the difference is utilizing the spectra option. Results has shown that the training data, that were constructed by using MeasureTool to average measurements data of different platform and export it to LAB, were not accurate as opposed to using MeasureTool to measure the LCD test chart across platform and manually linearizing the measurement data and averaging them in Excel to build the training data.

REFERENCES

[1] H. Johnson, *Mastering Digital Printing*, Thomson Course Technology, pp.115-126 (2005).

[2] X. Rong, "Color Management of Desktop input devices: Quantitative analysis of Profile Quality", M.S Thesis, Western Michigan University, MI, (2003)

[3] S. Hullfish and J. Fowler, *Color Correction for Digital Video: Using Desktop Tools to Perfect Your Image*, Focal Press, pp. 13-18 (2002).

[4] R. M. Adams II and J.B. Weisberg, *The GATF Practical Guide to Color Management*, 2nd Ed., GATFPress, Pittsburgh, pp. 2 (2002).

[5] A. Rodney, *Color Management for Photographers: Hands on Techniques for Photoshop Users*, Focal Press, pp. 26-36 (2005).

[6] M. D. Fairchild, *Color Appearance Models*, 2nd Ed., John Wiley & Sons, pp. 317-324 (2006).

[7] E. Reinhard, E. A. Khan, A. O. Akyuz and G. M. Johnson, *Color Imaging: Fundamentals and Applications*, A K Peters, pp. 833-839 (2008).

[8] M. Ebner, *Color Constancy*, John Wiley & sons, pp. 2 (2007).

[9] M. D. Fairchild, *Color Appearance Models*, 2nd Ed., John Wiley & Sons , pp. 3-4 (2006).

[10] R. S. Berns, *Billmeyer and Saltzman's Principles of Color Technology*, 3rd Ed., John Wiley & Sons, pp. 13 (2000).

[11] J. Y. Hardeberg, *Acquisition and Reproduction of Color Images: Colorimetric and Multispectral Approaches*, 2nd Ed, Universal-Publishers, pp. 10 (2001).

[12] A. Sharma, *Understanding Color Management*, Delmar Thomson Publishing, pp. 69-70 (2004).

[13] M. Ebner, *Color Constancy*, John Wiley & sons, pp. 10 (2007).

[14] E. Reinhard, E. A. Khan, A. O. Akyuz and G. M. Johnson, *Color Imaging: Fundamentals and Applications*, A K Peters, pp. 206-208 (2008).

[15] P. D. Fleming and A. Sharma, "Color Management with ICC Profiles: Can't Live without It so Learn to Live with It", Invited Review for *Gravure Magazine* (2002)

[16] A. Sharma, *Understanding Color Management*, Delmar Thomson Publishing, Chapter 3, pp. 81-82 (2004)

[17] H. Lee, *Introduction to Color Imaging Scienc*e, Cambridge University Press, pp. 107 (2005).

[18] G. Sharma, "Color fundamentals for digital imaging", in *Digital Color Imaging Handbook*, edited by G. Sharma, Chapter 1, CRC Press, pp. 28-29 (2003).

[19] M. D. Fairchild, *Color Appearance Models*, 2nd Ed., John Wiley & Sons, pp. 79 (2006).

[20] S. Westland and C. Ripamonti, *Computational Color Science: Using Matlab*, John Wiley & Sons, pp. 50 (2004).

[21] P. Green, "Colorimetry and colour difference", in *Colour Engineering: Achieving Device Independent Colour*, edited by P. Green and L. MacDonald, Chapter 3, John Wiley & Sons, Ed. pp. 56-57 (2002).

[22] J. Uroz, R. Luo and J. Morovic, "Perception of colour differences in large printed images", in *Colour Image Science: Exploiting Digital Media*, edited by L. W. MacDonald and M. R. Luo, Chapter 3 ,John Wiley & Sons, pp. 55 (2002).

[23] D. Wallner, "Color Management and transformation through ICC profiles", in *Colour Engineering: Achieving Device Independent Colour*, edited by P. Green and L. MacDonald, Chapter 11, John Wiley & Sons, pp. 248-257 (2002).

[24] A. Sharma, J. J. Suffoletto and R. M. Adams II, *Color Management Handbook*, PIA GATFPress (2008)

[25] R. M. Adams II and J.B. Weisberg, *The GATF Practical Guide to Color Management*, 2nd Ed., GATFPress, Pittsburgh, pp. 57-58 (2002).

[26] R. Bala, "Device characterization", In *Digital Color Imaging Handbook*, edited by G. Sharma, Chapter 5, CRC Press, pp. 273-331 (2003).

[27] A. Sharma, *Understanding Color Management*, Delmar Thomson Publishing, Chapter 1, pp. 34-35 (2004)

[28] E. Reinhard, E. A. Khan, A. O. Akyuz and G. M. Johnson, *Color Imaging: Fundamentals and Applications*, A K Peters, pp. 851-863 (2008).

[29] D. Wallner, "Building ICC Profiles - the Mechanics and Engineering", Corresponds to ICC Specification ICC.1:2000, pp. 6-10 (2000).

[30] ICC, "Specification ICC.1:2004-10 (Profile Version 4.2.0.0)" , pp. 15 (2004), see http://www.color.org

[31] A. Sharma, *Understanding Color Management*, Delmar Thomson Publishing, Chapter 5, pp. 137-146 (2004).

[32] P. Rao, M. R. Rosen, R. S. Berns and C. F. Carlson, "Performance Evaluation of the Profile Maker Professional 5.0 ICC Profiling Software", Munsell Color Science Laboratory (2005).

[33] P. Green, "Overview of characterization methods", in *Colour Engineering: Achieving Device Independent Colour*, edited by P. Green and L. MacDonald, Chapter 6, John Wiley & Sons, pp. 127-138 (2002).

[34] P. G. Engeldrum. "Computing Color Gamuts of Ink-Jet Printing Systems", In *Proc. of the Society for Information Display,* Vol. 27 , pp. 25-30 (1986).

[35] M. Mahy, "Calculating of Color Gamuts Based on the Neugebauer Model", *Color Research and Application*, Vol. 22 , pp. 365-374 (1997).

[36] P.-C. Hung, "Colorimetric calibration in electronic imaging devices using a look-up-table model and interpolation", *J. Electronic imaging*, Vol. 2 Issue 1, pp. 53-61 (1993).

[37] J. Y. Hardeberg, F. Schmitt, I. Tastl, H. Brettel and J.-P. Crettez, "Color management for color facsimile", In *Proc. of 4th IS&T and SID's Color Imaging Conf.*, Scottsdale, AR, pp. 108-113 (1996).

[38] J. M. Kasson, W. Plouffe and S. I. Nin, "Tetrahedral interpolation technique for color space conversion", In *Proc. of SPIE Conf. Device-Independent colour imaging*, Vol. 1909, San Jose, CA, pp. 127-138 (1993).

[39] J. M. Kasson, S. I. Nin, W. Plouffe, J. L. Hafner, "Performing color space conversions with three-dimensional linear interpolation", *J. Electronic Imaging*, Vol. 4 Issue 3, pp. 226-250 (1995).

[40] J. Morovic, "Gamut Mapping", in *Digital Color Imaging Handbook*, edited by G. Sharma, Chapter 10, CRC Press, pp. 641-669 (2003).

[41] V. Chovancova-Lovell and P. D. Fleming III, "Color Gamut – New Tool in the Pressroom?", *TAPPI J*, pp. 4-11 (2009).

[42] J. Morovic, "Colour gamut mapping", in *Colour Engineering: Achieving Device Independent Colour*, edited by P. Green and L. MacDonald, Chapter 13, John Wiley & Sons, pp. 298-306 (2002).

[43] J. Morovic, "Colour management for the graphic arts", in *The Colour Image Processing Handbook*, edited by S.J. Sangwine, R. E. N. Horne, Chapter 15, Springer, pp. 346 (1998).

[44] J. Morovic and M.R. Luo, "The Fundamentals of Gamut Mapping: A Survey", *Journal of Imaging Science and Technology*, Vol. 45 Issue 3, pp. 283-290 (2001).

[45] M. D. Fairchild, *Color Appearance Models*, 2nd Ed., John Wiley & Sons Ltd, pp. 184 (2006).

[46] P. Green and L. MacDonald, *Colour Engineering: Achieving Device Independent Colour*, John Wiley & Sons, pp. 301 (2002).

[47] F. Ebner and M.D. Fairchild, "Gamut mapping from below: finding minimum perceptual distances for colors outside the gamut volume", in *Color Research & Application*, Vol. 22, pp. 402-413 (1997).

[48] R. S. Berns, *Billmeyer and Saltzman's Principles of Color Technology*, 3rd Ed., John Wiley & Sons, pp. 196 (2000).

[49] A. Sharma, *Understanding Color Management*, Delmar Thomson Publishing, Chapter 8, pp. 261-266 (2004).

[50] ISO 12641, "Graphic technology - Prepress digital data exchange - Colour targets for input scanner calibration", see: http://www.iso.org/iso/iso_catalogue/catalogue_tc/catalogue_detail.htm?csnumber=2079 (1997)

[51] D. Q. McDowell, “Standards activities for colour imaging”, *in Colour Engineering: Achieving Device Independent Colour*, edited by P. Green and L. MacDonald, Chapter 18, John Wiley & Sons, pp. 421-442 (2002).

[52] ISO 12640-1, “Graphic technology -- Prepress digital data exchange -- Part 1: CMYK standard colour image data (CMYK/SCID)”, see: http://www.iso.org/iso/iso_catalogue/catalogue_tc/catalogue_detail.htm?csnumber=2105 (1997)

[53] P. Green, *Color Management: Understanding and Using ICC profiles*, John Wiley & Sons, Chapter 24, pp 184-204 (2010)

[54] ISO 13655, “Graphic technology -- Spectral measurement and colorimetric computation for graphic arts images”, see: http://www.iso.org/iso/catalogue_detail?csnumber=39877 (2009)

[55] H. R. Kang, *Computational color technology*, SPIE Press, Chapter 8, pp 135-150 (2006)

[56] Wikipedia, “Invertible matrix”, see: http://en.wikipedia.org/wiki/Invertible_matrix (2011)

[57] Wikipedia, “Jacobian matrix and determinant”, see: http://en.wikipedia.org/wiki/Jacobian_matrix#Jacobian_matrix (2011)

[58] M. Maria, ”Little CMS”, see: http://www.littlecms.com/ (2011)

[59] D. G. Zill, S. Wright and W. Wright, *Calculus: Early Transcendentals*, Jones & Bartlett Learning, 4th Ed, Chapter 14 , pp 749-796 (2009)

[60] Wikipedia, “Root mean square deviation”, see: http://en.wikipedia.org/wiki/RMSE (2011)

[61] V. Chovancova , “CRT Vs LCD monitors for soft proofing: Quantitative and Visual Considerations” ,MS Thesis, Western Michigan University, April (2003)

[62] V. Chovancova-Lovell, P. D. Fleming, B. Starr and A. Sharma, “Side by Side Soft Proofing with CRT and LCD Monitors”, *TAGA J.*, **3**, 144, 2007.

[63] A. Sharma, “Understanding Color Management”, Delmar Thomson Publishing, Chapter 7, pp. 193-224.(2004)

[64] M.D. Fairchild and D.R. Wyble, "Colorimetric characterization of the Apple Studio Display (Flat Panel LCD)", Munsell Color Science Laboratory Technical Report, see: http://www.cis.rit.edu/mcsl/research/PDFs/LCD.pdf (1998).

[65] Apple Computer, " What's New in ColorSync 2.5", Apple Technical Publications, pp. 15 , see: http://developer.apple.com/legacy/mac/library/documentation/mac/pdf/ColorSync 2.5.pdf (1998)

[66] R. El Asaleh, S. Sonmez, P. D. Fleming and A. Pekarovicova, "Customized ICC Display Profile Construction and Concerns ", *Proc. TAGA 62nd Annual Technical Conference*, March 14-17, San Diego, California (2010).

[67] E. A. Day, L. Taplin and R. S. Berns, "Colorimetric Characterization of a Computer-Controlled Liquid Crystal Display", *J. Color Research and Application*, Vol. 29, Issue 5, pp. 365-373 (2004).

[68] J. E. Gibson and M. D. Fairchild,"Colorimetric characterization of three computer displays (LCD and CRT)", Munsell Color Science Laboratory Report, Rochester Institute of Technology, Rochester, NY, see: http://www.cis.rit.edu/mcsl/research/PDFs/GibsonFairchild.pdf (2000).

[69] M. Xia, E. Saber, G. Sharma, and A. M. Tekalp, "End-to-End Color Printer Calibration by Total Least Squares Regression", *J. IEEE Transactions On Image Processing,* vol. 8, no. 5, pp 700-716 (1999)

[70] P. B. Plaisted and R. Chung, "Construction Features of Color Output Device Profiles", *Proc. of. IS&T's 5th Color Imaging Conference*, Scottsdale, AZ, November (1997)

[71] P. Green, "Characterizing hard copy printers", in *Colour Engineering: Achieving Device Independent Colour*, edited by P. Green and L. MacDonald, Chapter 10, John Wiley & Sons, Ed. pp. 242 (2002).

[72] R. El Asaleh, P. D. Fleming, "Customized ICC Printer Profile Construction and Concerns", *Proc. NIP 27th International Conference on Digital Printing Technologies*, Oct 2-6, Minneapolis, Minnesota (2011).

[73] M. Derhak, SampleICC, see: http://sourceforge.net/projects/sampleicc/?_test=beta

[74] Mitsubishi Electric, see: http://www.mitsubishi-imaging.com/photo/default.asp

[75] D. Donevski, “The Selection of Optimal Polynomial Device Model”, *The CREATE 2010 Conference / Simone*, Gabriele, Hardeberg, Jon Yngve , Farup, Ivar (ed). - Gjovik, Norveška (2010)

Appendix A

Scanner

A.1. ΔE Evaluation Results

Table A-1 Training Data vs. Polynomial fit

	Polynomial			Training Data			ΔE
	L	A	B	L	a	b	
GS0	91.08	0.57	0.39	91.48	-0.33	-0.45	1.29
GS1	88.12	-1.06	0.99	87.74	-0.86	1.74	0.87
GS2	83.53	-1.00	0.25	83.27	-0.85	0.82	0.64
GS3	79.41	-1.00	0.42	79.06	-0.81	1.06	0.76
GS4	74.76	-1.16	0.57	74.75	-1	0.97	0.43
GS5	70.61	-1.36	0.65	70.82	-1.12	0.68	0.32
GS6	65.74	-0.84	0.17	65.94	-0.71	0.25	0.25
GS7	62.02	-0.38	1.66	62.35	-0.36	1.57	0.34
GS8	57.69	-0.66	1.09	58.05	-0.63	0.87	0.42
GS9	53.87	-0.73	1.16	54.42	-1.1	1.06	0.67
GS10	49.78	-0.72	1.79	50.28	-0.93	1.47	0.63
GS11	45.45	-0.66	1.52	45.98	-1.18	1.12	0.84
GS12	42.00	-0.78	0.64	42.33	-1.17	0.35	0.59
GS13	38.18	-0.23	0.92	38.08	-0.82	0.74	0.63
GS14	34.65	-0.47	0.07	34.11	-1.18	0.2	0.91
GS15	31.32	-0.43	0.30	30.56	-1.34	0.6	1.22
GS16	27.59	-0.51	0.31	26.14	-1.47	0.48	1.75
GS17	25.00	0.40	-0.60	22.7	-0.72	0.24	2.69
GS18	21.92	0.26	-0.94	18.95	-0.97	0.23	3.42
GS19	18.25	0.76	-0.56	14.72	-0.43	0.93	4.01
GS20	16.12	0.46	-0.97	11.39	-0.48	0.59	5.07
GS21	15.10	-0.25	-1.03	9.3	-0.5	0.89	6.11
GS22	14.67	-1.00	-1.90	7.51	-0.27	-0.28	7.38
GS23	14.22	-0.97	-3.39	4.81	1.18	-2.9	9.67

Table A-1-Continued

	Polynomial			Training Data			ΔE
	L	A	B	L	a	b	
L13-C	54.60	-27.81	-35.23	53.48	-40.17	-38.87	12.94
L14-M	43.03	70.94	-41.63	43.47	69.2	-41.48	1.80
L15-Y	77.97	14.99	83.58	78.23	13.8	95.45	11.94
L16-K	18.65	2.98	0.35	11.88	0.2	0.28	7.32
L17-R	39.66	52.18	47.94	39.66	56.61	45.05	5.29
L18-G	43.40	-48.16	41.53	42.63	-49.76	39.23	2.90
L19-B	22.03	29.28	-62.28	19.58	34.53	-66.69	7.28
A1	23.64	10.66	1.75	18.8	10.95	3.92	5.31
B3	23.14	24.11	16.24	19.47	25.08	18.78	4.57
C7	55.01	25.94	68.20	54.56	26.3	60.76	7.46
D8	58.74	-0.74	69.33	58.12	-2.3	62.06	7.46
E10	70.49	-9.81	18.01	70.81	-9.7	17.71	0.45
F12	70.46	-20.09	6.49	70.74	-19.14	6.76	1.02
						Mean	**3.42**
						Max	**12.94**
						Std	**3.50**

Table A-2: Training Data vs. ProfileMaker Profile

	Photoshop			Training Data			ΔE
	L	a	b	L	a	b	
GS0	91.05	-0.90	-1.08	91.48	-0.33	-0.45	0.95
GS1	87.21	-1.48	0.45	87.74	-0.86	1.74	1.53
GS2	82.35	-1.75	-0.17	83.27	-0.85	0.82	1.62
GS3	77.91	-1.88	0.35	79.06	-0.81	1.06	1.72
GS4	73.19	-2.01	0.78	74.75	-1	0.97	1.87
GS5	69.01	-2.37	1.00	70.82	-1.12	0.68	2.22
GS6	64.04	-1.95	0.82	65.94	-0.71	0.25	2.34
GS7	60.36	-1.28	1.98	62.35	-0.36	1.57	2.23
GS8	56.11	-1.10	1.18	58.05	-0.63	0.87	2.02
GS9	52.29	-1.04	1.02	54.42	-1.1	1.06	2.13
GS10	47.98	-1.34	1.65	50.28	-0.93	1.47	2.35
GS11	43.25	-1.57	1.47	45.98	-1.18	1.12	2.78
GS12	39.45	-1.66	0.59	42.33	-1.17	0.35	2.93
GS13	35.18	-1.21	0.85	38.08	-0.82	0.74	2.93
GS14	31.13	-1.65	0.14	34.11	-1.18	0.2	3.02
GS15	27.15	-1.89	0.74	30.56	-1.34	0.6	3.45
GS16	22.51	-2.20	1.51	26.14	-1.47	0.48	3.84

Table A-2-Continued

	Photoshop			Training Data			ΔE
	L	a	b	L	a	b	
GS17	19.16	-1.41	1.24	22.7	-0.72	0.24	3.74
GS18	14.88	-1.74	1.72	18.95	-0.97	0.23	4.40
GS19	9.12	-1.38	3.33	14.72	-0.43	0.93	6.17
GS20	5.67	-1.23	3.14	11.39	-0.48	0.59	6.30
GS21	4.33	-1.55	3.17	9.3	-0.5	0.89	5.56
GS22	3.79	-2.13	2.56	7.51	-0.27	-0.28	5.04
GS23	3.24	-2.24	1.46	4.81	1.18	-2.9	5.76
L13-C	51.02	-39.09	-37.63	53.48	-40.17	-38.87	2.96
L14-M	40.78	65.03	-39.85	43.47	69.2	-41.48	5.22
L15-Y	76.76	12.68	89.86	78.23	13.8	95.45	5.89
L16-K	9.76	0.90	4.08	11.88	0.2	0.28	4.41
L17-R	36.55	51.90	47.36	39.66	56.61	45.05	6.10
L18-G	40.09	-45.64	37.45	42.63	-49.76	39.23	5.16
L19-B	16.24	31.18	-63.62	19.58	34.53	-66.69	5.64
A1	16.13	9.13	4.68	18.8	10.95	3.92	3.32
B3	15.64	23.50	20.04	19.47	25.08	18.78	4.33
C7	51.86	24.62	60.47	54.56	26.3	60.76	3.19
D8	55.62	-2.90	56.11	58.12	-2.3	62.06	6.48
E10	68.94	-10.53	16.32	70.81	-9.7	17.71	2.48
F12	69.24	-19.10	6.84	70.74	-19.14	6.76	1.50
						Mean	**3.61**
						Max	**6.48**
						Std	**1.64**

Appendix B

Monitor

B.1. Phase1: Monitor's Physical Behaviors Evaluation

It's important to note that the physical behavior of a device should not be affected by any applied ICC profile.

B.1.1. Brightness Test

B.1.1.1. Acer display

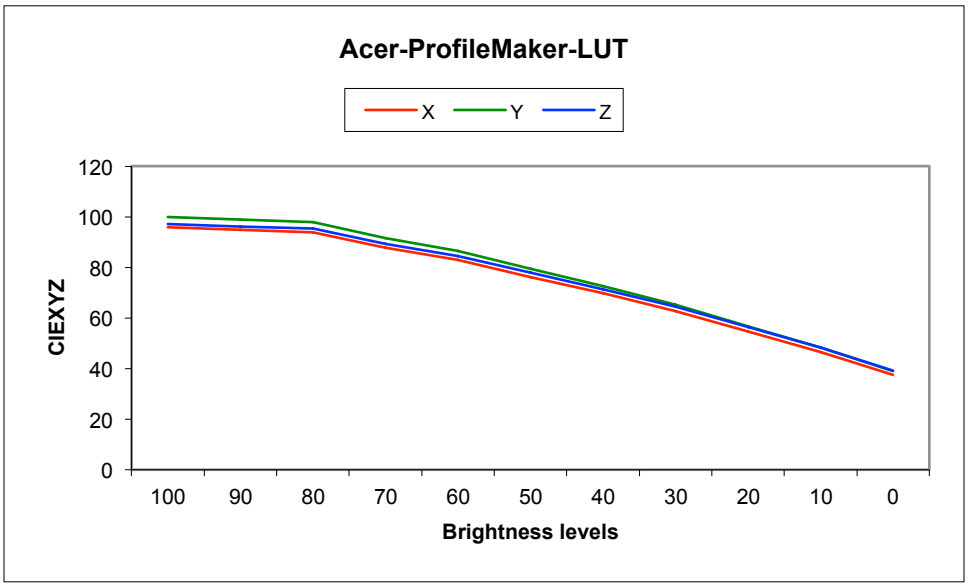

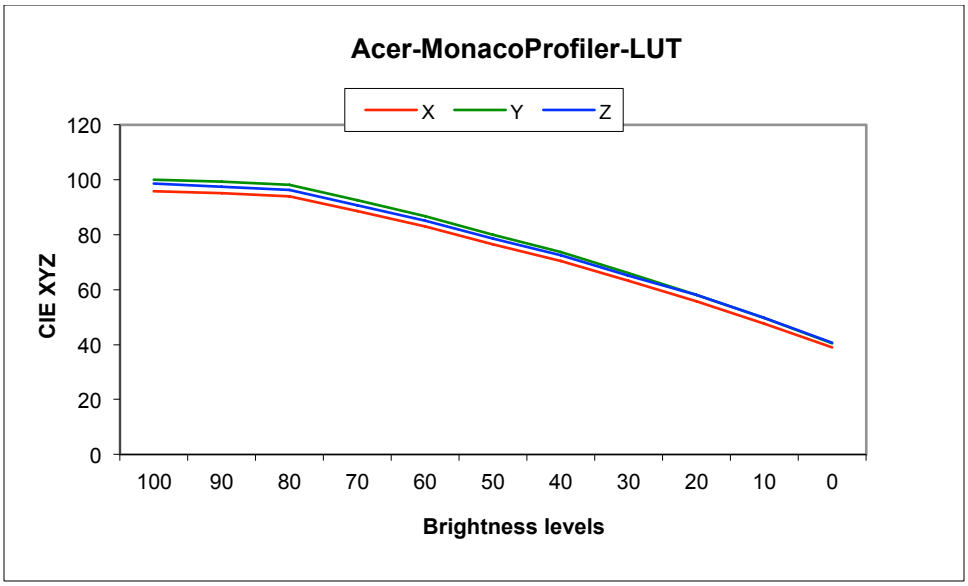

B.1.1.2. Apple Cinema display

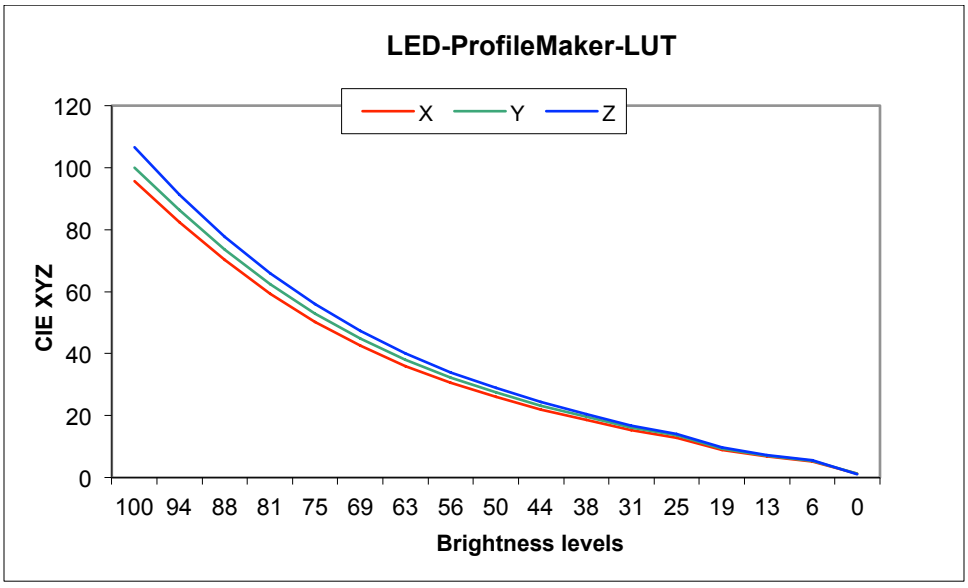

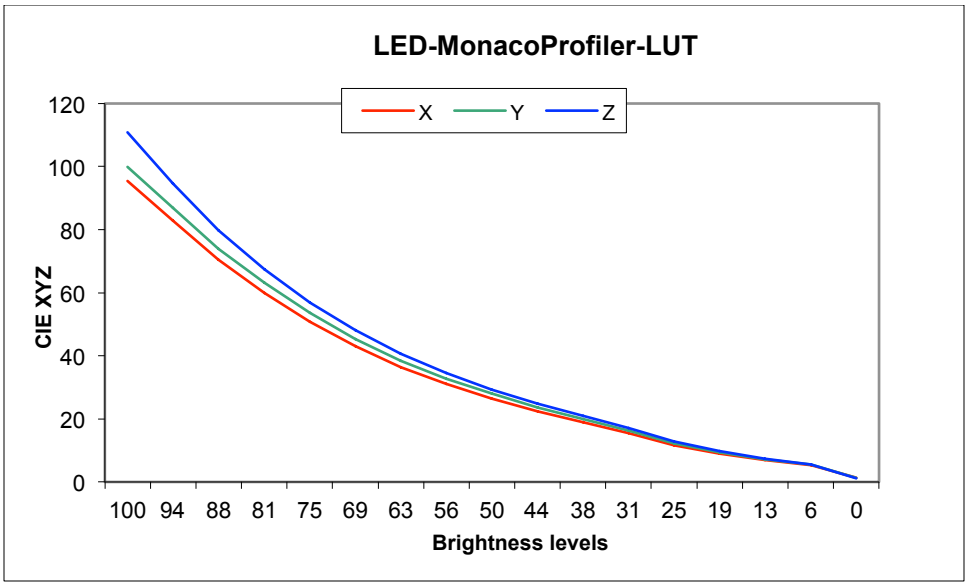

B.1.2. Warm-Up Test

The following data are the average and the standard deviation of the chromaticity xy values over 2 hours of the warm up test period. These values were calculated from the XYZ value for both displayed white and gray patches on both monitors. The Correlated Color Temperatures (CCT) were also calculated and listed in the same table.

Table B-1: White Patch data

		Acer			Apple Cinema		
		x	y	CCT	x	y	CCT
ProfileMaker Matrix-based	Avg	0.3057	0.3122	7100.3	0.3156	0.3297	6343.2
	STD	0.0009	0.0018	85.9	0.0007	0.0011	41.5
MonacoProfiler LUT-based	Avg	0.3254	0.3404	5816.6	0.3149	0.3295	6385.3
	STD	0.0005	0.0009	22.3	0.0011	0.0015	66.7
MonacoProfiler Matrix-based	Avg	0.3259	0.3398	5795.2	0.3172	0.3310	6255.1
	STD	0.0005	0.0011	26.7	0.0004	0.0005	21.1

Table B-2: Gray Patch Data

		Acer			Apple Cinema		
		x	y	CCT	x	y	CCT
ProfileMaker Matrix-based	Avg	0.3057	0.3122	7100.3	0.3170	0.3313	6260.5
	STD	0.0009	0.0018	85.9	0.0007	0.0009	37.9
MonacoProfiler LUT-based	Avg	0.3203	0.3349	6075.8	0.3145	0.3296	6406.7
	STD	0.0004	0.0012	25.3	0.0011	0.0012	62.9
MonacoProfiler Matrix-based	Avg	0.3221	0.3348	5990.9	0.3166	0.3295	6291.6
	STD	0.0007	0.0015	38.8	0.0007	0.0011	44.1

B.1.3. White Point Temperature Test

Table B-3: Acer Display

		X	Y	Z	x	y
Win	MeasureTool	177.89	186.85	176.92	0.328416	0.344958
	Photoshop	170.99	179.66	168.33	0.329473	0.346179
	Folder	161.79	170.14	160.14	0.328795	0.345764
	Avg				**0.328895**	**0.345634**
	CCT				**5654.2**	
	STD		**8.38**		**0.000535**	**0.000621**
Mac	MeasureTool	183.91	192.91	182.32	0.328916	0.345012
	Photoshop	172.71	181.58	172.15	0.328072	0.344921
	Folder	180.25	189.26	178.62	0.328845	0.345283
	Avg				**0.328611**	**0.345072**
	CCT				**5667.1**	
	STD		**5.78**		**0.000468**	**0.000189**
Cross Platform	**Avg**		**183.40**		**0.328753**	**0.345353**
	CCT				**5660.7**	
	STD		**8.12**		**0.000476**	**0.000513**

Table B-4: Apple Cinema Display

		X	Y	Z	x	y
Win	MeasureTool	344.83	360.53	385.27	0.316175	0.33057
	Photoshop	341.69	360.2	392.85	0.31212	0.329028
	Folder	342.13	358.82	383.38	0.315522	0.330914
	Avg				**0.314606**	**0.330171**
	CCT				**6394.4**	
	STD		**0.907138**		**0.002177**	**0.001005**
Mac	MeasureTool	359.44	378.83	393.56	0.317574	0.334706
	Photoshop	359.79	377.12	395	0.317861	0.333171
	Folder	350.47	369.32	391.53	0.315364	0.332326
	Avg				**0.316933**	**0.333401**
	CCT				**6254.1**	
	STD		**5.069586**		**0.001367**	**0.001207**
Cross Platform	**Avg**		**367.47**		**0.315769**	**0.331786**
	CCT				**6323.1**	
	STD		**8.960286**		**0.002066**	**0.002029**

B.2. Phase2: Finding the Native Gamma

The following tables represent the calculated slop of each RGB channel inside the video card gamma tag (vcgt) for each native profile under different platform and the calculated gamma value based on that slop.

B.2.1. Acer Display

Table B-5: Acer native matrix-base profile

	Mac		Win	
	Slop	**Gamma**	**Slop**	**Gamma**
Red	0.440	2.27	0.446	2.24
Green	0.447	2.24	0.458	2.19
Blue	0.473	2.11	0.466	2.15
Avg		**2.21**		**2.19**

Table B-6: Acer native LUT-base profile

	Mac		Win	
	Slop	**Gamma**	**Slop**	**Gamma**
Red	0.440	2.27	0.445	2.25
Green	0.447	2.24	0.457	2.19
Blue	0.473	2.11	0.467	2.14
Avg		**2.21**		**2.19**

B.2.2. Apple Cinema Display

Table B-7: Apple Cinema native Matrix-base profile

	Mac		Win	
	Slop	**Gamma**	**Slop**	**Gamma**
Red	0.471	2.12	0.472	2.12
Green	0.471	2.12	0.479	2.09
Blue	0.464	2.15	0.469	2.13
Avg		**2.13**		**2.11**

Table B-8: Apple Cinema native LUT-base profile

	Mac		Win	
	Slop	Gamma	Slop	Gamma
Red	0.463	2.16	0.472	2.12
Green	0.464	2.15	0.479	2.09
Blue	0.459	2.18	0.469	2.13
Avg		**2.17**		**2.11**

B.3. Training set Evaluation Results

The following tables represent a ΔE comparison between the measured set of primaries and white point color patches from MeasureTool and the LUT entries of the tested profiles that represents each fitting models for each monitor. The MeasureTool data are the average data of four attempted measurement under Mac platform and one measurement under Windows platform for each monitor.

B.3.1. Acer Display

B.3.1.1. Measure Tool Averaging Algorithm

	MeasureTool			Polynomial fit			ΔE
	L	a	b	L	a	b	
R	59.47	74.32	90.09	59.3	72.3	89.5	**2.1**
G	83.34	-90.62	78.44	84.0	-88.9	76.9	**2.4**
B	36.91	46.01	-111.93	35.4	37.3	-100.9	**14.2**
W	100.00	-2.68	-9.65	100.6	-6.6	2.0	**12.3**
						Avg	**7.7**

	MeasureTool			Least-Square			ΔE
	L	a	b	L	a	b	
R	59.47	74.32	90.09	59.2	75.1	91.2	**1.3**
G	83.34	-90.62	78.44	83.7	-91.0	78.8	**0.6**
B	36.91	46.01	-111.93	34.5	56.1	-116.2	**11.2**
W	100.00	-2.68	-9.65	99.5	-0.9	-10.6	**2.0**
						Avg	**3.8**

B.3.1.2. Manual Averaging Algorithm

	MeasureTool			Polynomial fit			ΔE
	L	a	b	L	a	b	
R	59.47	74.32	90.09	59.5	73.0	90.4	**1.4**
G	83.34	-90.62	78.44	83.6	-89.5	73.9	**4.7**
B	36.91	46.01	-111.93	36.3	48.3	-111.6	**2.4**
W	100.00	-2.68	-9.65	100.7	-2.3	-9.8	**0.8**
						Avg	**2.3**

	MeasureTool			Least-Square fit			ΔE
	L	a	b	L	a	b	
R	59.47	74.32	90.09	59.2	75.1	91.2	**1.3**
G	83.34	-90.62	78.44	83.7	-91.0	78.8	**0.6**
B	36.91	46.01	-111.93	36.6	46.9	-112.5	**1.2**
W	100.00	-2.68	-9.65	99.9	-2.7	-9.9	**0.2**
						Avg	**0.8**

B.3.2. Apple Display

B.3.2.1. Manual Averaging Algorithm

	MeasureTool			Polynomial fit			ΔE
	L	a	b	L	a	b	
R	52.73	80.17	75.00	53.2	80.2	71.5	**3.5**
G	88.20	-86.66	81.71	88.0	-88.0	81.0	**1.5**
B	32.36	78.80	-129.64	32.5	77.1	-127.5	**2.7**
W	100.00	-1.41	-19.79	100.0	-1.8	-18.2	**1.6**
						Avg	**2.3**

	MeasureTool			Least-Square fit			ΔE
	L	a	b	L	a	b	
R	52.73	80.17	75.00	53.1	80.6	75.8	**0.9**
G	88.20	-86.66	81.71	88.1	-88.4	81.7	**1.7**
B	32.36	78.80	-129.64	32.1	78.3	-128.5	**1.3**
W	100.00	-1.41	-19.79	100.1	-1.9	-18.3	**1.6**
						Avg	**1.4**

B.4. ΔE Evaluation Results

B.4.1. Acer Display

B.4.1.1. Polynomial fit

	Photoshop			Polynomial-LUT-entries			ΔE
	L	a	b	L	a	b	
R	60	75	93	60.1	74.9	93.8	**0.8**
G	83	-84	77	83.6	-84.1	77.2	**0.6**
B	35	42	-103	35.1	42.5	-104.0	**1.1**
W	100	0	0	100.7	0.0	0.0	**0.7**
						Avg	**0.8**

	DigitalColor Meter			Polynomial-LUT-entries			ΔE
	L	a	b	L	a	b	
R	60	72	91	60.1	74.9	93.8	**3.5**
G	80	-81	74	83.6	-84.1	77.2	**5.8**
B	37	35	-99	35.1	42.5	-104.0	**9.0**
W	100	0	0	100.7	0.0	0.0	**0.7**
						Avg	**4.7**

B.4.1.2. Least-Square fit

	Photoshop			Least-square-LUT-entries			ΔE
	L	a	b	L	a	b	
R	60	77	94	59.9	77.2	94.8	**0.9**
G	84	-85	82	83.6	-84.9	81.8	**0.4**
B	35	41	-105	35.4	40.9	-104.8	**0.5**
W	100	0	0	99.9	0.0	0.0	**0.1**
						Avg	**0.5**

	DigitalColor Meter			Least-square-LUT-entries			ΔE
	L	a	b	L	a	b	
R	60	76	94	59.9	77.2	94.8	**1.8**
G	81	-82	80	83.6	-84.9	81.8	**4.0**
B	38	34	-100	35.4	40.9	-104.8	**8.7**
W	100	0	0	99.9	0.0	0.0	**0.1**
						Avg	**3.7**

B.4.1.3. Photoshop vs. DigitalColor Meter

Table B-9: i1Profiler profile

	Photoshop			DigitalColor Meter			ΔE
	L	a	b	L	a	b	
R	60	75	92	60	75	91	**0.7**
G	84	-84	79	84	-84	78	**0.7**
B	35	46	-105	35	45	-104	**1.1**
W	100	0	0	100	0	0	**0.0**
						Avg	**0.6**

Table B-10: Polynomial fit profile

	Photoshop			DigitalColor Meter			ΔE
	L	a	b	L	a	b	
R	60	75	93	60	72	91	**3.1**
G	83	-84	77	80	-81	74	**5.3**
B	35	42	-103	37	35	-99	**8.1**
W	100	0	0	100	0	0	**0.0**
						Avg	**4.1**

Table B-11: Least-square fit profile

	Photoshop			DigitalColor Meter			ΔE
	L	a	b	L	a	b	
R	60	77	94	60	76	94	**1.2**
G	84	-85	82	81	-82	80	**4.4**
B	35	41	-105	38	34	-100	**9.0**
W	100	0	0	100	0	0	**0.0**
						Avg	**3.6**

B.4.2. Apple Display

B.4.2.1. Polynomial fit

	Photoshop			Polynomial-LUT-entries			ΔE
	L	a	b	L	a	b	
R	54.0	82.0	78.0	54.1	82.5	78.4	0.6
G	88.0	-80.0	87.0	88.1	-80.2	86.9	0.3
B	30.0	68.0	-114.0	29.8	67.8	-113.9	0.3
W	100.0	0.0	0.0	100.0	0.0	0.0	0.1
						Avg	**0.3**

	DigitalColor Meter			Polynomial-LUT-entries			ΔE
	L	a	b	L	a	b	
R	52.6	80.8	80.0	54.1	82.5	78.4	2.8
G	88.7	-72.3	87.7	88.1	-80.2	86.9	8.0
B	29.3	68.5	-114.4	29.8	67.8	-113.9	1.0
W	100.0	0.0	0.0	100.0	0.0	0.0	0.1
						Avg	**3.0**

B.4.2.2. Least-Square fit

	Photoshop			Least-square-LUT-entries			ΔE
	L	a	b	L	a	b	
R	54.0	83.0	82.0	54.1	82.9	82.6	0.6
G	88.0	-80.0	87.0	88.2	-80.4	87.4	0.6
B	29.0	69.0	-115.0	29.3	68.9	-115.0	0.4
W	100.0	0.0	0.0	100.1	0.0	0.0	0.1
						Avg	**0.4**

	DigitalColor Meter			Least-square-LUT-entries			ΔE
	L	a	b	L	a	b	
R	52.6	80.8	80.0	54.1	82.9	82.6	3.6
G	88.7	-72.3	87.7	88.2	-80.4	87.4	8.1
B	29.3	68.5	-114.4	29.3	68.9	-115.0	0.7
W	100.0	0.0	0.0	100.1	0.0	0.0	0.1
						Avg	**3.1**

B.4.2.3. Photoshop vs. DigitalColor Meter

Table B-12: i1Profiler profile

	Photoshop			DigitalColor Meter			ΔE
	L	a	b	L	a	b	
R	54.0	83.0	82.0	54.2	82.7	81.8	0.4
G	88.0	-81.0	87.0	88.0	-80.8	86.8	0.3
B	29.0	69.0	-115.0	29.2	68.5	-114.5	0.7
W	100.0	0.0	0.0	100.0	0.0	0.0	0.0
						Avg	**0.4**

Table B-13: Polynomial fit profile

	Photoshop			DigitalColor Meter			ΔE
	L	a	b	L	a	b	
R	54.0	82.0	78.0	52.6	80.8	80.0	2.7
G	88.0	-80.0	87.0	88.7	-72.3	87.7	7.8
B	30.0	68.0	-114.0	29.3	68.5	-114.4	1.0
W	100.0	0.0	0.0	100.0	0.0	0.0	0.0
						Avg	**2.9**

Table B-14: Least-square fit profile

	Photoshop			DigitalColor Meter			ΔE
	L	a	b	L	a	b	
R	54.0	83.0	82.0	52.6	80.8	80.0	3.3
G	88.0	-80.0	87.0	88.7	-72.3	87.7	7.8
B	29.0	69.0	-115.0	29.3	68.5	-114.4	0.8
W	100.0	0.0	0.0	100.0	0.0	0.0	0.0
						Avg	**3.0**

Appendix C

Printer

B.5. Gray and CMY Ramps Data

B.5.1. Training Data

Table C-1: Gray ramp data

R	G	B	X	Y	Z
0	0	0	1.16	1.11	1.10
16	16	16	2.08	2.07	1.66
32	32	32	2.16	2.22	1.87
32	32	32	3.03	3.01	2.25
48	48	48	4.46	4.48	3.51
64	64	64	5.67	5.98	5.42
64	64	64	7.07	7.13	5.56
80	80	80	11.07	11.14	8.73
96	96	96	14.13	14.86	12.93
96	96	96	15.92	16.21	12.74
112	112	112	19.87	19.65	16.20
128	128	128	23.42	24.25	20.02
128	128	128	24.88	24.49	19.85
144	144	144	31.94	31.94	25.95
160	160	160	38.16	40.09	32.67
160	160	160	39.56	40.03	32.18
176	176	176	48.72	49.80	39.43
192	192	192	58.02	59.22	47.70
192	192	192	59.47	60.83	47.72
207	207	207	68.51	69.51	56.57
208	208	208	72.03	74.31	58.19
224	224	224	78.77	81.48	67.99
224	224	224	80.64	83.64	69.11
233	233	233	82.21	85.04	72.29

Table C-1-Continued

R	G	B	X	Y	Z
240	240	240	84.24	87.19	74.26
244	244	244	83.74	86.73	73.95
255	255	255	86.93	90.03	76.92
255	255	255	86.60	89.80	76.57
255	255	255	87.07	90.33	77.56
255	255	255	86.67	89.85	76.74
255	255	255	86.99	90.25	77.50
255	255	255	86.74	89.87	76.75
255	255	255	86.95	90.21	77.12
255	255	255	86.63	89.82	76.51
255	255	255	86.95	90.16	77.47
255	255	255	86.77	89.92	76.92
255	255	255	86.87	90.10	77.56
255	255	255	86.71	89.89	76.85
255	255	255	86.92	90.15	77.54
255	255	255	86.57	89.76	76.75
255	255	255	87.03	90.24	77.62
255	255	255	86.73	89.83	76.78
255	255	255	86.90	90.13	77.39
255	255	255	86.61	89.78	76.70
255	255	255	86.56	89.78	77.10

Table C-2: Cyan ramp data

R	G	B	X	Y	Z
0	0	0	1.16	1.11	1.10
0	16	16	1.89	2.03	1.98
0	32	32	1.41	1.72	1.86
0	64	64	2.61	3.96	5.71
0	96	96	5.16	8.19	13.50
0	128	128	7.36	11.87	21.25
0	160	160	9.43	15.13	30.13
0	192	192	11.24	17.78	37.64
0	224	224	13.44	20.73	46.26
0	255	255	13.06	20.09	47.19

Table C-3: Magenta ramp data

R	G	B	X	Y	Z
0	0	0	1.16	1.11	1.10
16	0	16	1.9	1.71	1.57
32	0	32	1.8	1.47	1.43
64	0	64	4.22	2.70	3.18
96	0	96	8.66	4.74	6.28
128	0	128	13.80	6.97	9.29
160	0	160	18.57	8.92	12.39
192	0	192	25.69	11.84	15.59
224	0	224	29.07	13.09	17.73
255	0	255	30.18	13.55	18.62

Table C-4: Yellow ramp data

R	G	B	X	Y	Z
0	0	0	1.16	1.11	1.10
16	16	0	1.98	1.96	1.61
32	32	0	2.34	2.43	1.59
64	64	0	5.75	6.20	2.43
96	96	0	13.13	14.3	3.58
128	128	0	22.97	24.99	4.78
160	160	0	35.4	38.96	5.90
192	192	0	53.28	56.87	6.89
224	224	0	69.14	75.42	7.96
255	255	0	73.20	79.67	8.11

B.5.2. Constrained Fit LUT Entries

Table C-5: Gray ramp data

R	G	B	X	Y	Z
0	0	0	1.16	1.11	1.10
8	8	8	2.98	2.72	2.30
16	16	16	4.85	4.40	3.58
24	24	24	6.78	6.15	4.94
32	32	32	8.76	7.98	6.37
40	40	40	10.80	9.89	7.88
48	48	48	12.89	11.87	9.46
56	56	56	15.03	13.93	11.12
64	64	64	17.24	16.06	12.85

Table C-5-Continued

R	G	B	X	Y	Z
72	72	72	19.49	18.27	14.66
80	80	80	21.81	20.55	16.54
88	88	88	24.17	22.91	18.50
96	96	96	26.59	25.34	20.54
104	104	104	29.07	27.85	22.65
112	112	112	31.60	30.43	24.84
120	120	120	34.19	33.09	27.10
128	128	128	36.83	35.82	29.44
135	135	135	39.52	38.63	31.85
143	143	143	42.28	41.51	34.34
151	151	151	45.08	44.47	36.90
159	159	159	47.94	47.51	39.54
167	167	167	50.86	50.62	42.26
175	175	175	53.83	53.80	45.05
183	183	183	56.86	57.06	47.92
191	191	191	59.94	60.40	50.86
199	199	199	63.07	63.81	53.88
207	207	207	66.26	67.29	56.97
215	215	215	69.51	70.86	60.14
223	223	223	72.81	74.49	63.38
231	231	231	76.17	78.20	66.70
239	239	239	79.58	81.99	70.10
247	247	247	83.04	85.85	73.57
255	255	255	86.56	89.79	77.12

Table C-6: Cyan ramp data

R	G	B	X	Y	Z
0	0	0	1.16	1.11	1.10
0	8	8	1.65	2.05	2.28
0	16	16	2.13	2.98	3.50
0	24	24	2.61	3.88	4.76
0	32	32	3.09	4.77	6.05
0	40	40	3.56	5.63	7.39
0	48	48	4.03	6.47	8.76
0	56	56	4.49	7.30	10.16
0	64	64	4.95	8.10	11.61
0	72	72	5.40	8.89	13.09
0	80	80	5.85	9.65	14.61
0	88	88	6.29	10.39	16.17

Table C-6-Continued

R	G	B	X	Y	Z
0	96	96	6.73	11.12	17.77
0	104	104	7.17	11.82	19.40
0	112	112	7.60	12.50	21.07
0	120	120	8.03	13.17	22.78
0	128	128	8.45	13.81	24.52
0	135	135	8.87	14.44	26.31
0	143	143	9.28	15.04	28.13
0	151	151	9.69	15.62	29.98
0	159	159	10.09	16.19	31.88
0	167	167	10.49	16.73	33.81
0	175	175	10.89	17.25	35.78
0	183	183	11.28	17.76	37.79
0	191	191	11.67	18.24	39.84
0	199	199	12.05	18.70	41.92
0	207	207	12.43	19.15	44.04
0	215	215	12.80	19.57	46.20
0	223	223	13.17	19.97	48.40
0	231	231	13.54	20.35	50.63
0	239	239	13.90	20.72	52.90
0	247	247	14.25	21.06	55.21
0	255	255	14.61	21.38	57.56

Table C-7: Magenta ramp data

R	G	B	X	Y	Z
0	0	0	1.16	1.11	1.10
8	0	8	2.63	1.78	1.98
16	0	16	4.06	2.43	2.84
24	0	24	5.45	3.06	3.70
32	0	32	6.80	3.67	4.55
40	0	40	8.11	4.27	5.39
48	0	48	9.38	4.85	6.22
56	0	56	10.62	5.41	7.04
64	0	64	11.81	5.95	7.86
72	0	72	12.97	6.48	8.66
80	0	80	14.09	6.99	9.46
88	0	88	15.17	7.48	10.25
96	0	96	16.21	7.95	11.03
104	0	104	17.21	8.41	11.80

Table C-7-Coninued

R	G	B	X	Y	Z
112	0	112	18.17	8.84	12.56
120	0	120	19.09	9.27	13.32
128	0	128	19.97	9.67	14.06
135	0	135	20.82	10.05	14.80
143	0	143	21.62	10.42	15.52
151	0	151	22.39	10.77	16.24
159	0	159	23.12	11.11	16.95
167	0	167	23.80	11.42	17.66
175	0	175	24.45	11.72	18.35
183	0	183	25.06	12.00	19.03
191	0	191	25.63	12.26	19.71
199	0	199	26.17	12.51	20.37
207	0	207	26.66	12.74	21.03
215	0	215	27.11	12.95	21.68
223	0	223	27.53	13.14	22.32
231	0	231	27.91	13.31	22.95
239	0	239	28.24	13.47	23.58
247	0	247	28.54	13.61	24.19
255	0	255	28.80	13.74	24.80

Table C-8: Yellow ramp data

R	G	B	X	Y	Z
0	0	0	1.16	1.11	1.10
8	8	0	2.78	2.65	1.40
16	16	0	4.45	4.25	1.70
24	24	0	6.15	5.92	2.02
32	32	0	7.90	7.64	2.34
40	40	0	9.70	9.44	2.68
48	48	0	11.53	11.30	3.02
56	56	0	13.41	13.22	3.38
64	64	0	15.33	15.20	3.75
72	72	0	17.29	17.25	4.12
80	80	0	19.29	19.36	4.51
88	88	0	21.34	21.54	4.91
96	96	0	23.43	23.78	5.32
104	104	0	25.56	26.08	5.73
112	112	0	27.73	28.45	6.16
120	120	0	29.95	30.88	6.60

Table C-8-Continued

R	G	B	X	Y	Z
128	128	0	32.21	33.38	7.05
135	135	0	34.51	35.93	7.51
143	143	0	36.85	38.56	7.98
151	151	0	39.24	41.24	8.46
159	159	0	41.66	43.99	8.95
167	167	0	44.13	46.81	9.45
175	175	0	46.65	49.68	9.96
183	183	0	49.20	52.63	10.48
191	191	0	51.80	55.63	11.01
199	199	0	54.44	58.70	11.55
207	207	0	57.12	61.84	12.10
215	215	0	59.85	65.03	12.66
223	223	0	62.62	68.29	13.23
231	231	0	65.43	71.62	13.82
239	239	0	68.28	75.01	14.41
247	247	0	71.18	78.46	15.01
255	255	0	74.11	81.97	15.62

B.6. ΔE Evaluation Results

Table C-9: Training Data vs. Constrained fit

	Constrained fit			Training data			ΔE
	L	a	b	L	A	B	
W	96.00	0.00	-3.00	95.99	0.04	-2.41	**0.59**
C	53.00	-32.00	-58.00	51.94	-36.06	-48.87	**10.05**
M	44.00	77.00	-31.00	43.58	82.67	-19.03	**13.71**
Y	93.00	-10.00	73.00	91.54	-7.40	93.11	**21.32**
K	10.00	3.00	-3.00	9.88	3.03	-2.81	**0.23**
R	39.00	66.00	47.00	42.11	72.06	52.06	**7.93**
G	46.00	-70.00	25.00	46.32	-74.32	26.32	**4.53**
B	16.00	38.00	-58.00	15.95	41.76	-62.42	**5.80**
						Avg	**8.02**
						Max	**21.32**
						STD	**7.03**

Table C-10: Training Data vs. ProfileMaker

	ProfileMaker			Training data			ΔE
	L	a	b	L	A	B	
W	96.00	0.00	-2.00	95.99	0.04	-2.41	**0.41**
C	52.00	-36.00	-49.00	51.94	-36.06	-48.87	**0.16**
M	44.00	83.00	-19.00	43.58	82.67	-19.03	**0.53**
Y	92.00	-7.00	93.00	91.54	-7.40	93.11	**0.62**
K	10.00	3.00	-3.00	9.88	3.03	-2.81	**0.23**
R	42.00	72.00	52.00	42.11	72.06	52.06	**0.14**
G	46.00	-74.00	26.00	46.32	-74.32	26.32	**0.56**
B	16.00	42.00	-62.00	15.95	41.76	-62.42	**0.49**
						Avg	**0.39**
						Max	**0.62**
						STD	**0.19**